Teaching the Cellular and Molecular Basis of Breast Cancer Metastasis: A Novel Workflow for Incorporating Time-lapse Microscopy Data into 3D Animation

by
Brittany Celeste Bennett

A thesis submitted to Johns Hopkins University
in conformity with the requirements for the degree of
Master of Arts.

Baltimore, Maryland
March, 2019

ABSTRACT

Time-lapse confocal microscopy and organotypic 3D culture allow biologists to capture 3D movies of cells moving in real time. The Ewald Lab at Johns Hopkins School of Medicine developed this method to determine how molecular variables affect the growth of breast cancer tumors and cells' ability to metastasize. The results support a new model of breast cancer metastasis, called Collective Epithelial Metastasis (CEM). Existing visuals of CEM are limited to microscopy and schematic model figures. Although informative to biologists, these are not intuitive to non-specialist audiences such as patient advocates and research investors. There is a need for visuals that explain the molecular and cellular basis of CEM within an anatomical context, and make conclusions of complex research more accessible.

The animation teaches the role of two proteins, E-cadherin and Keratin-14, during collective invasion and dissemination. The visual challenge was to contextualize molecular concepts for an audience that first needs introduction to mammary gland anatomy, histology, and epithelial cancer definitions. Learning objectives, a script, and twenty-four page partial-color storyboard were created to teach these concepts in an appropriate level of detail. A website was developed to display the animation and provide additional information and citations.

The technical project goal was to incorporate the Ewald Lab's time-lapse microscopy datasets into an educational animation. Selected datasets show cellular events that correspond to storyboarded scenes. Volumetric data was converted into 3D surface meshes in Bitplane Imaris and imported into MAXON Cinema 4D with an OBJ Sequence Importer plugin. In Cinema 4D, the "re-animated" surface meshes were modified before being merged into a scene of the mammary duct microenvironment.

Other data-derived 3D models created for the animation include: 1) breast anatomy and a metastatic tumor, segmented from DICOM data and 2) a ductal tree created in Cinema 4D, based on mouse mammary tissue.

This project demonstrates that 3D time-lapse microscopy datasets can be incorporated into Cinema 4D and blend within the built anatomical and histological scene. The merging of data-derived animation with artist-created animation can improve scientific communication to audiences outside of cell biology.

Brittany Celeste Bennett

CHAIRPERSONS OF THE SUPERVISORY COMMITTEE

Timothy Phelps, MS, FAMI, Department Advisor
Professor, Department of Art as Applied to Medicine, Johns Hopkins University, School of Medicine

Andrew Ewald, Ph.D., Preceptor
Professor, Center for Cell Dynamics, Department of Cell Biology, Johns Hopkins University, School of Medicine

ACKNOWLEDGEMENTS

I would like to express my gratitude to **Tim Phelps** for his role as my faculty advisor. I am grateful for his narrative imagination and critical eye, which strengthened my project without a doubt. His guidance is helpful in many ways, but his efforts in empowering me to believe in myself is one that I appreciate the most.

Thanks to my Preceptor, **Dr. Andrew Ewald,** whose role was not only as a scientific advisor, but also as a professional mentor. I'm thankful that he proposed a thesis topic with remarkably captivating visual data and presented the story of the Ewald Lab research. I am also thankful that he allowed me the opportunity to learn and experiment with Imaris.

I am deeply grateful to **Andrew Fraser**, member of the Ewald Lab, for generously sharing his time and morphogenesis datasets, and providing guidance through the technical aspects of Imaris. His patience and commitment to figuring out many unexpected technical issues went above and beyond expectations and undoubtedly contributed to the success of the Imaris export workflow.

I am thankful to the dedicated researchers who generously shared their datasets with me for the creation of this project. Thanks to **Katarina Sirka,** member of the Ewald Lab, for sharing the confocal microscopy datasets of myoepithelial cell recapture events. Her thesis presentation on the topic of myoepithelial cells was both informative and a model of incredibly clear scientific communication. Thanks to **Dr. Kevin Cheung** of the Fred Hutchinson Cancer Research Center, for his words of encouragement and sharing his data set of collective invasion.

A special thanks to my classmates, **Alisa Brandt**, **Insil Choi**, **Cecilia Johnson**,

Lohitha Kethu, and **Vondel Mahon**. These five individuals are some of the most hard working and passionate artists I've ever had the pleasure to work beside. Also I would like to thank the class of **'18** for their guidance through our first year and efforts to help us relax.

I am eternally grateful for the opportunity to study in the Department of Art as Applied to Medicine. Thanks to all of the faculty and staff for their unwavering enthusiasm for the field and support of blossoming medical illustrators. **Corinne Sandone, Jennifer Fairman, David Rini, Gary Lees, Juan Garcia, Ian Suk, Ann Altemus, Norm Baker, Donald Bliss, Sandra Gabelli, Lydia Gregg, and Fabian De Kok-Mercado** and **Carol Pfeffer**. I would like to give a special thanks to **Dacia Balch** for lifting spirits on a daily basis and expert narration of the project script.

I send my thanks to my undergraduate professors at the Pennsylvania Academy of Fine Arts (PAFA) who supported my growth as a young artist. I am grateful to **Tony Rosati, Cindy Hodgeson, Dr. Danielle Bassett,** and **Jeff Brown**, my mentors as an undergraduate student who encouraged my focus on medical illustration, despite being deep in the Fine Art world.

A heartfelt thanks to my family, especially my parents, **Bret Bennett** and **Connie Bennett,** and my grandparents, **Fred Casmay** and **Gloria Jacobs** for their unrelenting encouragement and support. Thanks to my sister, **Emily Bennett**, for a steady supply of biomedical memes.

To **Steve Goldman**, thank you for being a source of strength and support over a great distance. Your kindness, wisdom, humor, and wit is deeply cherished and very marketable.

Thanks to **Graham Johnson** of the Allen Institute for Cell Science for sharing his knowledge on workflows similar to the one developed in this project. Thanks to **Megan Riel-Mehan**, for making her tutorial and scripts for the related workflow available on her portfolio website.

Thanks to the **Association of Medical Illustration (AMI)** for providing a valuable collection of resources and fostering a network of inspiring professionals.

I would like to thank the developers of the scripts and plugins used to create this project. The OBJ Sequence Importer 2.1.0 plugin developed by **Matteo Porchedda** for **C4Dzone.com** made this method of data visualization possible. The Python script published on C4D Café, by the user **Kalugin**, was helpful for importing coordinates into Cinema 4D as a spline. A Python workflow script written by **Lasse Clausen**, called Simple Object Renamer Script, within the C4D Renamer Pack v1.1, significantly streamlined the OBJ export process.

ABBREVIATIONS

Collective Epithelial Metastasis – CEM

Epithelial-Mesenchymal Transition – EMT

Johns Hopkins Medical Institutions – JHMI

Extracellular Matrix – ECM

Glycosaminoglycan – GAG

Invasive Ductal Carcinoma – IDC

Invasive Lobular Carcinoma – ILC

Cinema 4D – C4D

Region of Interest – ROI

Time Frame of Interest – TOI

TABLE OF CONTENTS

LIST OF TABLES

LIST OF FIGURES

INTRODUCTION

Abnormal Cell Growth

Cells that make up the tissues of the body undergo regulated cycles of growth, division, maintenance, and death. Under normal conditions, cells divide when the body requires tissue growth, die when they become old or damaged, and are replaced by new cells. During cell division, a cell can acquire abnormal mutations that disrupts this cycle (Coleman 2018). Instead of undergoing programmed cell death in response to the mutation, an abnormal cell proliferates out of physiological control. This type of abnormal cell growth is called neoplasia and results in the formation of an irregular mass, or tumor (National Institutes of Health 2019).

Neoplastic tumors are either benign or malignant. Cells in a benign tumor proliferate, but do not invade surrounding tissue. Conversely, cells in a malignant tumor proliferate aggressively and breach a histological barrier called the basement membrane, and invade into surrounding tissue (National Institutes of Health 2019). A malignant tumor is also commonly referred to as cancer.

Biological Hallmarks of Cancer

Cancer represents a collection of over 100 distinct neoplastic diseases with vast diversity in tissue origin, etiological mechanisms, and clinical presentations (Coleman 2018). However, there are six biological properties true to neoplastic cells that apply to cancers. These six “hallmarks of cancer” include: 1) sustained proliferative signaling, 2) evasion of growth suppressors, 3) resistance to cell death, 4) replicative immortality, 5) induced angiogenesis, and 6) activation of invasive and metastatic behavior (Hanahan and Weinberg 2011).

Overview of Breast Cancer

Sarcoma versus Carcinoma

There are twenty-one distinct histological subtypes and four presently-identified molecular subtypes of breast cancer (American Cancer Society 2017). These subtypes of breast cancer are divided into two categories: sarcomas and carcinomas. Sarcomas are rare cancers that originate from the connective tissue component of the breast. However, most breast cancers are carcinomas, which arise from the cellular lining of the lobules and ducts of the mammary gland, called *epithelium* (American Cancer Society 2017).

Ductal versus Lobular Carcinoma

A carcinoma is classified by the location within the epithelium. Ductal carcinomas, develop in the duct wall, while lobular carcinomas develop in the lobules. Both types can present as either In Situ or Invasive (Johns Hopkins Medicine Pathology Department 2019).

I*n Situ versus Invasive Carcinoma*

In situ carcinomas grow within the ducts and lobules but do not invade past the basement membrane. Invasive carcinomas grow within the ducts and lobules and then progress to invade through the basement membrane and into the surrounding tissue (Johns Hopkins Medicine Pathology Department 2019).

In 2017, there were 266,120 new cases of invasive breast cancer diagnosed in the United States (American Cancer Society 2017). According to the Johns Hopkins Medicine Pathology Department website, “Approximately 80% of breast carcinomas

are invasive ductal carcinoma, followed by invasive lobular carcinomas which account for approximately 10-15% of cases." (Johns Hopkins Medicine Pathology Department 2019) The prevalence of invasive ductal carcinoma cases makes it a significant target for clinical research to develop new approaches to prevent and treat the disease.

Breast Cancer Metastasis

Metastasis describes the spread of invasive cancer from the primary tumor site to a distant tissue location. This poses the greatest danger for patients with breast cancer because it means that the cancer is no longer confined to one the site of origin, where it can often be surgically removed (American Cancer Society 2015). The five-year survival rate for patients with local and regional breast cancer is high, 99% and 85% respectively. However, this figure drops to 27% for patients with metastatic breast cancer (American Cancer Society 2017).

Models of Metastasis

Metastasis is a complex, multi-step process mediated by a multitude of interactions between cancer cells and their microenvironment. There is great diversity in expert views on exactly how metastasis works. Even in a general model of metastasis (**Figure 1**), experts disagreed on which processes were most important (Divoli et al. 2011). The consensus view of metastasis includes the following steps: local invasion by the primary tumor, intravasation into the blood or lymphatic system, survival in circulation, extravasation from blood or lymphatic system, survival in a new environment, and secondary metastatic colonization.

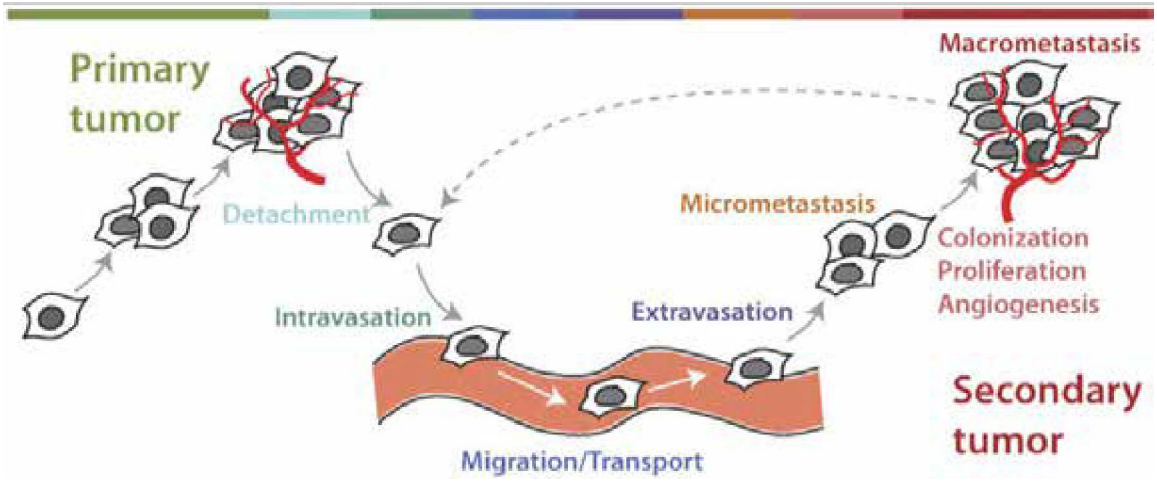

Figure 1. Consensus view of metastasis. This model Figurere includes the steps of metastasis upon which experts agree. Figure originally published in PLoS Computational Biology under a Creative Commons License (Divoli et al. 2011, figure 1). Text not intended to be read.

Collective Epithelial Metastasis Model

In the 1950's it was reported that both single and clustered tumor cells were found in blood samples from cancer patients (Watanabe 1954). It is now known that cells of many types of cancers, including epithelial cancers, can invade tissue independently or collectively (Friedl 2012). In this model of metastasis, cells rely on their adhesive connections to survive as they disseminate through tissue and circulate through the blood or lymphatic system as cell clusters (Shamir et al. 2016). This model helps to identify which cells in a tumor are the most dangerous to the patient because clusters of tumor cells were found to be more effective metastatic seeds (Cheung 2016).

Treating Breast Cancer

Over the past two centuries, treatment for invasive breast cancer has changed drastically in some ways and remained analogous in others. In 1894, William Halsted,

a surgeon at Johns Hopkins Hospital, published a procedure for the surgical removal of an invasive breast tumor. Halsted's procedure, called the radical mastectomy, remained the standard treatment for breast cancer until 1970 when a less invasive procedure was developed (Sakorafas and Safioleas 2010).

An important concept in oncology is that of tumor heterogeneity. Cancerous proliferation generates new cells that are derived from the same "parent" cell, but are also individually distinct. As the tumor grows, it amasses a complex mixture of cells with different genotypes (Turashvili 2017).

For this reason, there is no single standardized treatment plan, and great efforts have been made in clinical research to develop multiple therapeutic strategies. Technological advancements in the later decades of the 20th century enabled new treatments to gradually emerge, including radiation therapy, chemotherapy, hormone therapy, and *targeted therapy* (American Cancer Society 2015).

Targeted Therapy

Rapid advances in molecular biology, genetics, and microscopy have enabled researchers to learn more about the molecular mechanisms that drive cancer progression. Targeted therapies are drugs that are designed to target these molecular mechanisms to prevent and treat cancer (American Cancer Society 2015).

Prognostic Tests Assist Therapeutic Decision-Making

There are numerous factors that physicians take into account during therapeutic decision-making (Sparano 2018). Prognostic tests can analyze the genomic profile of a patient's tumor and indicate the presence of biomarkers,

hormone receptors, and human epidermal growth factor receptor 2 oncoproteins (Turashvili 2017). These results assist the prediction of how the individual patient's cancer will progress and respond to certain treatments (Cleator 2004).

However, there is no clinical prognostic test presently used to determine the metastatic potential of an individual patient's tumor (Weigelt et al. 2005). The need for more individualized treatment strategies relies on the discovery of prognostic biomarkers that would indicate which tumors have the highest risk of becoming metastatic (Weigelt et al. 2005). An improved understanding of the molecular mechanisms that drive the metastatic process enables both the development of targeted therapies and identification of prognostic biomarkers.

Molecular Approaches to Metastatic Breast Cancer Research

Background on Molecular Biology

In 1957, Francis Crick delivered a lecture where he asserted what is now known as the "Central Dogma" of molecular biology (Cobb 2017). The Central Dogma states that genetic material (genes) in DNA is transcribed into RNA, and finally translated by a ribosome into a particular protein. Genes govern the amino acid sequence of proteins which determines their structure and function. Proteins orchestrate many aspects of the cell, including cell-signaling, motility, structure, cell division, and apoptosis (Cooper 2016). Therefore, the expression or inhibition of certain genes has significant downstream impact on the behavior of the cell

Molecular Biology Research in the Ewald Lab

The Ewald lab is a part of the Center for Cell Dynamics at Johns Hopkins Medicine that studies the molecular conditions that cause epithelial cancer cells to

develop invasive and metastatic behavior.

The lab began with investigation into the migratory behavior of typically-stationary epithelial cells during the development of mammary ducts (see section on "Epithelial Cells" for more detail). From there, the lab investigated how epithelial cells use structural proteins and signaling molecules to build tissues like mammary ducts and mammary tumors.

Researchers in the lab use transgenic mouse models (MMTV-PyMT) that develop highly invasive mammary tumors that metastasize to the lung (Cheung, 2013). A gene is identified that encodes a protein of interest and the model can be genetically engineered to turn that gene's level of expression either "up," "down," or "off." As a result, the model develops a tumor with cells that have the specified genetic background and gene expression profile. This method enables the analysis of the roles specific genes play in regulating cell behavior in the MMTV-PyMT epithelial tumor (Shamir and Ewald 2014).

Creation of Tumor Organoids

Experimental study of mammalian tissues in real-time is considered difficult due to the tissue's inaccessibility to experimental manipulation and optical observation. The development of 3D organotypic culture methods allows mammalian tissues, including epithelium, to be visualized and studied in real time (**Figure 2**).

Additionally, 3D organotypic culture is used to observe cell behavior in MMTV-PyMT epithelial tumors (Cheung 2013). For this method, the epithelium is isolated from the primary tumor by mechanical disruption and enzymatic digestion. The resulting mass of approximately 200-1000 tumor cells is called a *tumor organoid*.

A benefit of this method is that the organoid reflects the tumor heterogeneity exhibited *in vivo*. Tumor organoids are embedded in 3D ECM gels that mimic the tumor's microenvironment *in vivo*, which enables the cells to self-assemble to both interpret and remodel the ECM during proliferation (Shamir and Ewald 2014). This model system offers the opportunity to test the effect of microenvironmental factors on the growth of the tumor organoid.

Figure 2. Time-lapse video of growing organoid. A mammary organoid embedded in a 3D matrix gel containing Matrigel. Time-lapse video shows progression of epithelial dissemination over seven days. Figure adapted from time-lapse video published under a Creative Commons License (Shamir and Ewald 2014, video 7).

Imaging with 4D Confocal Microscopy

Optical imaging of tumor organoid growth over time is challenging due to the location of the cells within a thick ECM gel (Shamir & Ewald 2014). Cellular components, such as actin, microtubules, nuclei mitochondria, membranes, and tight junctions, can be labeled with immunofluorescent markers to visualize them under a microscope. The tumor organoid's growth in the ECM gel is captured over time (approx. 48-72 hours) with confocal microscopy (Cheung 2013). The resulting time-lapse microscopy images are also referred to as *4D confocal microscopy*, because the organoid is visualized in 3D space over time, the fourth dimension.

Anatomy of the Mammary Gland

Organizational Hierarchy in Anatomy and Biology

A fundamental concept in biology is that the structure of living things can be understood as a hierarchy in both complexity and scale. The framework for understanding a complex system can be approached by either a top-down or bottom-up perspective (Novartis Foundation et al. 2001). In the human body, the body is organized into organ systems, which are made of discrete tissues further composed of a variety of cell types. The cell itself is composed of macromolecules that can be further subdivided into individual subunits units and then the atoms by which they are comprised. The organizational hierarchy within the human body, from atom to human body, spans ten orders of magnitude.

Anatomical Structure of the Mammary Gland

The structure of the mammary gland differs depending on biological sex and reproductive status. The mature mammary gland is made up of a compound branching system of ducts. In the inactive, non-lactating state, each duct branches into the tissue of the breast and terminates as a non-functional bud.

During pregnancy, the lactating mammary gland undergoes a morphological change in which the buds at the end of each branching duct become alveolar *acini*, the functional secretory unit of the gland that contains milk-producing cells. A group of acini is called a *lobule*, and a group of lobules is called a *lobe*. The gland is organized into 10-20 separate lobes that are each drained by one lactiferous duct (Kierzenbaum 2016).

Histology of the Mammary Gland

The ducts and lobules of the mammary gland are lined by a thin, cellular tissue called epithelium. The epithelial structures are supported and protected by fatty, yet highly vascular, loose connective tissue (Adriance et al. 2005). Both the epithelial and connective tissue components contain discrete cell types that play unique roles in tissue maintenance (Gartner 2017).

The epithelium is comprised of two cell types: epithelial cells and myoepithelial cells. In the most fundamental view, the mammary duct can be schematized as tube where epithelial cells form a wall around a central space called the lumen. A layer of myoepithelial cells interfaces with the basal surface of the tightly packed epithelial cells. The outer-most layer of the duct is a thin basement membrane.

Components of the Mammary Gland Epithelium

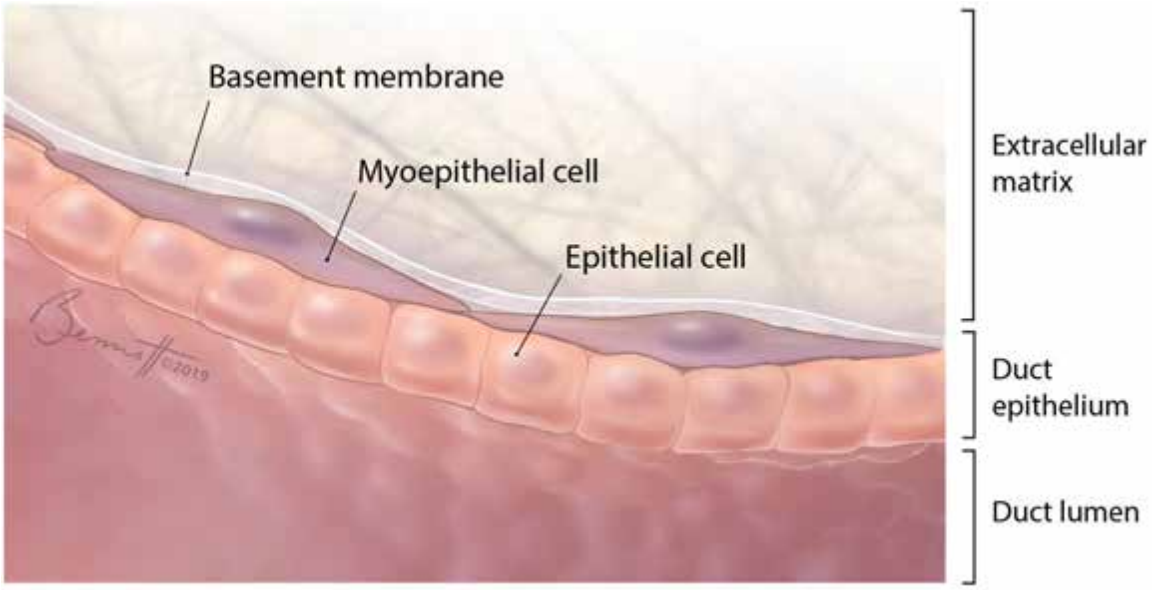

Figure 3. Components of the mammary duct epithelium. The epithelium is comprised of myoepithelial cells and cuboidal epithelial cells surrounded by a basement membrane. The epithelial cell layer separates the lumen of the duct from the extracellular matrix.

- *Epithelial Cells*

The cells of the duct wall are cuboidal epithelial cells with microvilli on their apical surface (Clearmont 2013). Epithelial cells require cell polarity, a term that refers to the asymmetric organization of their shape, structure, and cellular components. Epithelial cell polarity defines two opposing axis of the cell: an apical surface that is exposed to the lumen, and a basal surface that interacts with a basement membrane (MBInfo 2018).

Loss of cell polarity is one of the six hallmarks of cancer (Hanahan and Weinberg 2011). It is also a requirement for the Epithelial-Mesenchymal Transition (EMT), in which epithelial cells undergo biochemical changes and revert to a mesenchymal phenotype. The mesenchymal phenotype inhibits migratory behavior necessary for cells to form ducts in developing mammary glands, a process called morphogenesis. However, the activation of EMT programs after morphogenesis, initiates invasive and metastatic behavior in luminal epithelial cells (Kalluri and Weinburg 2010).

- *Myoepithelial Cells*

Myoepithelial cells are responsible for the contractile forces that assist the outward passage of milk from the ducts during lactation (Gartner 2017). Networks of actin and myosin filaments in their cytoplasm allow the cell to contract and relax (Adriance 2005). The contractile ability plays a key role in retaining the structural integrity of the epithelium during cancer progression (Sirka 2018).

Myoepithelial cells that surround the ducts are spindle shaped, and elongated along the length of the duct, while those surrounding the lobules are branched to

cover multiple cells. The extent of myoepithelial coverage is positively correlated with the amount of collagen in the extracellular environment (Nguyen-Ngoc and Ewald 2013).

- *Basement Membrane*

The basal surface of epithelial cells interfaces with a histological layer called the basement membrane. This layer is roughly 20-100 nm (0.1 µm) and best visualized with an electron microscope (Hohenester et al. 2013). The basement membrane is a layer of laminin 5 and type IV collagen that links the basal surface of epithelial cells to the extracellular matrix. Interactions between cellular receptors and proteoglycans on the cell surface anchor the basement membrane to the basal surface of the epithelial cells. The basement membrane is then anchored to the extracellular matrix of the connective tissue stroma by fibrils made of type VII and type XV collagen (Hohenester et al. 2013).

Components of the Mammary Gland Stroma

Organ tissues of the body contain functional cells and stroma, the structural part of the tissue that surrounds the epithelium. The stroma of the mammary gland contains loose connective tissue and adipose tissue. Connective tissue of the mammary gland is a network of collagen I and elastic fibers with other wandering and static cells scattered in extracellular matrix (ECM) (Gartner 2017).

The ECM contains a structural scaffolding proteins and signaling molecules that regulate cell growth, migration, and differentiation (MBInfo 2018). Due to the macromolecular composition, ground substance appears “fibrillar to granular” in electron microscopy images (Martinez-Hernandez 1977).

- *Collagen I*

The ECM's ability to resist tensile forces is due to the abundance of rigid collagen I fibers. Although the protein itself is rigid, Collagen I proteins band together to form flexible fibrils, which merge to form a collagen fiber. Collagen fibers in connective tissue range from 1-20 μm in diameter (Wang 2006). Fibers are colorless when unstained, but appear glistening white in vivo (Gartner 2017). Observation of collagen (and elastin) fibers in a carcinoma under light microscopy revealed that the fibers "may appear increased or decreased either in number or in degree of aggregation or both," (Ozzello 1970).

- *Elastic fibers*

Elastic fibers are responsible for the flexibility of connective tissue. In loose connective tissue, the fibers are long and branched (Gartner 2017). Compared to collagen fibers, elastic fibers are thinner in diameter (10–12 nm) and less abundant in the stroma. However, elastic fibers are more abundant than collagen fibers in the stroma surrounding invasive lobular and ductal carcinomas (Martinez-Hernandez 1977).

- *Fibroblasts*

These cells are responsible for synthesizing the ECM and are the most widely distributed cell type in connective tissue (Gartner 2017). Fibroblasts are either active or in a smaller, quiescent state. Active fibroblasts are found closely associated with collagen fibers, where their elongated cell body is parallel with the long axis of the fiber. The nucleus stains dark and granular, but the cytoplasm stains pale, making it difficult to distinguish from the associated collagen fiber (Gartner 2017).

Current Visuals of Breast Cancer Metastasis

Visualization Challenges

One of the challenges of visualizing metastasis is that it is a complex multi-step process that bridges scales from organ to tissue, to groups of cells, individual cells, and molecules. Another challenge is that there is a new layer of complexity to consider at every scale at each step of metastasis. The view of metastasis at the organ level might depict the anatomical or physiological complexity while on the cellular level, an entire molecular ecosystem of intracellular and microenvironmental factors drives the process. Researchers in the Ewald Lab need a better way to incorporate molecular information into structural visualizations without overwhelming the image with excessive layers of complexity.

Microscopy Imaging

The 3D time-lapse microscopy movies produced by the Ewald Lab show the complex cellular dynamics and stromal interactions that take place during proliferation, collective invasion, dissemination. In these movies, the glow of fluorescent proteins such as tdTomato and membrane eGFP visualize specific cellular structures which reveal the morphology and movement of the cell or cells (Cheung 2016). Although these movies are informative to researchers, they require additional explanation for audiences with less experience in immunofluorescent microscopy. Because only specific cellular structures are visualized against a black or minimal background, the movies lack anatomical context.

2D Illustration

A search for “cancer metastasis” on Google Images and a survey of figures in both relevant literature and conference presentations demonstrates that there are

numerous available 2D images of breast cancer metastasis. The majority of visuals are vector illustrations where graphic representations of general steps in metastasis are connected by arrows to communicate progression (**Figure 4**). In this discussion, these are referred to as *model figures*.

An informal survey was conducted to analyze the figures used during nineteen presentations at the 5th Annual Metastatic Breast Cancer conference at Johns Hopkins University School of Medicine in Baltimore, MD, on November 16th 2018. Model figures were the most commonly used visual component of these presentations, following images of data. Representation of anatomical or cellular components varies in level of sophistication; however, it is debatable whether this impacts the didactic efficacy of the image. A study by Elizabeth Rowley-Jolivet on the content of 2,048 presentations in geology, medicine, and physics quantified that an average of 59.2% of slide content was visual (figurative and graphical) (Rowley 2000). This percentage has likely increased since first published due to the ubiquity of digital media.

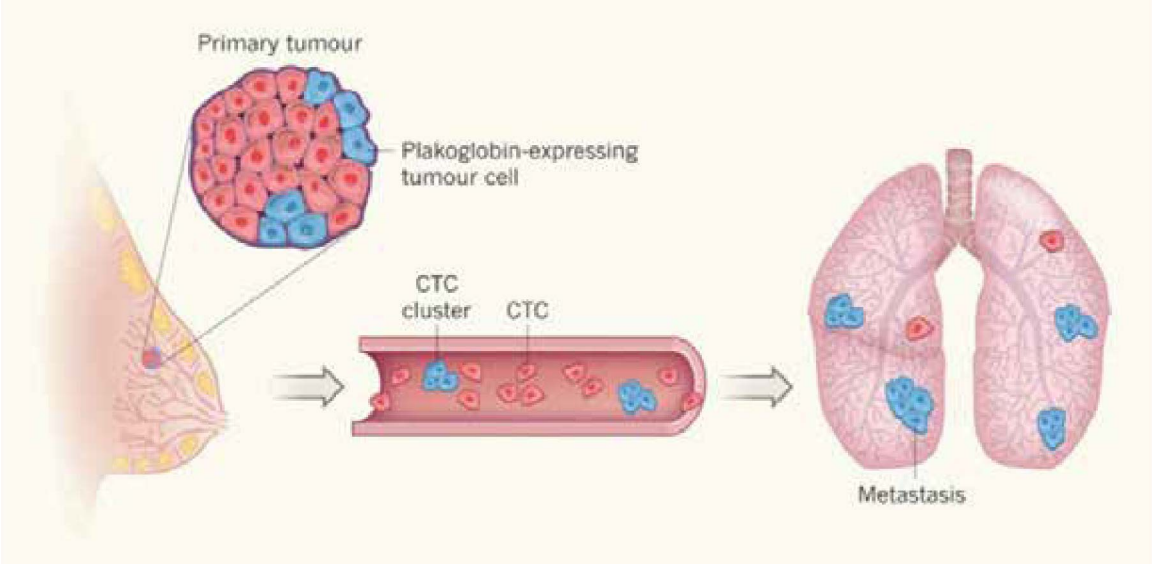

Figure 4. Example of current illustration of Circulating Tumor Cells. Reprinted from "Staying together on the road to metastasis," by A. Bottos and N. Hynes, 2014, Nature, 514(7522), 309-310. Copyright 2014, Springer Nature. Reprinted with permission. Text not intended to be read.

While 2D illustrations visuals communicate sequential steps and differences in scale, they are often limited in their scope of conceptual complexity. Model figures compress the complexity of metastasis and serve as a general overview of the process in order to represent multiple steps across a range of scales in one frame. Molecular information is rarely incorporated and anatomical context is highly schematized.

Several animated short films depict cancer metastasis and the metastatic progression of breast cancer in 2D and 3D. These animations are deployed on the web for educational purposes and either communicate broad concepts to a lay audience or more detailed cellular and molecular concepts to a medical audience. Similar to the 2D illustrations, the animations also vary in their level of technical sophistication. While animations often require more production time than illustrations, there are advantages to their use. Animations can transition between levels of scale by utilizing visual effects such as cross-fades and rapid camera zooms. Additionally, the animator can selectively incorporate or filter out visual information at any level of scale. This gives animation great power as a teaching tool for complex biological systems (Iwasa 2015).

Although there are several animated representations of breast cancer metastasis, there are currently no animated depictions of Collective Epithelial Metastasis. Present visuals of this new model of metastasis include 2D illustrations (**Figure 4**) and microscopy images. There is a need for visuals that explain the molecular and cellular basis of collective epithelial metastasis within its anatomical context to audiences who cannot independently interpret existing visuals.

Current Visualization of Time-lapse Microscopy Data

Recent advances in microscopy technology have made it possible to image the spatial relationships of moving and non-moving cells at high resolution (Chen 2014). The resulting datasets can be visualized as 3D surface meshes to more clearly demonstrate morphology, topology, and spacial relationships (Chen 2014). The field of scientific visualization shows trends towards developing workflows to visualize high-resolution 3D surface meshes of cells outside of microscopy analysis software to improve scientific communication. Workflows are currently used to create manuscript figures (Fritz-Laylin 2017), educational web modules (Visual Guide to Human Cells 2019), and for viewing in virtual reality (University of Glasgow 2016).

Although 3D surface meshes can be created from the volumetric data within microscopy analysis software, there are limited options for modifying the visual style of the 3D surface. For this reason, 3D surfaces are commonly exported from the microscopy software and imported into a sophisticated animation or sculpting program for further modification (Daly 2014). Modifications typically include the application of materials for didactic color-coding, 3D rendering with Ambient Occlusion for shading, and optimizing the surface topology. Surface topology optimization can be particularly useful for reducing polygon count, which improves display performance on the web, or for smoothing away extraneous surface noise.

While this method of 3D rendering has been used to visualize non-moving volumetric data of cells and organelles (Mindek 2018), 3D rendering *time-lapse* volumetric data in animation programs like Cinema 4D is a newly emerging method (Fritz-Laylin 2017). Python scripts have been developed to import OBJ files of cell surfaces from frames of time-lapse microscopy datasets into Cinema 4D (Reil-Mehan

2019). Presently, the animations produced by this method are used in cell biology manuscripts as figures (Fritz-Laylin 2017).

Project Objectives

This project seeks to visualize the Collective Epithelial Metastasis model of breast cancer through the following objectives:

1. Produce a short animation for a non-specialist audience that explains CEM on an anatomical, cellular, and molecular level.

2. Create a series of infographic, 3D still scenes that allows users to explore the research behind the animation through interactive insets that display more information, publication hyperlinks, diagrams, and microscopy imaging data related to that element of the scene.

3. Develop a website to display the animation and interactive infographic insets

4. Increase the level of accuracy in the 3D animation of dynamic cellular behaviors by integrating volumetric time-lapse microscopy data into the animation workflow.

Audience

The project is intended for a primary audience of non-specialists who have a vested interest in metastatic breast cancer research, such as donors, patient advocates, and healthcare professionals. These individuals have some knowledge of terminology and general concepts in metastasis, but do not have the specialized background to independently interpret immunofluorescent time-lapse microscopy of tumor cells growing in a 3D culture. This audience would benefit from a visualization

that makes the conclusions of complex research accessible, and easy to understand.

The project can also be used by a secondary audience of graduate students and post-doctoral fellows interested in a summary of current research on this topic. In the future, audiences can access the project through the Ewald Lab website and the Cancer Invasion and Metastasis Program website.

Learning Theories

A number of learning theories are useful guides for the creation of visual media that teaches complex scientific concepts. Cognitive Load theory emphasizes the distinction between a learner's working memory and long term memory (Pollock 2002). Information should be structured in a way that reduces extraneous details to reduce the cognitive load on working memory.

Use of the Completion Principle in the design of information is one strategy to reduce cognitive load on the learners working memory (Merrienboer 2003). This principle is most commonly used for teaching multi-step math problems; however, the same principle can be applied to teaching a multi-step biological process like metastasis. In the Completion Principle, the learner is first presented with the fully solved result, then elements are gradually removed so the learner fills in more and more of the information each time until they understand all steps. A progressive presentation of information enables the learner to construct a schema for the information. A schema is a cognitive construct that organizes elements of information categorically, often in a hierarchy, and stores them in long-term memory.

In this project, the Completion Principle manifests as a summary of all steps of metastasis before describing each of the steps in progressively greater detail.

Cognitive load on the working memory is reduced because the learner is able to build a schema for the concept of metastasis to which they can gradually add more complex information.

Cognitive theory of multimedia learning states that meaningful learning occurs when learners are able to make connections between corresponding visual and verbal representations in working memory (simultaneous presentation) (Mayer and Moreno 2002). For this reason, on-screen labels are frequently used, and animated events are timed to correspond with narration.

The decision to include visuals from the animation deployed secondarily as interactive infographics is based on the Information Delivery Theory. This theory suggests that multimedia learning is improved when information is presented to the learner in multiple ways (Pollock 2002).

MATERIALS AND METHODS

Software Overview

A variety of software and software plugins were employed to analyze datasets, build 3D models, animate, and composite footage. Adobe Photoshop CC 2018® was used to add text and didactic color to storyboards and composite still scenes. Imaris® from Bitplane was used to analyze volumetric time-lapse microscopy datasets and export cellular 3D surface meshes. An open source medical image processing software, 3D Slicer 4.10.1®, was used to segment a tumor and breast anatomy from a DICOM MRI datasets and export segmentations as 3D surface meshes.

Zbrush® from Pixologic was used to preform additional sculpting and texture optimization on the 3D surface meshes. MAXON Cinema 4D R20® was used to build cellular models, animate scenes, and render footage. It is important to note that the tools used to build several of the models, the Volume Builder and Volume Mesher tool, are new features in the 2019 R20 release (MAXON 2019). Cellular 3D surface meshes from Imaris were imported into Cinema 4D with an OBJ to C4D Importer plugin. Animation footage was composited in Adobe After Effects CC 2018® and the Collective Metastasis website was created with Wix® website builder.

Content Aggregation

A summary of research from the Ewald Lab from 2008 to 2018 was obtained in the form of three slide presentations (The Ewald Lab 2019). The first, entitled ‘Cellular and molecular mechanisms of breast cancer invasion and metastasis,’ (Ewald 2018) contained 301 slides. The second, ‘Molecular programs of migration, invasion, and metastasis in epithelial organs’ contained 207 slides (Ewald 2018).

The third, entitled ‘Visualizing breast cancer invasion and metastasis’ contained 138 slides. These presentations provided an overview of each experiment, the results, conclusions, microscopy movies, and brief discussions of the key findings in relation to the broad view of metastatic breast cancer. Further information on specific experiments was gathered from the associated publications.

Learning Objectives

The amount of information and images provided by Ewald Lab in the slide presentations was vast. In order to select what main concepts needed to be communicated to the specified audience, the primary research questions, experiments, and conclusions needed to be identified. To do this, a detailed outline of research topics was created from the slide presentations provided by the Ewald Lab. The most important topics were selected from the outline to be taught in narration or visualized in the animation. A list of enabling learning objectives was written to detail what knowledge a successful viewer will have gained after watching the animation (**Appendix A)**.

Script and Narration

The script was written to address the defined learning objectives (**Appendix B**). The script went through four iterative revisions before being finalized. The tone of the script was intended to best suit the knowledge level of the target audience (see Audience section for more details). Additionally, phrases were carefully chosen to convey scientific content in a general and accessible way, while remaining accurate to the current science. The script was narrated by voice talent and the audio was edited in Adobe Audition CC 2018®.

Storyboard

A storyboard was created using a combination of traditional and digital materials. Each frame was sketched with pencil on a printed storyboard template. The pages were scanned into the computer and opened in Adobe Photoshop where text and didactic color was added digitally.

The storyboard underwent three iterative revisions before being finalized. Feedback from the Principal Investigator of the Ewald lab and non-specialist viewers was incorporated into the final storyboard design.

Website Design

The Collective Metastasis website was developed with the Wix website builder following a general site map created with Draw.io online diagram software (**Figure 14**). The website was designed to contain four main pages: (1) Home, (2) Watch the Film, (3) Explore the Research, and (4) About Ewald Lab. The 'Explore the Research' section functions as an online exhibit that offers additional published information about the topics covered in the animation. Change-state hover boxes were used for interactive labeling (**Wix web editor > Add > Interactive>Hover Boxes**) and transparent video boxes were used to display 3D models (**Wix web editor > Add > Video > Transparent Video**).

Data Visualization

Datasets Utilized

Multiple 3D confocal time-series datasets were provided by The Ewald lab from which 3D cell surface meshes were exported (**Table 1**). Each dataset contained

z-stacks of multiple TIFF images captured at specified time intervals over the course of several hours, called a multi-TIFF series. Images were collected from a Solamere Technology Group spinning-disk confocal microscope with a 40× C-Apochromat LD LCI. Datasets were provided as either an Imaris Scene File (.imx), or a folder that contained the multi-TIFF series and a metadata file (.txt). Multi-TIFF series were opened in Imaris with the Imaris File Converter (**File > Batch Convert**) and saved as an Imaris Scene File for analysis.

Katarina Sirka of the Ewald Lab shared videos and Imaris Scene Files that demonstrate myoepithelial cells restraining and recapturing invasive luminal epithelial cells in a tumor organoid (**Table 1, #1**) (Sirka 2018). This dataset imaged a proliferating organoid, although the event of myoepithelial recapture was observable in one region.

Dr. Kevin Cheung, of the Fred Hutchinson Cancer Research Center shared a multi-TIFF series that captured a group of breast cancer cells collectively invading extracellular matrix in organotypic culture (**Table 1, #2**) (Cheung 2016)

#	Structures	Width x height x depth (µm)	Time points	Time interval (hh:mm:ss)	Total time (hh:mm:ss)
1	Twist1+ luminal epithelial cells, Twist1- myoepithelium	004 x 1002 x 13	158	00:20:00	12:00:00
2	Luminal epithelial cell migration during morphogenesis	247 x 228 x 26	84	00:10:00	14:00:00
3	Luminal epithelial cells	512 x 512 x 21	51	00:10:00	10:00:00

Table 1. Select microscopy datasets used in project.

Andrew Fraser of the Ewald Lab provided Imaris Scene Files that tracked the movement of a luminal epithelial cell in developing mammary epithelium during morphogenesis (**Table 1, #3**) (Ewald et al. 2012)

Data-Derived 3D Assets

External Breast Anatomy and Tumor

An anonymized DICOM dataset (BreastDx-01-0004) from the Breast-Diagnosis collection was downloaded from The Cancer Imaging Archive (Clark et al. 2013). The Breast-Diagnosis collection contains DICOM files of cases that are high-risk normals, DCIS, fibroids and lobular carcinomas. According to the Data Usage Policies and Restrictions page of the TCIA User Guide, the dataset is free to use for commercial, scientific, and educational purposes under the Creative Commons Attribution 3.0 Unported License (The Cancer Imaging Archive User Guide 2019).

The BreastDx-01-0004 dataset was selected because the tumor lesions were visibly circumscribed within the breast tissue and could be easily segmented. The Short TI Inversion Recovery (STIR) sequence was selected from the dataset folder for segmentation because the STIR imaging modality had the greatest tumor-stroma contrast since STIR nulls the signal from fat (Krinsky et al. 1996).

The sequence, "501: STIR SENSE" from the BreastDx-01-0004 dataset was imported into 3D slicer by selecting the *DCM* icon in the Load/Save panel. In the Segmentation Module, the volume "501: STIR SENSE" was selected as source geometry. A new segment was added in the **Segmentations Module**. All tumor lesions were selected as Regions of Interest (ROI) by using Renyi Entropy Threshold segmentation in the **Effects Panel**. The threshold was applied and one main tumor

mass was isolated by using the **Scissors** tool from the **Effects Panel**.

A new segment was added and renamed "External anatomy." The external anatomy was selected as Regions of Interest (ROI) by using Renyi Entropy Threshold segmentation in the Effects panel. "Export Segments to Files" was selected from the "Segmentations" drop-down menu (**Segmentations Module > Edit Selections**).

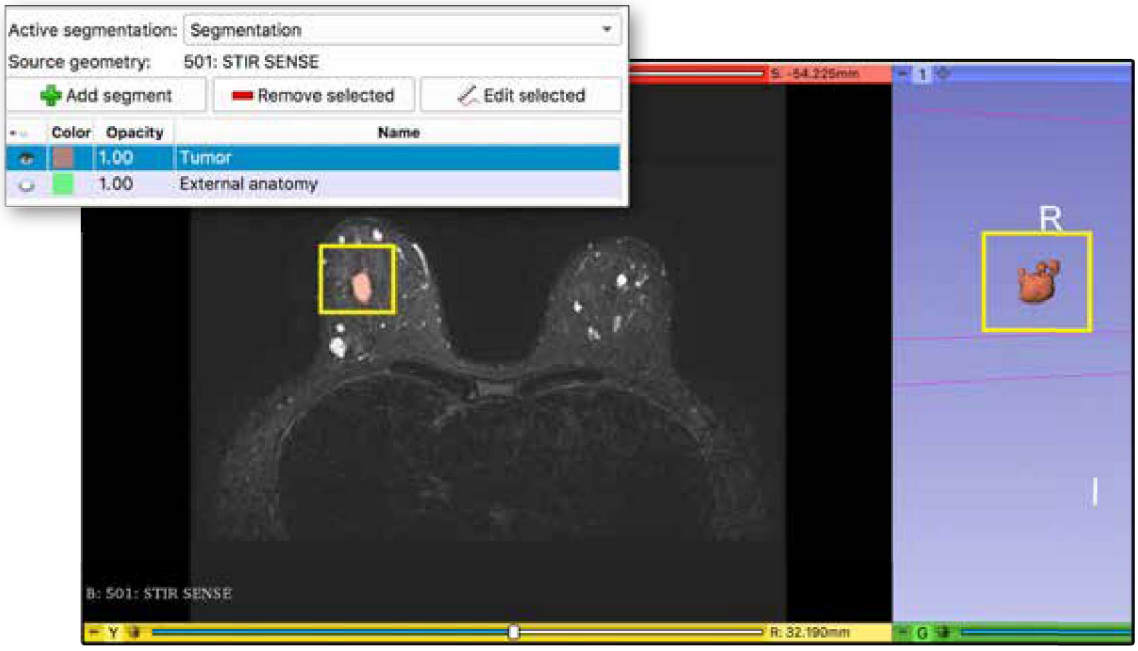

Figure 5. Segmentation in 3D Slicer. A breast tumor (pink) segmented from a Short TI Inversion Recovery (STIR) sequence and reconstructed in 3D Slicer. Text not intended to be read.

The breast anatomy was exported as an OBJ file and imported into Pixologic Zbrush (**Tool > Import**) (**Figure 6b**). In Zbrush, the breast anatomy model was appended to a standard Ztool of a female model, Julie.ztl, (**Subtool > Append**) (**Figure 6a**). The legs and head of Julie.ztl were trimmed from the torso with the **Trim Rectangle** brush to reduce polygon count. Geometry of Julie.ztl was subdivided to increase surface detail (**Geometry > Subdivide**), and the two subtools were combined (**Subtool > Merge > Merge Down**) (**Figure 6c**). Texture was refined with the **Smooth** brush to create a seamless anatomical model of a female torso (**Figure 6d**).

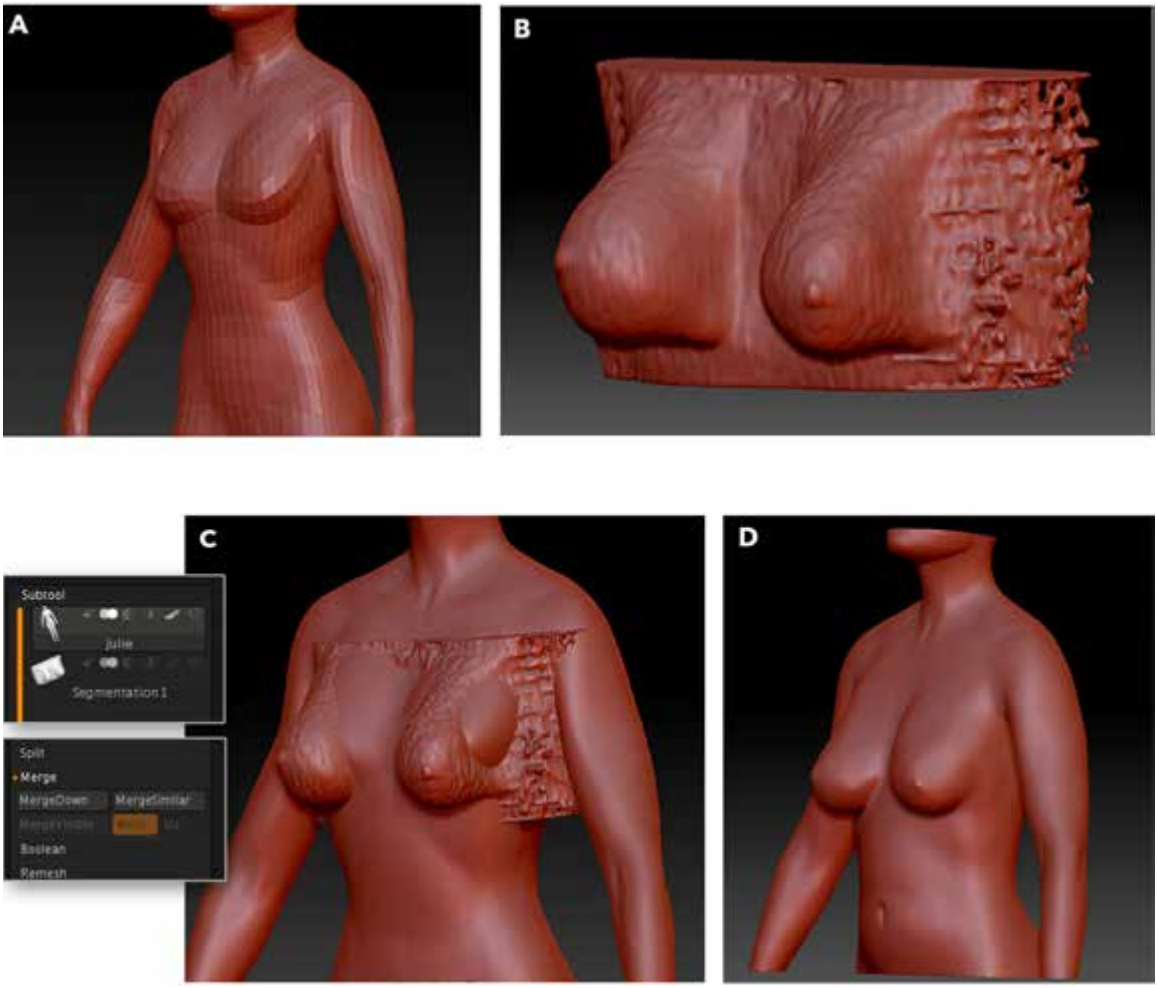

Figure 6. Combining external anatomy with a default Ztool in Zbrush. a) The standard Ztool of a female figure, Julie.ztl, with clothing subtools removed. b) OBJ file of segmented external breast anatomy. c) Merged Julie.ztl and external anatomy segmentation subtools **(Merge > Merge Down).** d) Final female external anatomy model. Text not intended to be read.

Creating Mammary Gland Ductal Tissue in Cinema 4D

A mammary gland ductal tree was created in Cinema 4D using a reference image of a wholemount virgin adult mouse mammary gland (Andrecheck et al. 2008). Mouse mammary tissue was used as a visual reference because the human mammary tissue images were not available due to their difficulty to image in whole mount and confocal microscopy. A new document was opened and a plane was placed in the (front-facing) axis. A new material was applied to the plane and the reference image (.png) was loaded into the color channel of the material to project the image onto the plane surface. The **Sketch Spline** tool was used to trace the general branching pattern shown in the reference image (**Figure 7**).

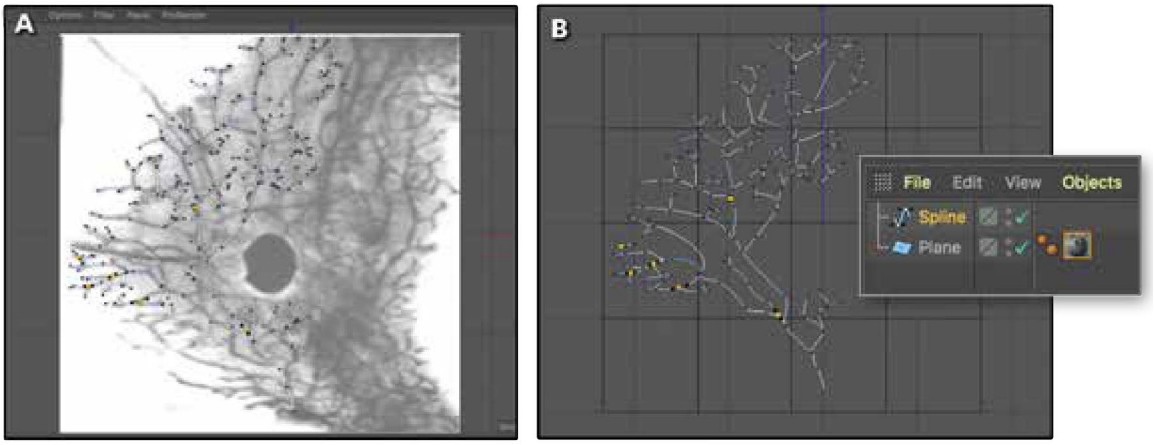

Figure 7. Creating a human mammary ductal tree in Cinema 4D. a) Branching duct structure created over a plane with reference image. The lymph node (large ovoid shape) in the image was not included in the asset. b) Plane material hidden to show spline. Text not intended to be read.

To add volume and geometry to the spline, the spline was made a child of a **Volume Builder**, and then the **Volume Builder** was made child of a **Volume Mesher**. Each branch of the resulting geometry was repositioned and rotated to create an

organic structure which branched in different directions (**Figure 8**). Branching dimensionality was created based on 3D confocal images of virgin mouse mammary tissue (Lloyd-Lewis et al. 2016).

The resulting model represented one ductal tree, while the entire mammary gland contains 18-20 ductal trees. This model was made editable, then the **Smooth** brush was used to taper the ends of the ductal branches, and the **Inflate** brush was used to sculpt the ductal buds (**Figure 9**). Finally, the object was cloned in a radial array. The resulting cloned object was duplicated three times and adjusted to appear organically dispersed (**Figure 10**).

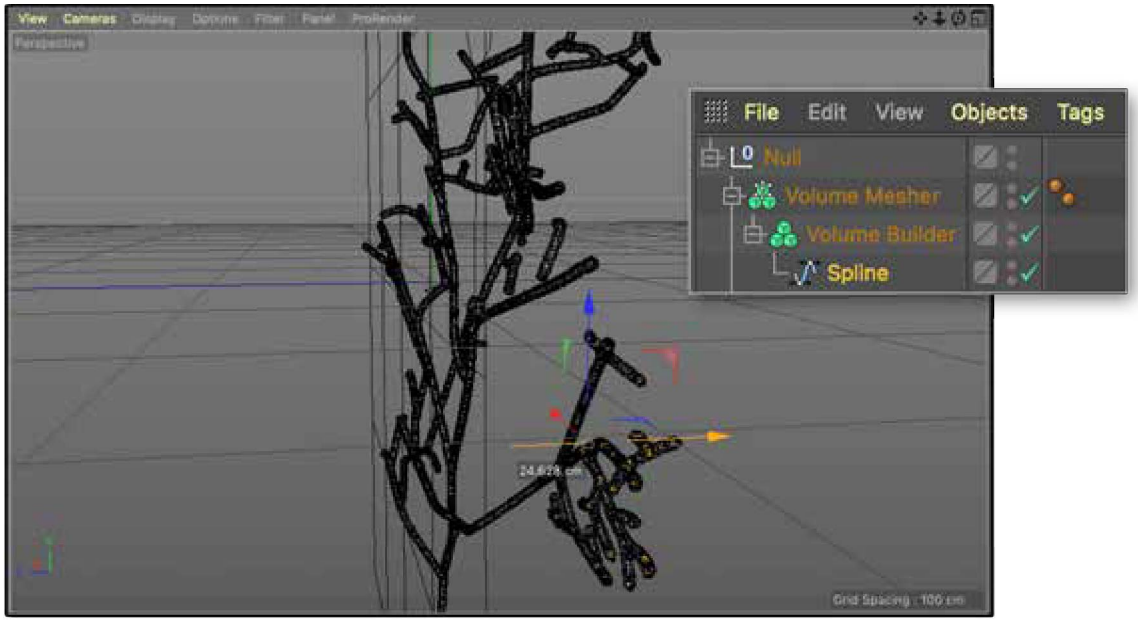

Figure 8. Creating geometry from splines. The ductal tree spline was placed as a child of a Volume Builder and nested within a Volume Mesher to create geometry from the spline. The spline was manually offset in the z-axis to mimic organic branching. Text not intended to be read.

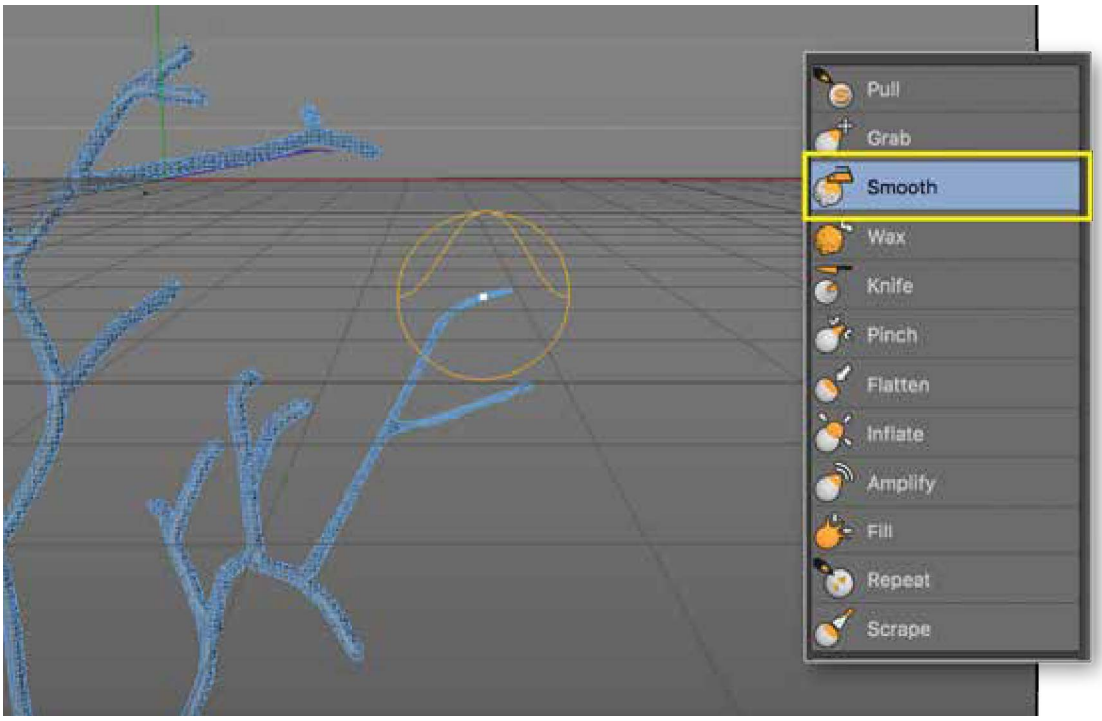

Figure 9. Sculpting duct branches. Smooth brush used to taper the ends of the ductal branches. Text not intended to be read.

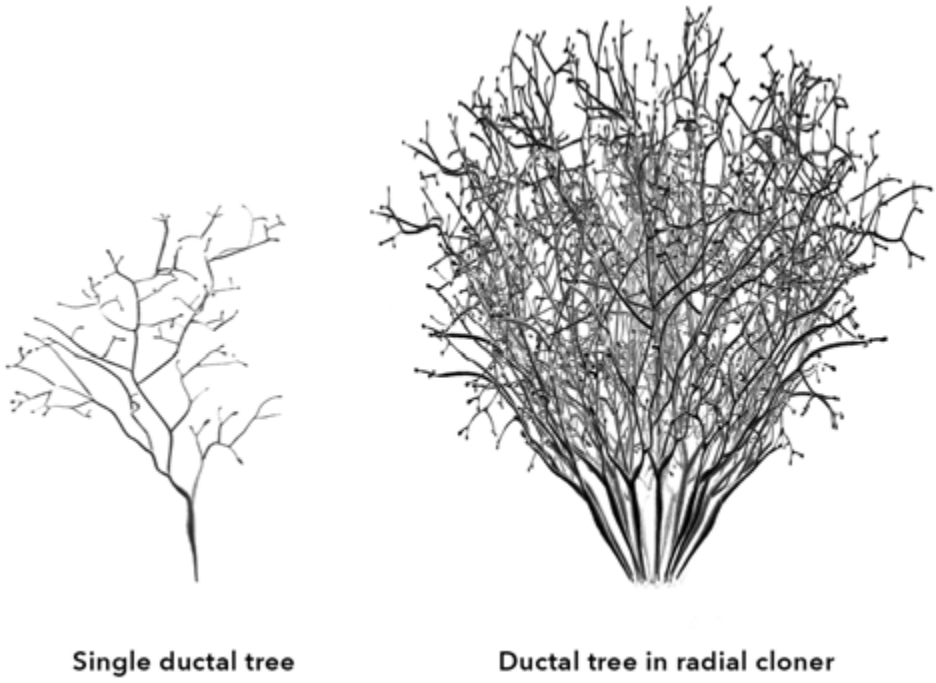

Figure 10. Creating mammary gland ductal tissue. Comparison of the modeled ductal tree before (left) and after (right) cloning and positioning into the full ductal tissue structure.

Creating a Ductal Epithelium Cross Sectional Model in Cinema 4D

A cell-level model of an intralobular duct for scene two was created with the Volume Builder and Volume Mesher. Tube objects were created with an outer and inner radius corresponding to histological measurements in **Table 2**. The tubes were made children of a Volume Builder to combine the objects as voxels. The Volume Builder was then made a child of a Volume Mesher, to create geometry from the voxels and the resulting geometry was made editable. To achieve a cellular surface texture, a **Displacer Effector** with a custom **Noise Shader** was applied to the duct object. A draw back of the **Displacer Effector** is that there is minimal control of the cross-section edges, which required a uniform cell lining for clarity. Where the duct wall is visible in cross-section, cells were separately modeled. The cells needed to appear cuboidal and tightly adherent to each other. A sphere was created with the radius of a cuboidal epithelial cell following the method in section "Creation of Cells to Scale." The sphere was made editable and sculpted with **Grab** and **Smooth** brushes in **Polygon Mode**. The resulting cell was placed in a cloner and cloned along a spline.

#	Structure	Known dimensions (µm)
1	Lactiferous duct	800 diameter
2	Intralobular duct	80 diameter
3	Terminal ductule	50-60 diameter
4	Lobe	12544 L x 7077 W
5	Lobule	1198 L x 1574 W
6	Ductal bud	512 L x 512 W x 21 D

Table 2. Dimensions of mammary histological structures measured from digital microscopy slides (Christensen 2019).

Incorporating Time-lapse Microscopy Datasets into 3D Animation

Exporting a Moving Cell Model from Imaris

The 3D time-lapse microscopy dataset, 11_04)07_Pos0_Crop.ims, was opened in Imaris in **3D View** and **Surpass Mode (Figure 10).** The dataset, comprised of 99 frames, captures luminal epithelial cells migrating during ductal morphogenesis (red channel of **Figure 10**). The movement and position of a single luminal epithelial cell (green channel of **Figure 10**) was tracked over sixteen hours. In this dataset, a 3D surface for the luminal epithelial cell had already been created by another researcher. To export a 3D surface mesh of the cell, the surface (*Surfaces 1*) was selected in the **Scene Manager** and all other objects were deselected except for the negligible *Light Source 1* (**Figure 11**).

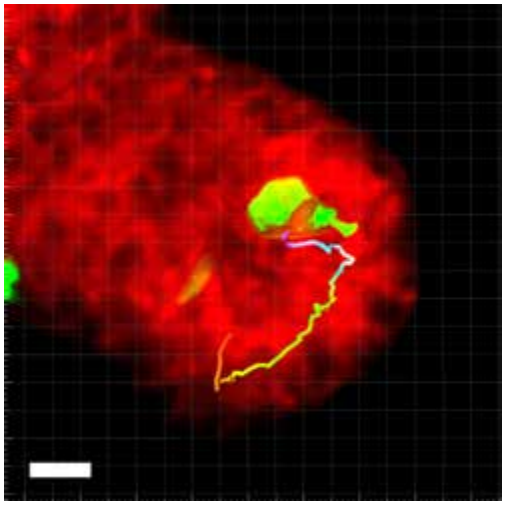

Figure 11. 3D confocal microscopy dataset of ductal morphogenesis. Imaris scene file (.ims) viewed in Imaris. Single epithelial cell in green and collective epithelial cells in red. Scale bar equals 10 µm.

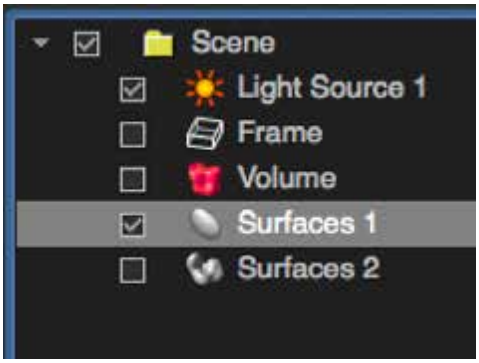

Figure 12. Selecting objects in Imaris. Surfaces 1 selected in Scene Manager to prepare for export.

A 3D surface object of *Surfaces* 1 was exported as a VRML2 file (**3Dviewer > Export selected objects**). Cinema 4D was opened and the VRML2 file was imported (**File > Open**)

Importing a VRML2 File of a Moving Cell into Cinema 4D

A VRML2 file opened in C4D contains objects in a deeply nested parent-child hierarchy in the object manager. To reorganize the object manager into a simple two-level hierarchy, the file was re-exported as an OBJ (**File > Export > Wavefront OBJ**) and the OBJ file was re-imported into C4D (**Figure 13**). When the OBJ was opened, material was set to "No Material", "Invert Transparency" was deselected, and no axes were flipped. The axis of all children was re-centered (**Select all children + Mesh > Axis center > Center axis to**).

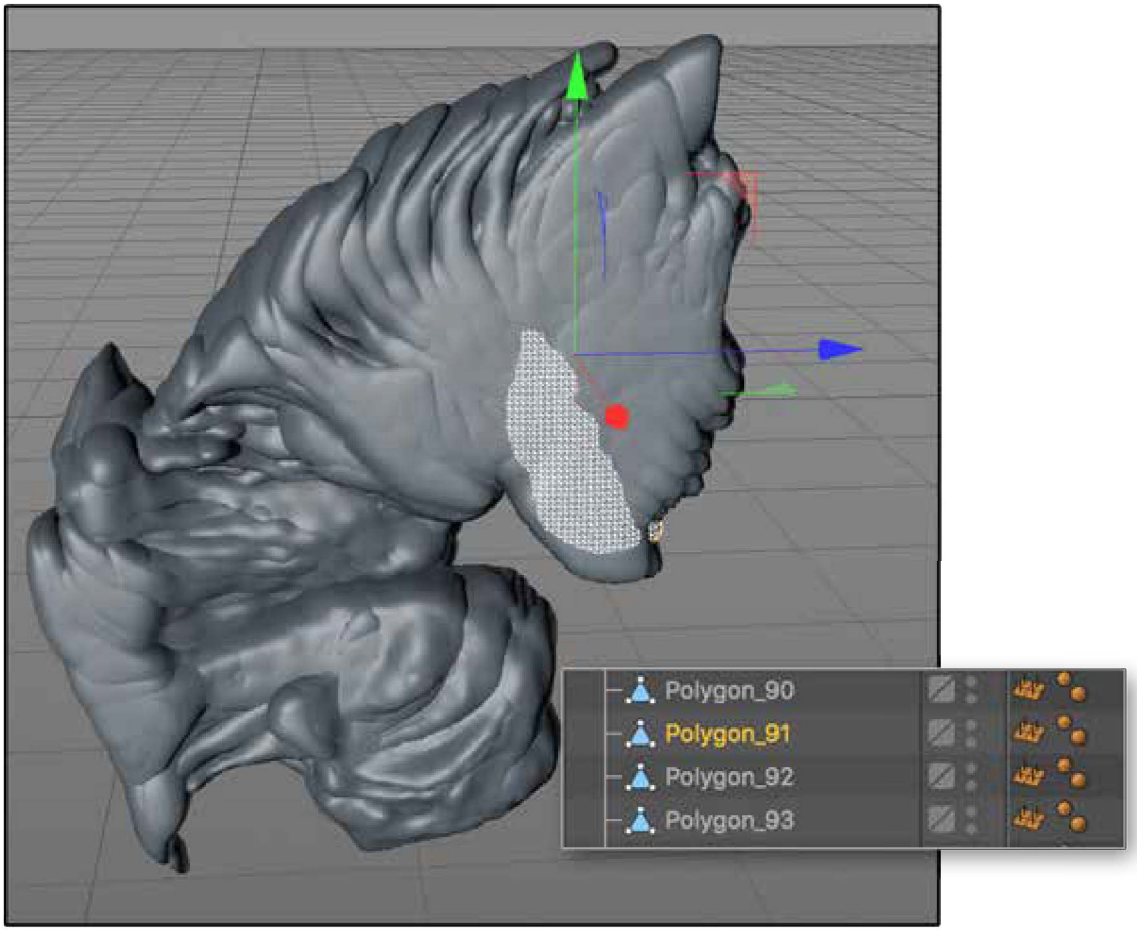

Figure 13. Result of OBJ file re-import into Cinema 4D. The OBJ file contained 95 polygon objects (inset), where each polygon object correlates to a 3D cell surface from each of the 95 frames in the time-lapse dataset. Viewport shows 95 non-moving polygon objects stacked on top of each other. Position of polygon object is retained from coordinate data in Imaris.

Re-exporting Moving Cell OBJ Files

A **Simple Object Re-namer Script**, within the C4D Re-namer Pack v1.1, was used to rename the polygon objects "Surface_1"-"Surface_96." Each object was selected, individually exported as an OBJ (**File [in the object manager] > Export selected object as... > Wavefront OBJ**), and saved to a destination folder titled "Morphogenesis_Surfaces_1-96". To expedite the process as each file was saved, all options in the export menu were kept at default. As a result, a material file (.mtl) was exported along with each OBJ file. At the end of the export process, the "Morphogenesis_Surfaces_1-96" folder contained 96 OBJ files and 96 material files

Re-importing Moving Cell OBJ Files as an Animated Sequence

Before the OBJ sequence was re-imported into C4D, an important step was performed in the computer's file manager to prepare the files to overcome a bug in one of the program's numeric sorting systems. In the folder containing the 96 OBJ files, OBJ's 1-9 were renamed using the following convention: from "Surface_1" to "Surface_001".

In a new document, the **OBJ Sequence Importer 2.1.0 plugin** was used to import the folder containing the OBJ files. In the OBJ Sequence Importer menu, the source folder, "Morphogenesis_Objs_1-96" was selected. The value for Frame Start determines on which frame in the **Animation Palette** timeline the animated sequence begins. By default, the plugin began the animated sequence on the frame number that corresponded to the number of OBJ files in the source folder. For example, when the Frame Start value was 0, and the folder contained 96 files, the animated OBJ sequence began on frame 96 of the timeline in the **Animation Palette**. To begin the

animation on frame 0, the Frame Start was set to -96. The option to "Flip z-axis" and "Flip x-axis" was selected to match the orientation of the dataset in Imaris. All other settings were left at default.

When the import was complete, the object manager contained a null group called "*Sequence Controller*" containing 96 empty polygon objects. The sequence controller was rotated 90 degrees counter-clockwise in the z-axis to match the orientation of the dataset in Imaris.

Importing a Cell Track From Imaris into Cinema 4D

To export the track that shows the trajectory of the cell, the corresponding surface (*Surfaces 1*) was first selected in the **Scene Manager**. In the **Statistics Panel**, choose the **Selection Tab**, and choose "Position" from the drop down menu that says "Area" by default. Coordinates for the locus of the cell at the current frame were displayed in the Statistics panel. Cell coordinates for the entire time-lapse were exported with the *Export Statistics on Tab Display to File* icon in the lower right corner of the Statistics Tab (**Figure 13**, yellow rectangle). The coordinates were exported and saved as a Command Separated Values (CSV) (.csv) file which can be opened in

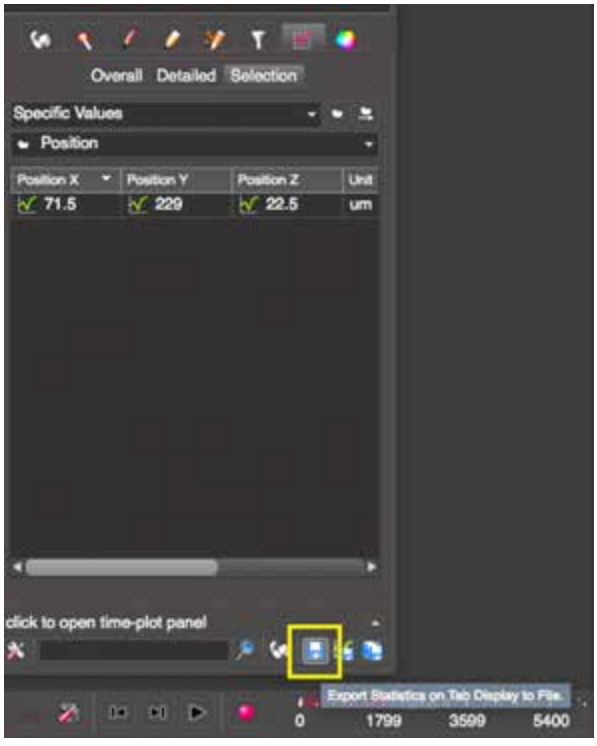

Figure 14. Imaris Statistics Panel. Yellow rectangle highlights *Export Statistics on Tab Display to File* icon. Text not intended to be read.

Excel. Non-numerical inputs in the spreadsheet were deleted (**Figure 14**) and the CSV file was saved. In the Cinema 4D document that contains the Sequence Controller, the track was imported by executing a python script, written by C4DCafe.com user, Kalugin, that creates a spline based on coordinates in a CSV file.

The resulting spline was significantly increased in scale until it matched the scale of the imported cell surfaces in the Sequence Controller. The spline was made a child of a Volume Builder, and the Volume Builder was made a child of a Volume Mesher to generate geometry for the spline, although step is not generally necessary.

	A	B	C	D
1	71.5095	228.789	22.5303	
2	71.7933	229.522	23.0102	
3	71.7098	229.613	23.1382	
4	71.7094	229.639	23.1891	
5	71.4591	229.549	23.2067	
6	69.9772	230.439	22.9471	

Figure 15. Command Separated Values file. (Left) Correct formatting of cell track coordinates in the CSV file. Columns A,B, and C correspond to axes x, y, and z, respectively.

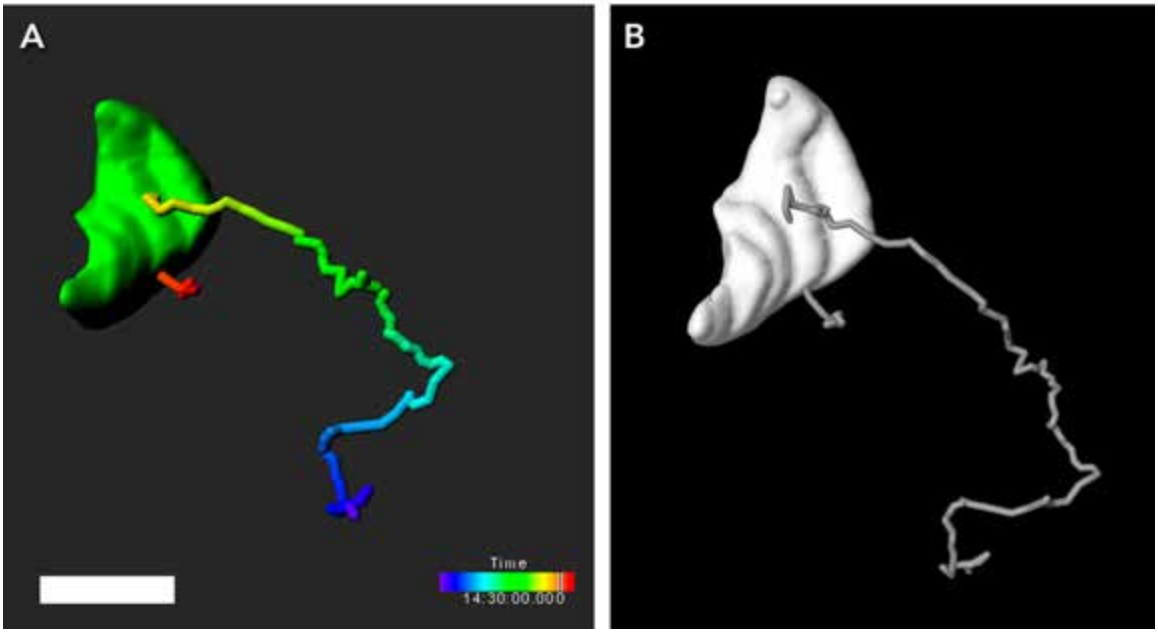

Figure 16. Comparison of Imaris scene to Cinema 4D render. (Above) A) Frame 83 of Dataset #2 showing a 3D cell surface and a corresponding position track. Scale bar equals 10 µm. Text not intended to be read. B) Result of Spline import process in Cinema 4D. Rendered with Ambient Occlusion.

Creating a 3D Surface for the Myoepithelial Recapture Dataset

The 3D time-lapse microscopy dataset, Video02_17_0629_Pos1_analyzed.ims, was opened in Imaris in **3D view** and **Surpass Mode (Figure 16).** The dataset, comprised of 158 frames, captures an invasive tumor organoid made of two cell types: myoepithelial cells, visualized in the red channel, and epithelial cells, visualized in the green channel. From frame 50-90, myoepithelial cells were observed to recapture and restrain a luminal epithelial cell invading into the surrounding matrix.

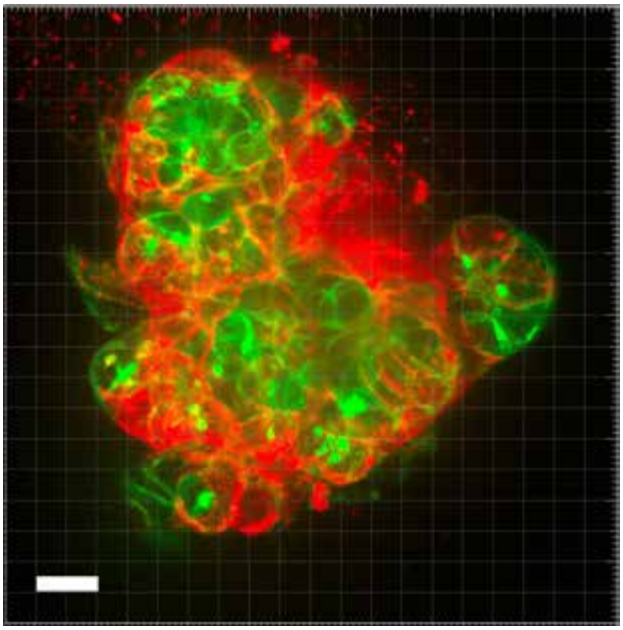

Figure 17. 3D confocal microscopy dataset of myoepithelial recapture event. Imaris scene file (.ims) viewed in Imaris. Myoepithelial cells are in red and epithelial cells are in green. Scale bar equals 100 µm.

The dataset was natively compressed in the z-axis because of the way the microscope header information was calibrated. The z-axis needed to be returned to its original geometry in order for surfaces to be created. The 3D image geometry was modified (**Edit > Image Properties**) such that the voxel size of the 3D image matched the pixel size of the microscope resolution found in a metadata file contained within the dataset folder. The pixel size in the x, y, and z planes was copied from the dataset metadata file and pasted in the respective values for voxel size (x = 0.1374 µm, y = 0.1374 µm , and z = 2.000 µm).

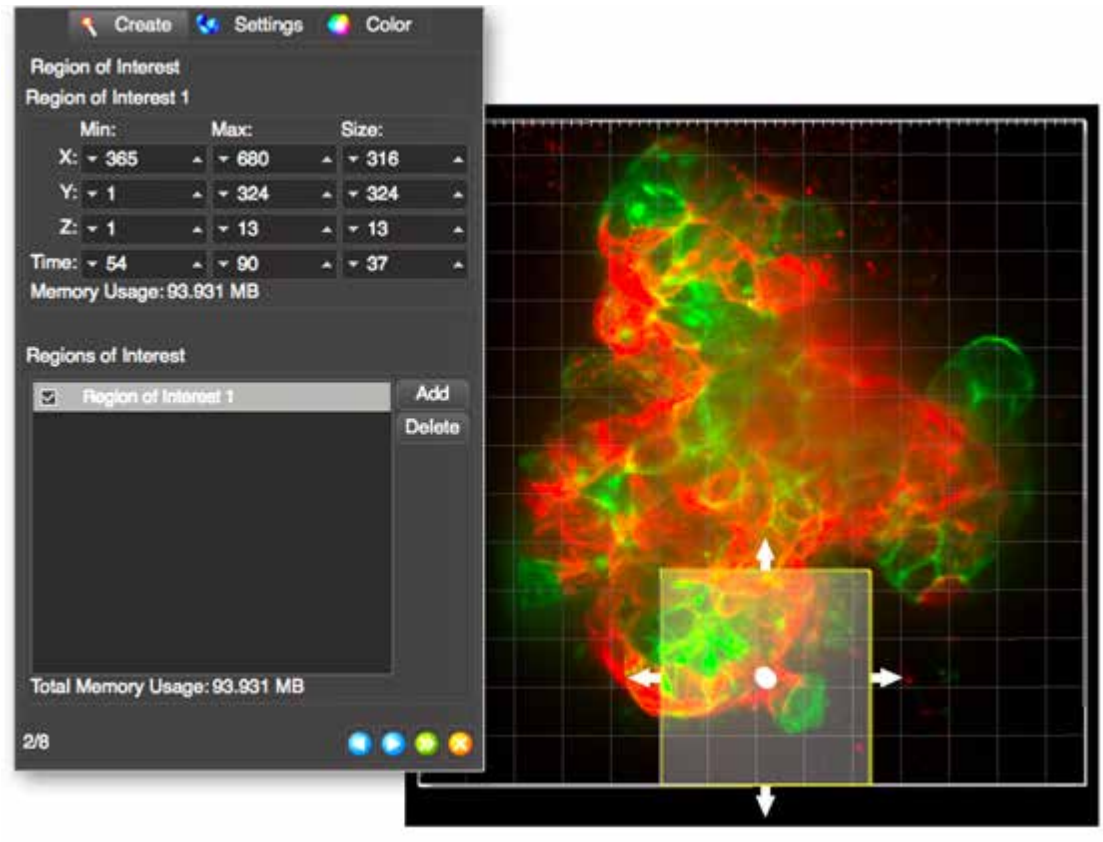

Figure 18. Selecting a Region of Interest and Time Frame of Interest. A ROI and TOI parameters were defined so the Surface Creation Wizard create surfaces only within the specified spacial and temporal region. Dataset displayed at frame 64. Text not intended to be read.

Surfaces of the two cell types were made by creating a surface for each corresponding color channel. The **Surface Creation Wizard** was initialized with the *Add New Surfaces* button in the **Surpass Tool Palette**. Algorithm settings were set to "Segment only a Region of Interest" and "Track Surfaces (over time)." The coordinates of the Region of Interest (ROI) were identified manually with the arrows in the viewport (xMin = 365, xMax = 680, yMin = 1, yMax = 324, zMin = 1, xMax = 13). The Time Frame of Interest (TOI) was input as values corresponding to the frames that capture the cellular event (time: min = 54, max = 90) (**Figure 18**).

Channel 1, the green channel visualizing epithelial cells, was selected as the source channel. With "Smooth" checked, Surfaces Detail was set to 0.850 µm. Thresholding was set to Absolute Intensity and the threshold value was manually set to 406. Surface detail and Threshold values were determined by qualitatively assessing the values required to reduce excessive noise, yet also maintain the integrity of the cell's morphology over the course of the time series.

After the wizard creates a surface for all 37 frames of Channel 1 (**Figure 19**), the same method was used to create a surface for Channel 2, the red channel that visualized myoepithelial cells. Surface Detail was set to 0.3 µm and Threshold was set to 479. A 3D surface object of the epithelial cells, *Surfaces 1*, and myoepithelial cells, *Surfaces 2*, was separately exported as two different VRML2 files (**3D viewer > Export selected objects**).

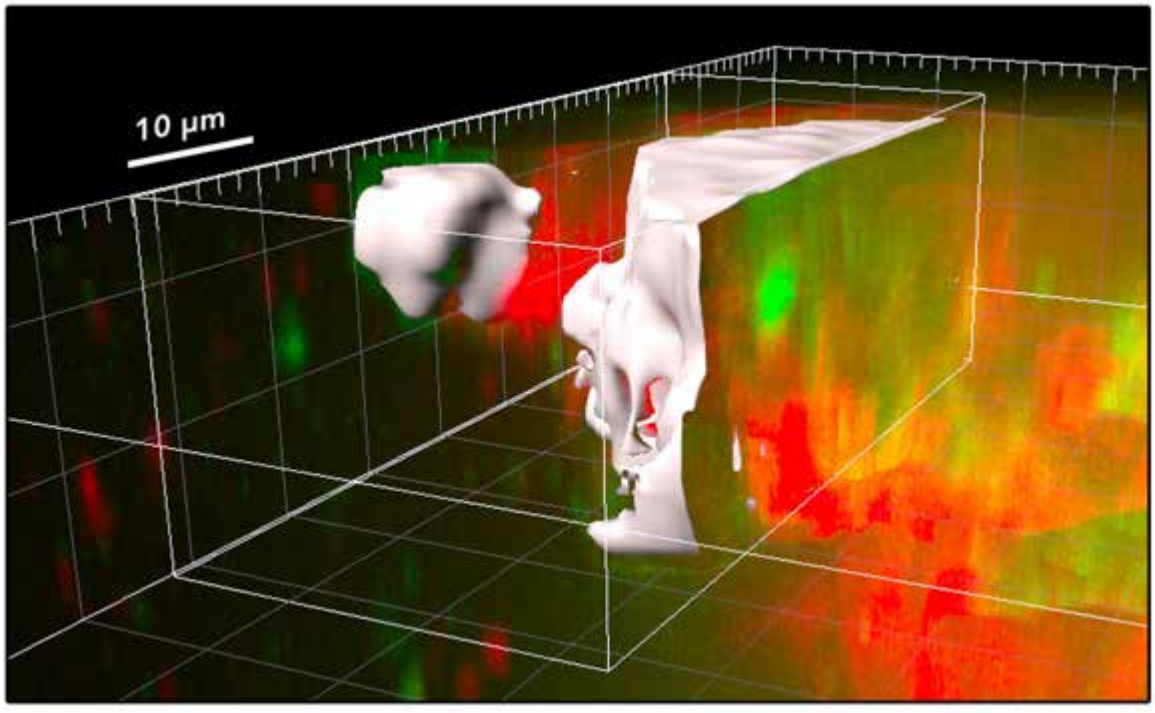

Figure 19. Creating 3D surfaces of cells in Bitplane Imaris. 3D surface created for Channel 1. Dataset displayed at frame 64 in perspective view. Scale bar equals 10 µm.

Animating the Myoepithelial Recapture Dataset

The VRML2 of the epithelial cell surface was opened in Cinema 4D (C4D). A VRML2 file opened in C4D contains objects in a deeply nested parent-child hierarchy in the object manager. To reorganize the polygon objects in the Object Manager into a simple two-level hierarchy, the file was exported as an OBJ (**File > Export > Wavefront OBJ**) and the resulting OBJ file was opened in C4D. When the OBJ was opened, material was set to "No Material", "Invert Transparency" was deselected, and no axes were flipped. The axis of all children was re-centered (**Select all + Mesh > Axis center > Center axis to**).

The OBJ file contained 174 separate polygon objects even though there were only 37 frames in the TOI, and there should have been one polygon object per 3D surface per frame. The excessive number of polygon objects was a result of two issues.

First, small fragments of the main 3D surface of the epithelial cells (generated from imperfect threshold segmentation in the **Create Surfaces** wizard) were exported in the VRML2 file as separate 3D surface objects. Therefore, the OBJ file contained multiple polygon objects that were small fragments (**Figure 20**). The small fragments were identified by selecting each polygon object in the null group, isolating it from the other polygon objects (large mass of objects in the viewport of **Figure 20**) with the **Transpose** tool, and deleting any objects that appeared small and fragmentary (**Figure 20**).

Second, during VRML2 export, frames of the time series where the 3D surface of the migratory epithelial cell had separated from the main 3D surface were also imported as separate polygon objects. These polygon objects were combined with the previous polygon object (**Right click > Connect Objects + Delete**) (**Figure 21**).

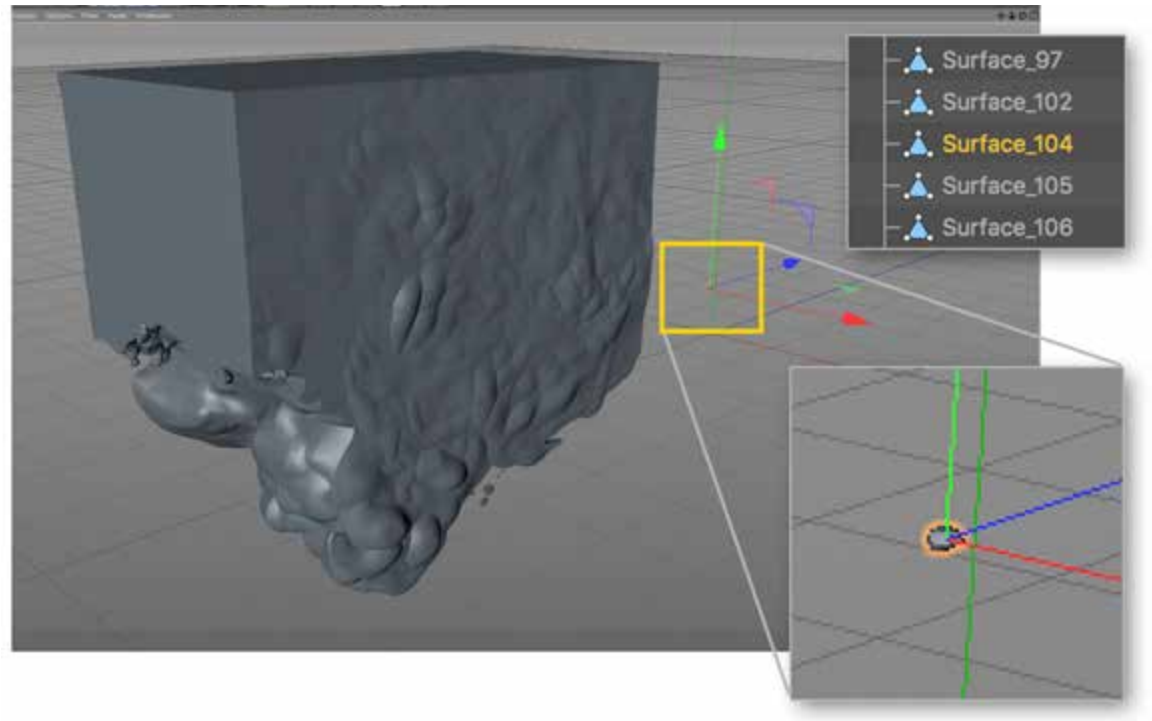

Figure 20. Deletion of stray surfaces fragments. Surface_104 was moved from its original location in the z-axis (Transpose tool) to illustrate that some surfaces in the OBJ file, like Surface_104, are fragments of the larger group of epithelial cells.

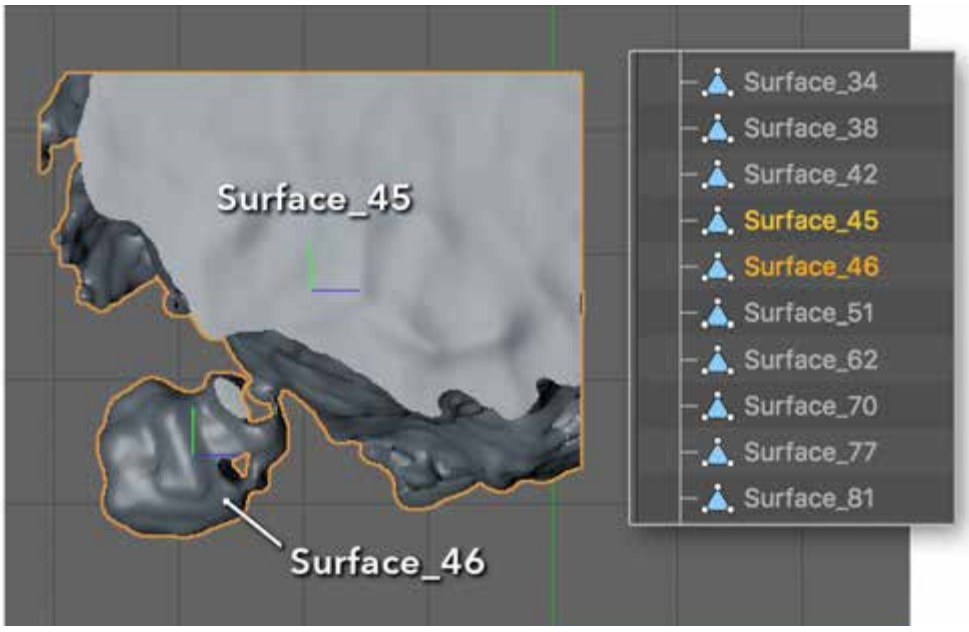

Figure 21. Combining two polygon objects on the same time-lapse frame. Two polygon objects before combination.

A **Simple Object Re-namer** script, within the C4D Re-namer Pack v1.1, was used to rename the polygon objects outside of the null "Surface_54" through "Surface_90." Each object was selected, and individually exported as an OBJ file following the same method as the (**File [in the object manager] > Export selected object as > Wavefront OBJ**), and saved to a destination folder titled "Epithelial_ Surfaces_54-90." To expedite the process as each file was saved, all options in the export menu were kept at default. As a result, a material file (.mtl) was exported along with each OBJ file. At the end of the export process, the "Epithelial_ Surfaces_54-90" folder contained 36 files.

Before the OBJ sequence was re-imported into C4D, two important steps were performed in the computer's file manager to prepare the files to overcome a bug in the OBJ Sequence Importer 2.1.0 plugin. First, the material files were deleted. Second, OBJ's 1-9 were renamed (eg. "Surface_1" to "Surface_001").

In a new document, the OBJ Sequence Importer 2.1.0 plugin was used to import the folder containing the OBJ files. In the OBJ Sequence Importer menu, the source folder, "Epithelial_Objs_54-90," was selected. The value for Frame Start determines on which frame in the **Animation Palette Timeline** the animated sequence begins. By default, the plugin began the animated sequence on the frame number that corresponded to the number of OBJ files in the source folder. For example, when the Frame Start value was 0, and the folder contained 37 files, the animated OBJ sequence began on frame 37 of the timeline in the **Animation Palette**. Frame start was set to -37. The option to "Flip y axis" and "Flip z axis" was selected because the z-axis was flipped by default when the OBJ objects were individually exported. All other settings were left at default.

When the import was complete, the object manager contained a null group

called "*Sequence Controller*" containing 73 empty "polygon objects." The sequence controller was rotated 90 degrees counter-clockwise in the z-axis to match the orientation of the dataset in Imaris. A comparison of the 3D surface in Imaris (**Figure 22a**) with the corresponding polygon object in Cinema 4D (**Figure 22b**) is shown in **Figure 22**.

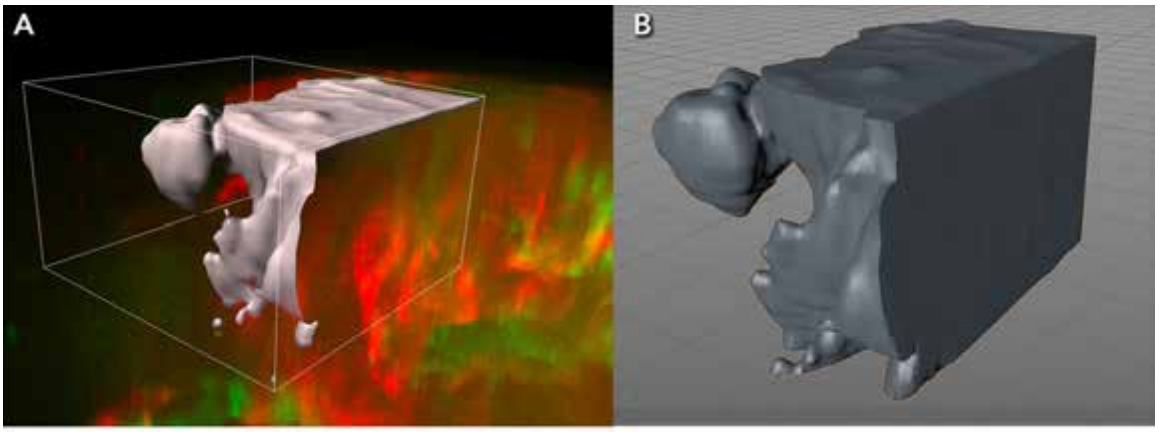

Figure 22. Comparison of Imaris 3D surface with same frame in Cinema 4D. A) Frame 63 of the epithelial cell (green channel) 3D surface created in Imaris. B) The corresponding 3D surface mesh of the same frame after OBJ sequence import.

Creating a 3D Surface for the Collective Invasion Dataset

Dataset #2 (**Table 1**), which visualizes the collective invasion of K-14+ epithelial cells, was opened in Imaris in 3D view and Surpass mode. The dataset is comprised of 51 frames, with only one channel which visualized epithelial cancer cells in red. As before, the **Surface Creation Wizard** was initialized with the "add new Surfaces" button in the **Surpass Tool Palette**. The cellular event of interest takes place across all frames and all regions of the frame, thus there was no need to crop the dataset to define a region of interest.

Channel 1, the red channel, was selected as the source channel. With "Smooth" checked, Surfaces Detail was set to 0.850 µm. Thresholding was set to

Absolute Intensity and the threshold value was manually set to 403.

After the wizard created a surface for each frame, extraneous cell debris was removed from the surface object by adding the filter, "Number of Voxels Img = 1" and setting the threshold to 9377. The new 3D surface was selected and exported as VRML2 file (.wrl) (**3D viewer > Export selected objects**).

Animating the Collective Invasion Dataset

The VRML2 file of the cell surfaces was opened in Cinema 4D (C4D) and exported as an OBJ (**File > Export > Wavefront OBJ**). The OBJ file contained 110 separate polygon objects even though there were only 51 frames in the time series. Filtering by voxel size reduced the amount of excessive polygon objects due to small fragments that exported as surfaces. There were nearly double the amount because the time series contained 2-3 surfaces per frame that were not connected to each other, and thus exported as separate surface objects in the VRML2 file. Objects that were discontinuous with the main 3D surface (showing the cellular event of interest) were deleted by selecting the Sequence Controller in model mode and selecting and deleting the discontinuous object with the **Lasso** tool in **Polygon Mode**. Further optimization of the cell surface polygon objects included use of the **Polygon Reduction** deformer and the **Smoothing** effector.

The Simple Object Re-namer Script, within the C4D Re-namer Pack v1.1, was used to rename the polygon objects according to their time series frame number in the same way as previously described. Individual polygon objects were also exported as OBJ files following the same method, but saved in a new folder. Material files were deleted from the folder and OBJ's 1-9 were renamed (eg. "Obj_1" to "Obj_001")

In a new document, the OBJ Sequence Importer 2.1.0 plugin was used to import the folder containing the 51 OBJ files. When import was complete, the object

manager contained a null group called "*Sequence Controller*" containing 51 empty polygon objects. Rotate the parent 90 degrees counter-clockwise in the z-axis to match the orientation of the dataset in Imaris.

Creating Cells to Scale

To determine the relative scale of the cells visualized in the project, a list of published measurements and average dimensions (diameter, length) of the relevant cell types was compiled (**Table 3**). General 3D models of each cell were created in Cinema 4D using sphere and cylinder objects of the same dimensions. By default, Cinema 4D measures space in centimeters. While the world scale can be changed to micrometers (**Edit > Preferences**), it was kept in centimeters because C4D processes the geometry and displacement maps better at that scale. Where dimensional data was not available, the cell volume was recorded. A formula was used to determine the radius of a sphere given the volume:

$$\text{Given volume: } r = (3\ V/4\pi)^{(1/3)}$$

The resulting radius was used to create a sphere in Cinema 4D that reflects the relative scale of the cell of interest. The sphere was futher modified with sculpt brushes, such as **Grab**, Inflate, and **Smooth**.

#	Structure	Known dimensions (µm)	Volume ($µm^3$)	Radius in C4D (cm)	Source/citation
1	Cuboidal epithelial cell	10–15 basal to apical	1010	6.22	Nandakumar 2010
2	Myoepithelial cell	~10 cell body diameter ~50 protrustions	n/a	n/a	Haaksma 2011
3	Basement membrane	0.1 µm (20–100 nm) thick	n/a	n/a	Junqueira 1992
4	Collagen I	1–20 diameter	n/a	n/a	Wang 2018
5	Fibroblast	~50 width	2,000	7.82	Christensen 2019
6	Adipocyte	n/a	600,000	24,286	Christensen 2019

Table 3. Dimensions, volumes, and calculated radius for cellular components of animation scene.

RESULTS

Novel Workflow for Importing Time-lapse Microscopy Data into Cinema 4D

A flowchart (**Figure 23**) was created to summarize the novel workflow used in the creation of this project. The flowchart is color-coded to organize the main steps: Open (document), Create, Modify, Import, and Export. Each step was written about in detail in the Materials and Methods section.

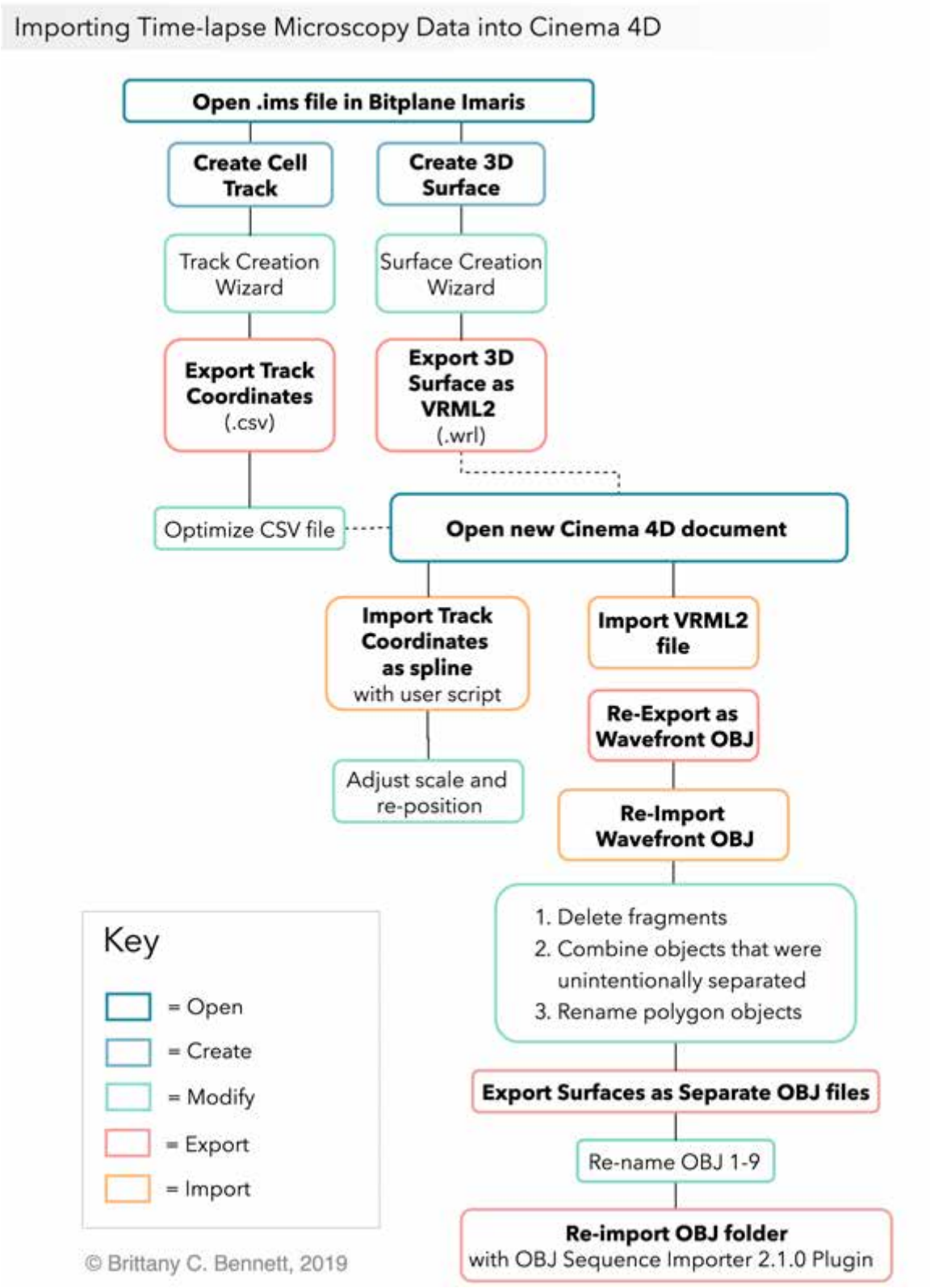

Figure 23. Workflow flowchart. Summary of Imaris-to-Cinema 4D import process.

Flowchart and Website

A flowchart (**Figure 24**) was created to map out the organizational structure of the Collective Epithelial Metastasis website. A website (**Figure 25-26**) was developed to display the animation, provide additional information, and include links to published manuscripts related to the animation content.

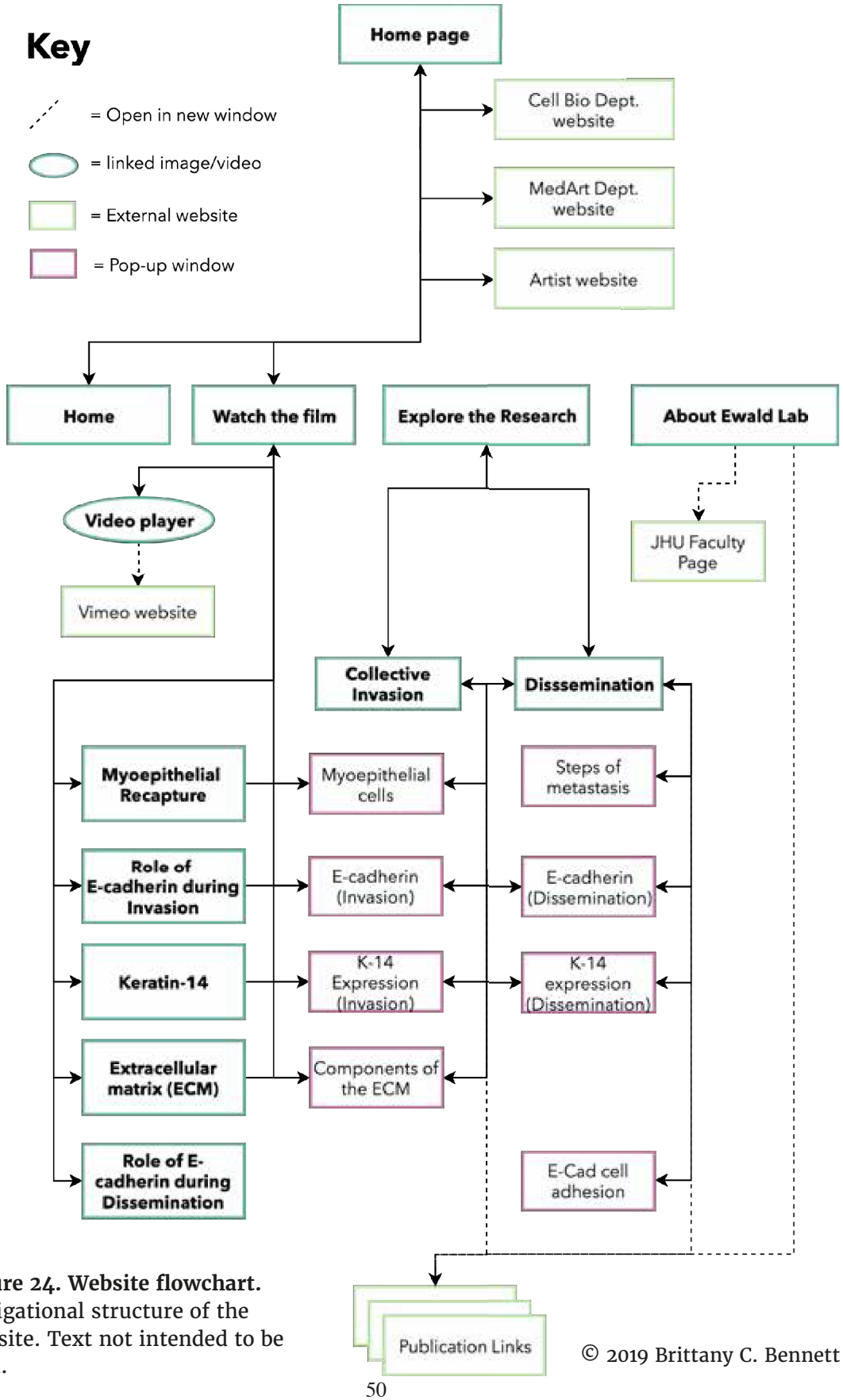

Figure 24. Website flowchart. Navigational structure of the website. Text not intended to be read.

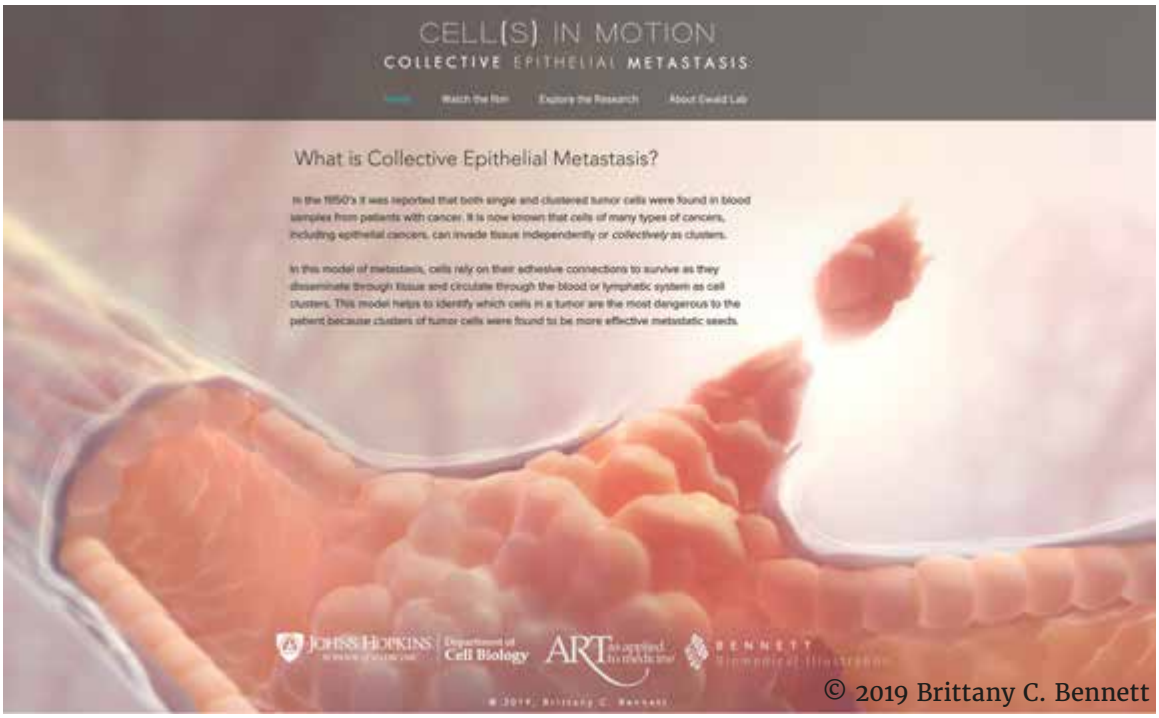

Figure 25. Website homepage. Homepage of the website demonstrating fonts and color palette. Background image composited in Adobe Photoshop from scene built in Cinema 4D. Text not intended to be read.

Figure 26. Website "Watch the Film" page. Page of the website that includes the animation video player and "Learn More" section with additional information and links to related publications. Text not intended to be read.

Collective Epithelial Metastasis Animation Storyboard

Learning objectives (**Appendix A**), a script (**Appendix B**), and twenty-four page partial-color storyboard (**Figures 27.1-27.22**) were created to teach these concepts in an appropriate level of detail. The animation teaches the role of two proteins, E-cadherin and Keratin-14, during collective invasion and dissemination.

Shot numbers 17 and 18 (**Figure 27.8**) were selected to be animated based on two time-lapse microscopy datasets. Shot 17 was animated based on dataset #1 (**Table 1**), and Shot 18 was animated based on dataset #2 (**Table 1**).

Video: Small tumor organoid proliferating slowly and migrating.

Audio: Music plays (minimal, but engages curiosity)

Video: Translucent generalized anatomical model rotates slowly to lateral view of breast. Mammary gland simultaneously fades in. Tumor glows red.

Audio: "Which cells in a breast tumor…"

Figure 27.1. Animation storyboards 1–2.

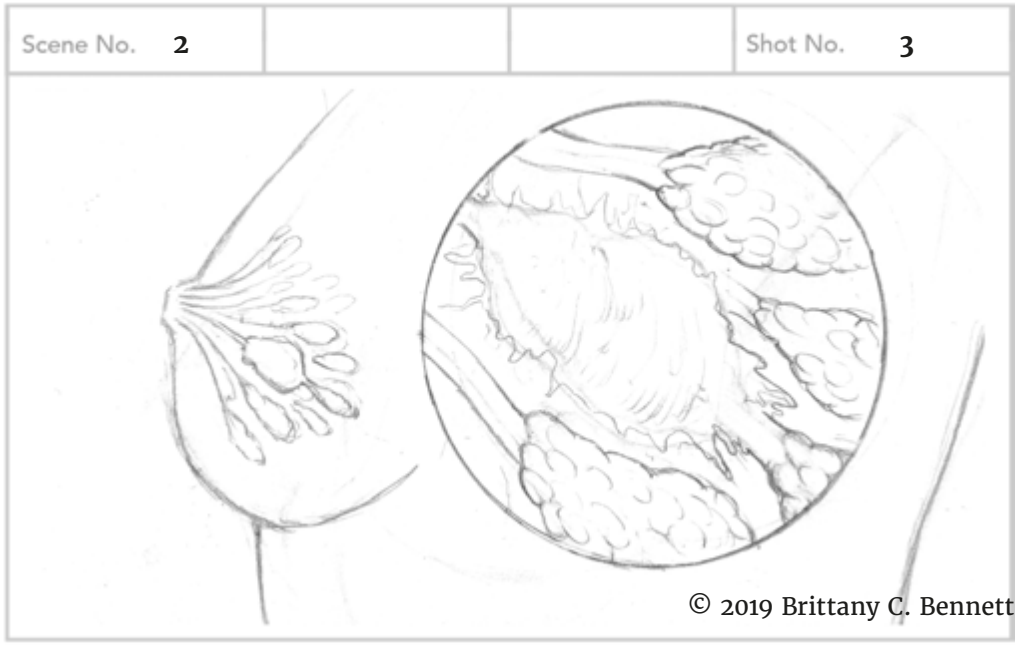

Video: Circular inset appears and magnifies tumor, then camera zooms into the inset which takes full screen.

Audio: "...are the most dangerous to the patient?"

Video: Inset takes full screen then background blurs. On-screen text: "Metastasis"

Audio: "The most dangerous cells are those that enable metastasis..."

Figure 27.2. Animation storyboards 3-4.

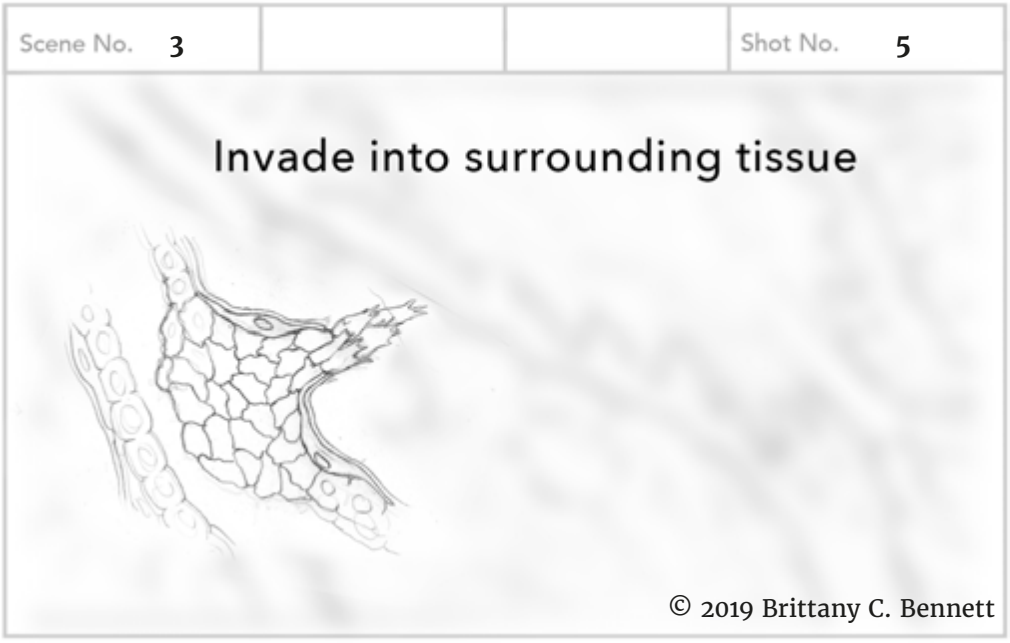

Video: Schematic appears, cells break through basement membrane and invade.

Audio: "A process in which cancer cells invade into the surrounding tissue…"

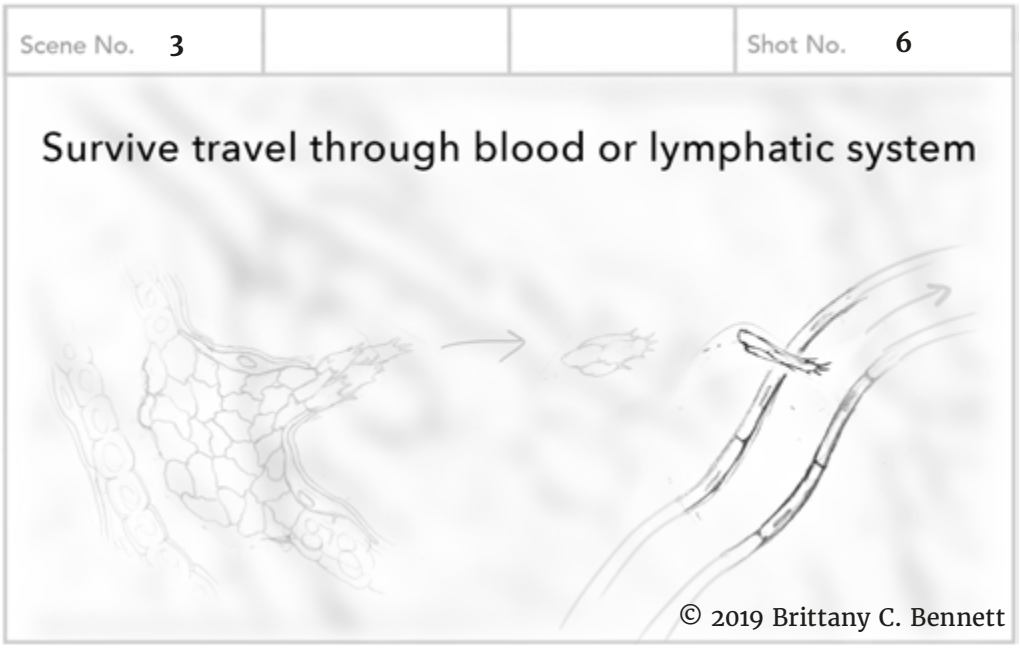

Video: Schematic cell cluster disseminates accross screen, enters vessel, and travels out of scene.

Audio: "…and survive as they travel through the blood or lymphatic system…"

Figure 27.3. Animation storyboards 5-6.

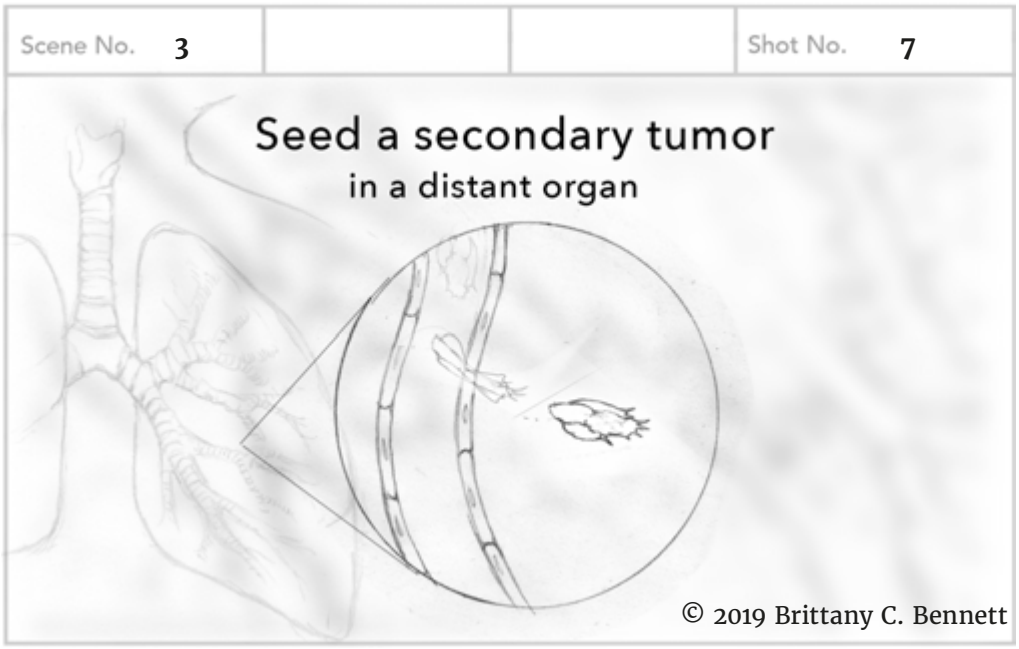

Video: Schematic lung appears, then circular inset appears and magnifies extravasation. Color scheme shifts to indicadte another organ environment.

Audio: "...to seed a secondary tumor..."

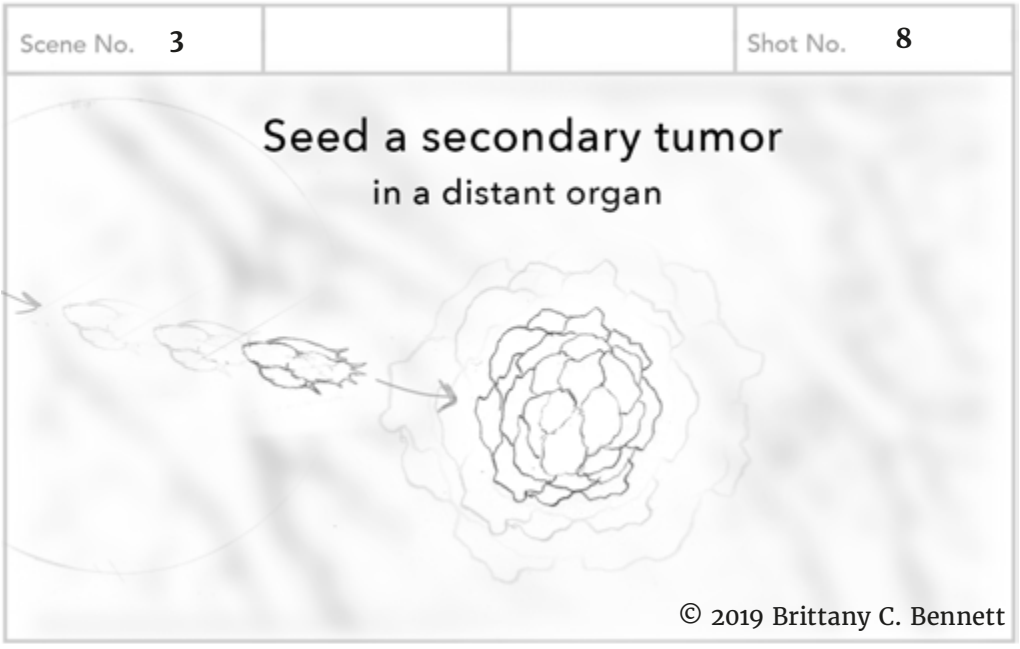

Video: Cluster disseminates tpo center of scene and proliferates into tumor.

Audio: "... in a distant organ. A deeper understanding of the mechanisms that drive dangerous cell behaviors enables scientists to develop new therapies to prevent and treat metastasis."

Figure 27.3. Animation storyboards 7-8.

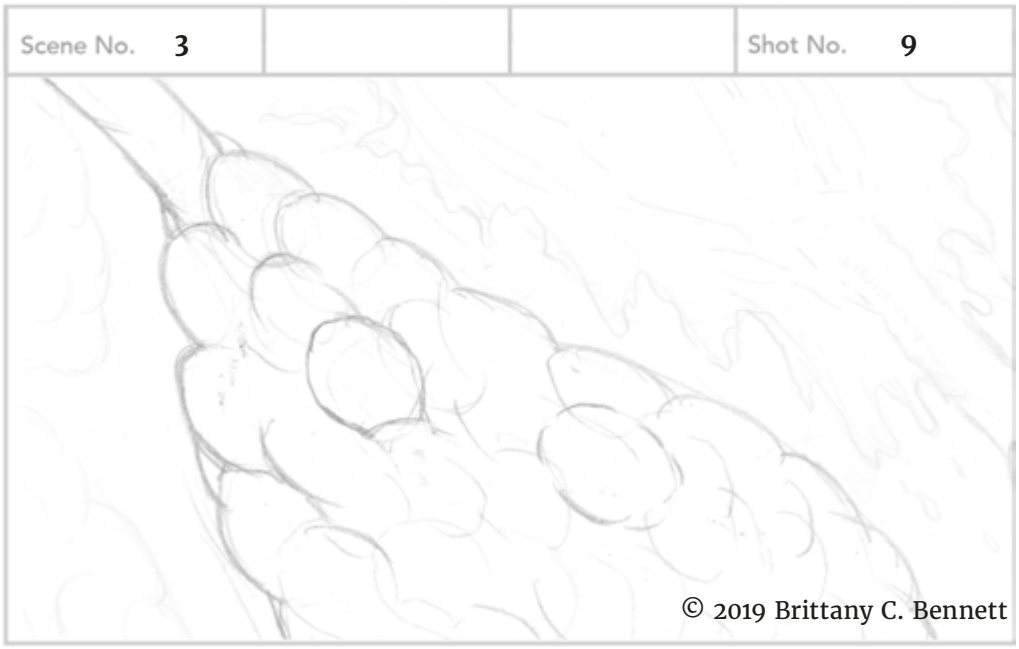

Video: Scene unblurs. Background lobes fade out as camera zooms in on the hero lobe
Audio: "Most breast cancers arise from cells that line the..."

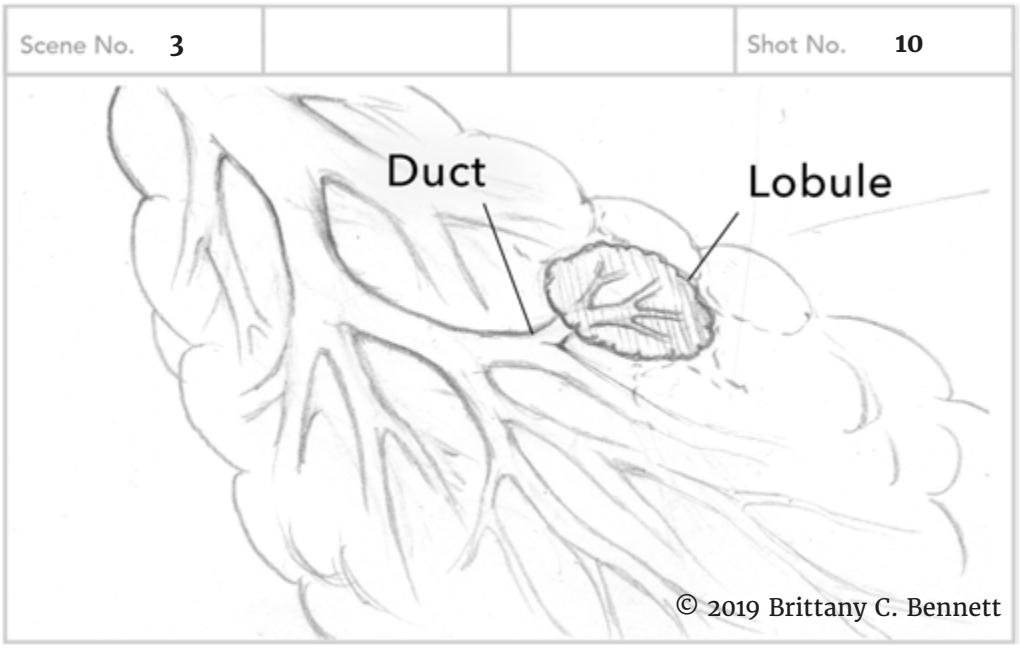

Video: Slow pan accross ducts. Duct and lobule labeled on screen.
Audio: "...ducts and lobules of the mammary gland..." **subtle woosh sound with transition to next scene**

Figure 27.4. Animation storyboards 9-10.

Video: Camera skims backwards along the surface of the duct epithelium. Fibroblast and collagen fibers in the background out of focus.

Audio: "...called the Epithelium."

Video: With camera fully zoomed out. Half cross-section cut of duct appears with "made of" narration cue.

Audio: "Mammary duct epithelium is made of..."

Figure 27.5. Animation storyboards 11-12.

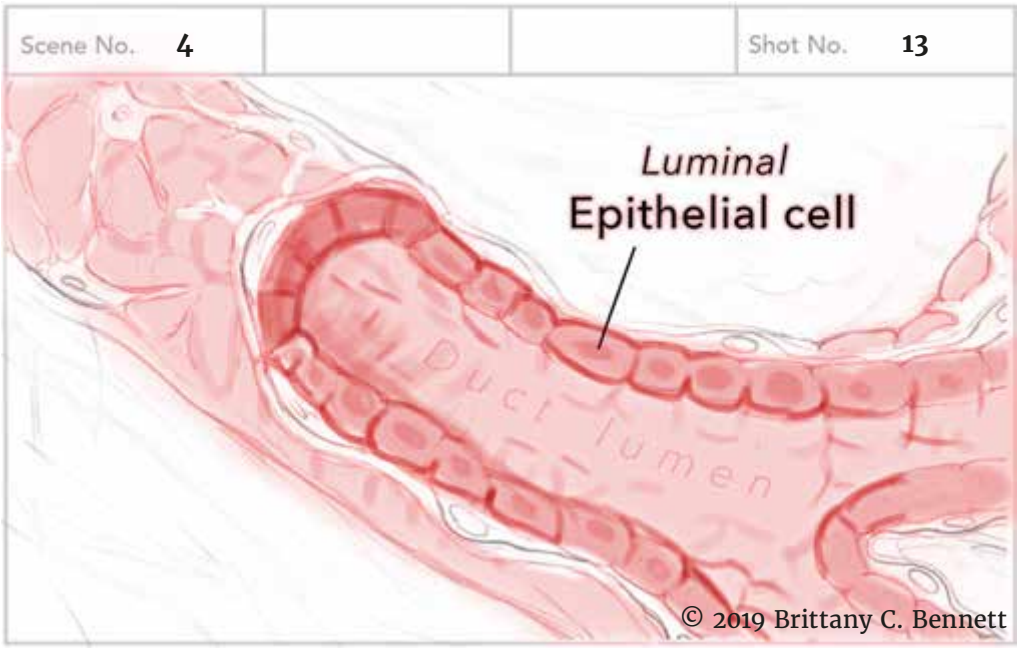

Video: Label luminal epithelial cell. Epithelial cells glow red. Basement membrane and myoepithelial cells turn low-opacity and low-saturation.

Audio: "...luminal epithelial cells,..."

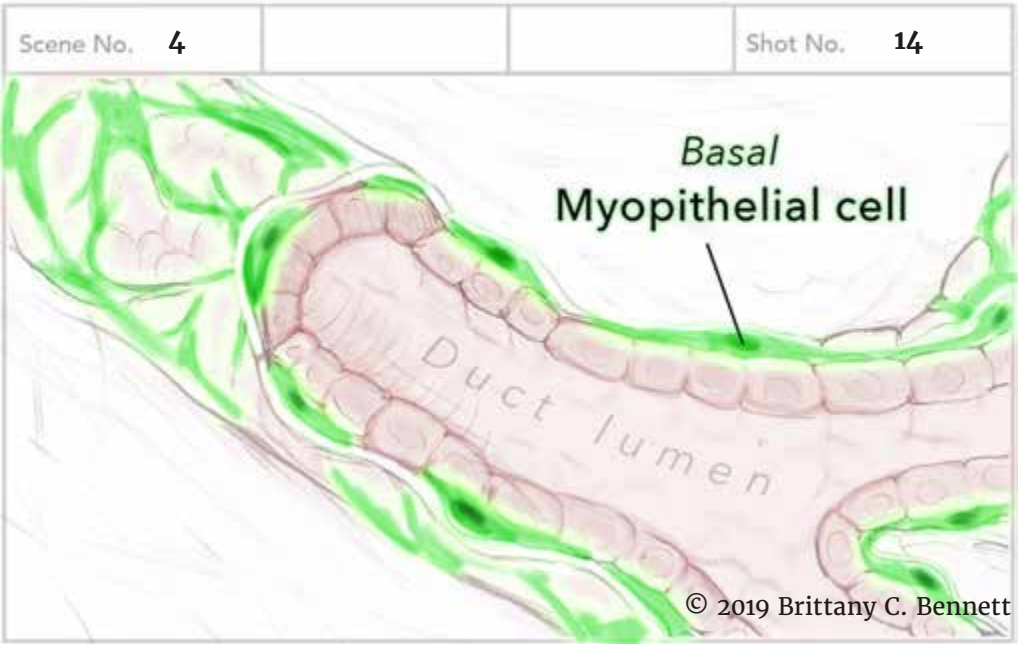

Video: Label basal myoepithelial cell. Myoepithelial cells glow green.

Audio: "...basal myoepithelial cells,..."

Figure 27.6. Animation storyboards 13-14.

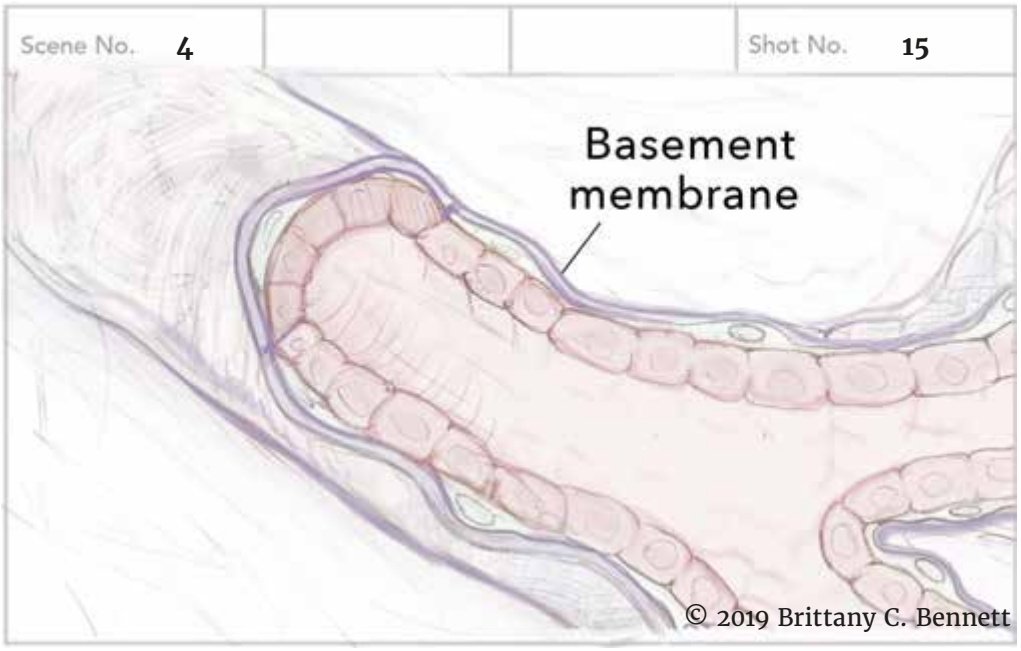

Video: Label basement membrane. BM opacity intensifies then returns to normal.

Audio: "...surrounded by a basement membrane."

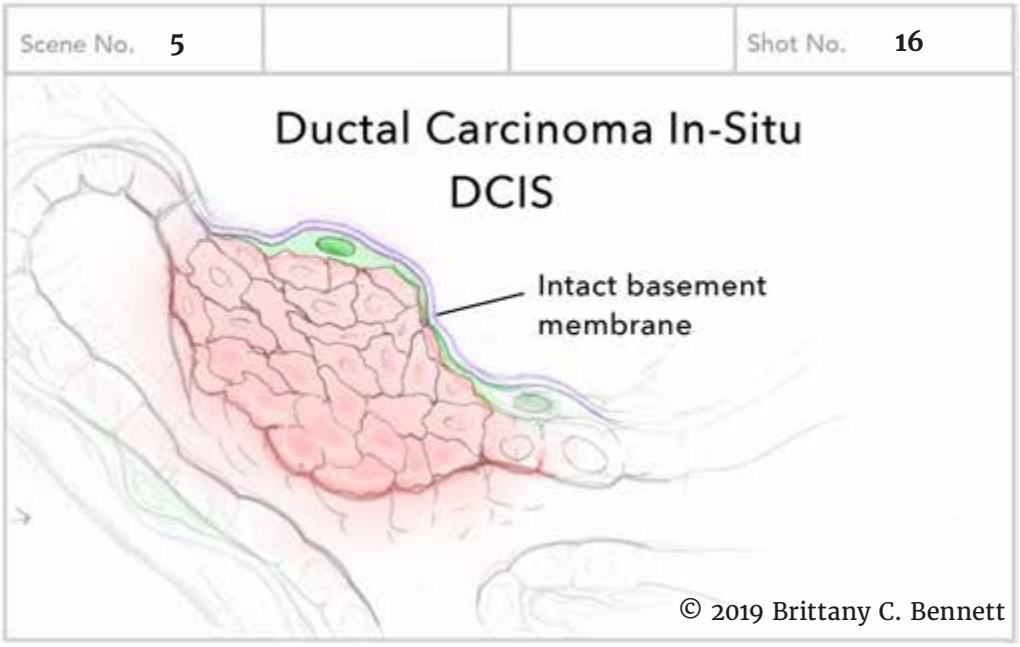

Video: Majority of previous scene fades, slight zoom in on duct. Selective blur and color intensity used as focal device. On screen text: DCIS, then label basement membrane.

Audio: "When luminal epithelial cells proliferate into the duct, but do not penetrate the basement membrane, this is called Ductal Carcinoma In Situ."

Figure 27.7. Animation storyboards 15-16.

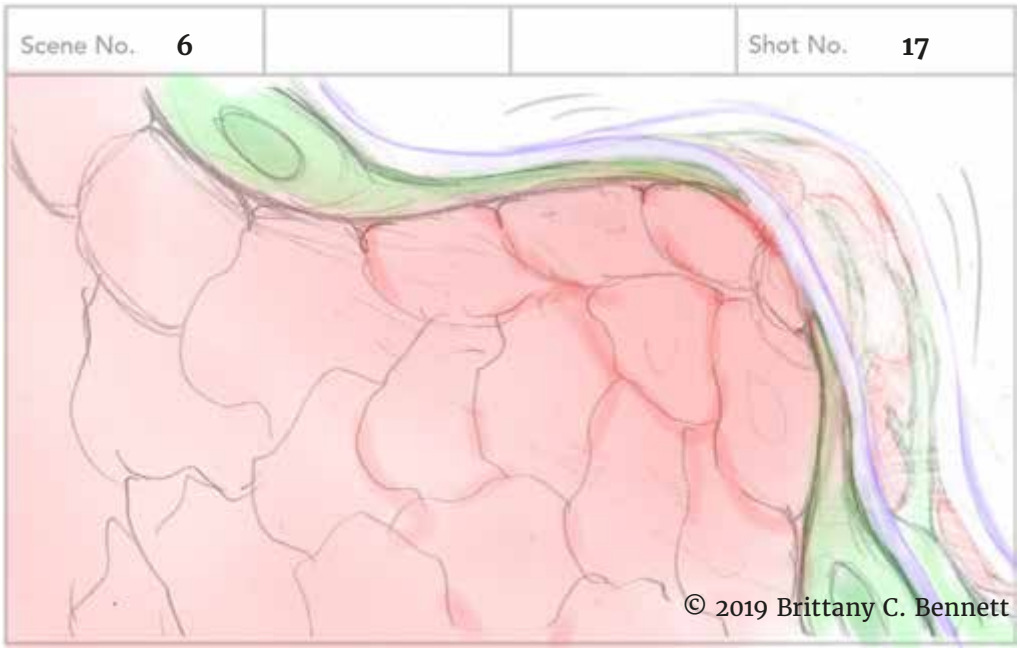

Video: Myoepithelial cells try to re-capture the luminal cells, but it eventually breaks through basement membrane.

Audio: "During cancer progression, myoepithelial cells can contract to restrain and re-capture luminal cancer cells..."

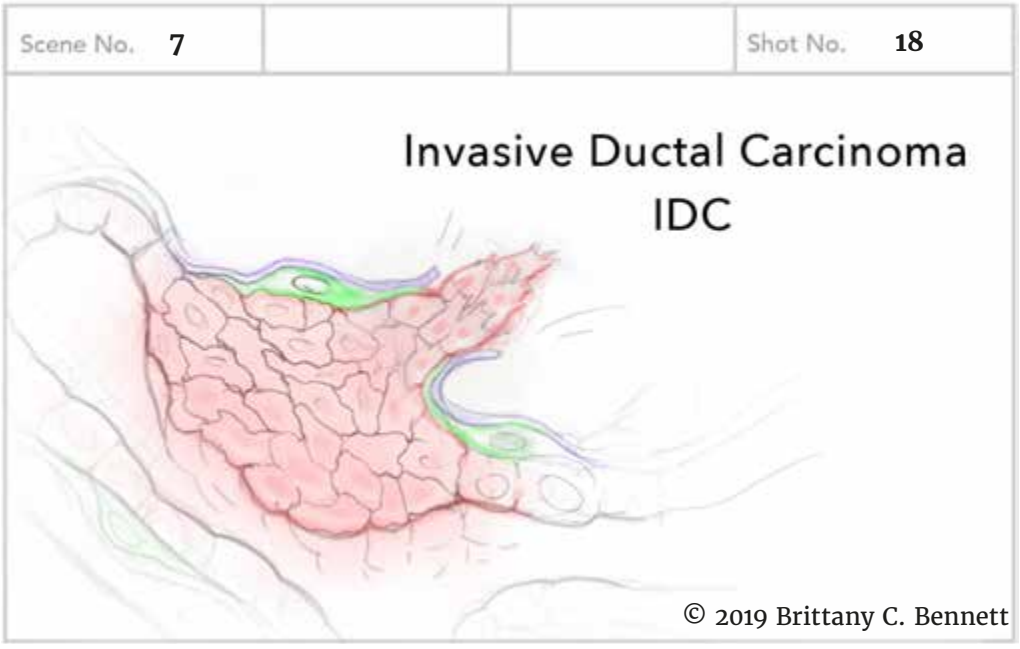

Video: Majority of previous scene fades, slight zoom in on duct. Zoom far above. 3D scene becomes schematic outline.

Audio: "...but if they penetrate the basement membrane, the tumor becomes Invasive Ductal Carcinoma, a malignant tumor that can become metastatic." Music shifts tone.

Figure 27.8. Animation storyboards 17-18.

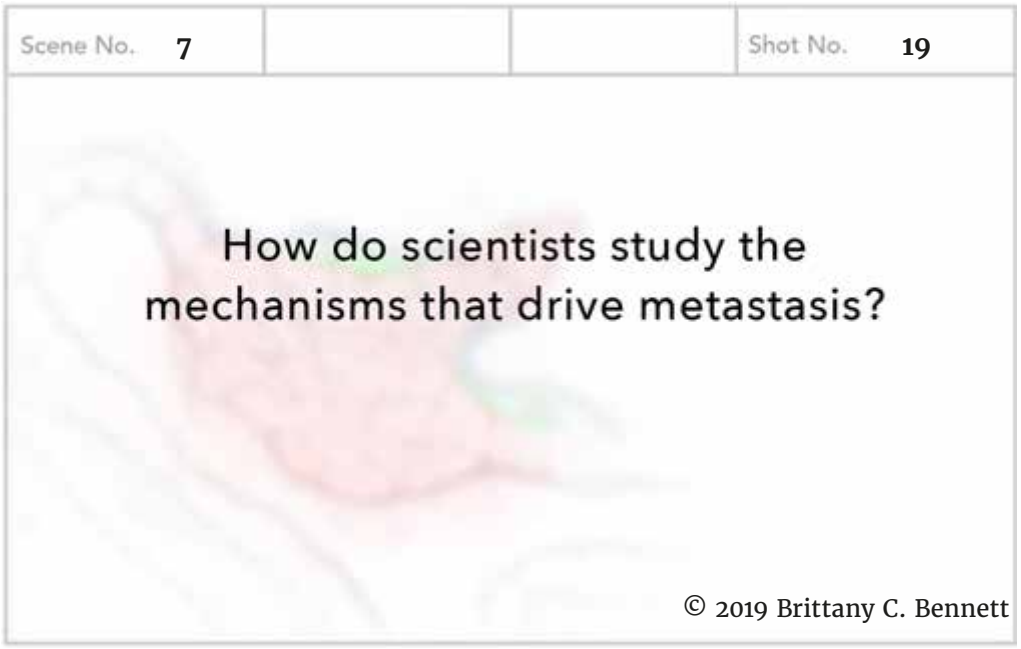

Video: Previous scene blurs. On-screen text appears.

Audio: "...and seeds a distant organ."

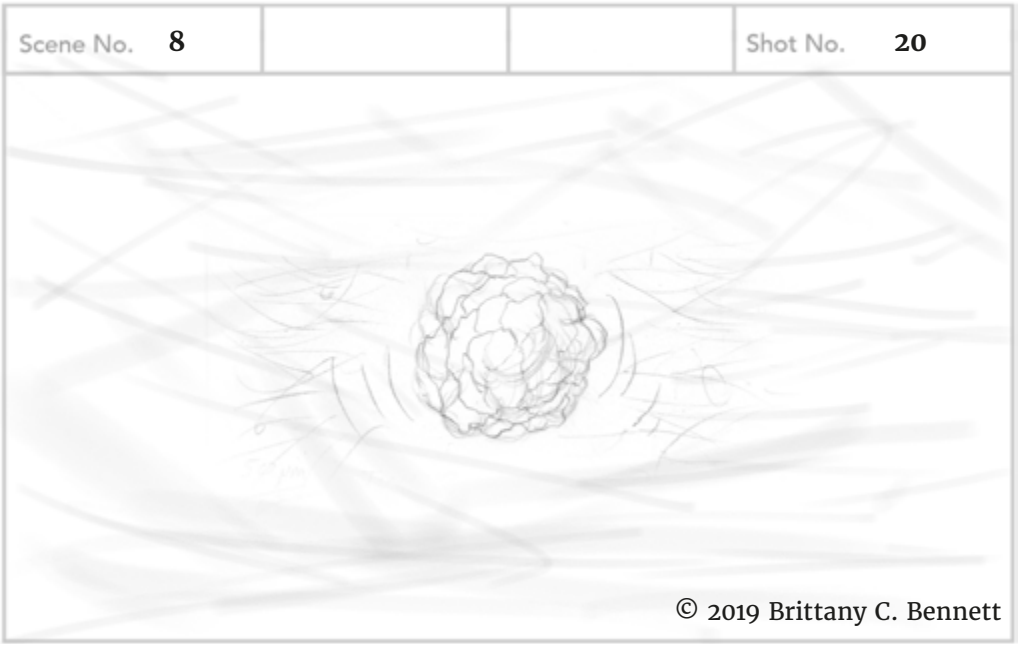

Video: Previous scene fades, this scene fades in. Growing tumor now in center of shot. Collagen fibers come into view.

Audio: "Scientists use a novel combination of genetics,..."

Figure 27.9. Animation storyboards 19-20.

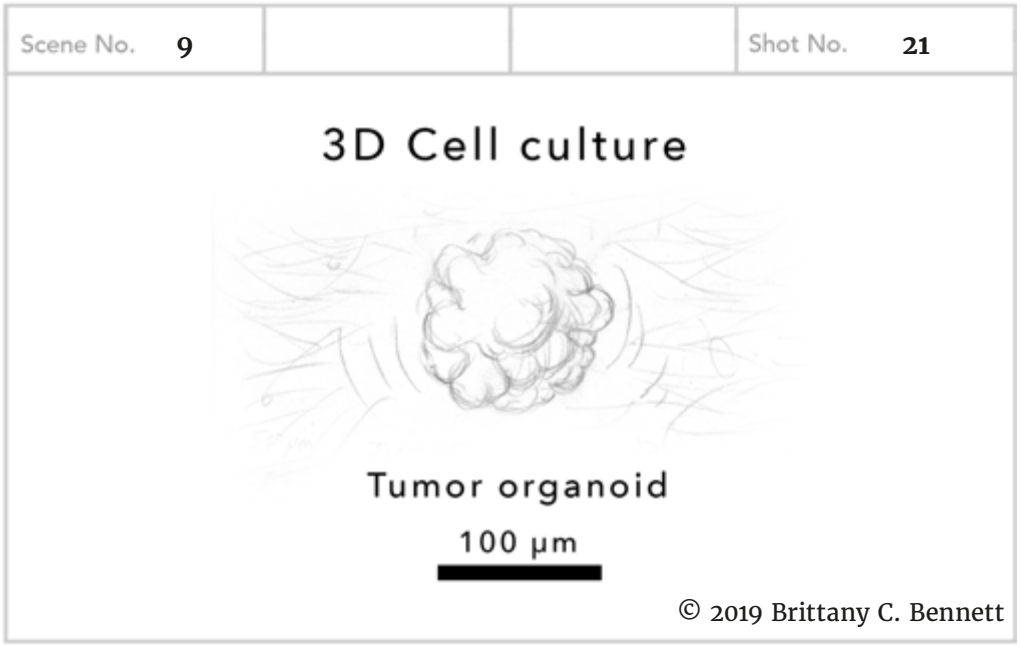

Video: Previous scene zooms out, this scene fades in and cells proliferate.

Audio: "...3D cell culture..."

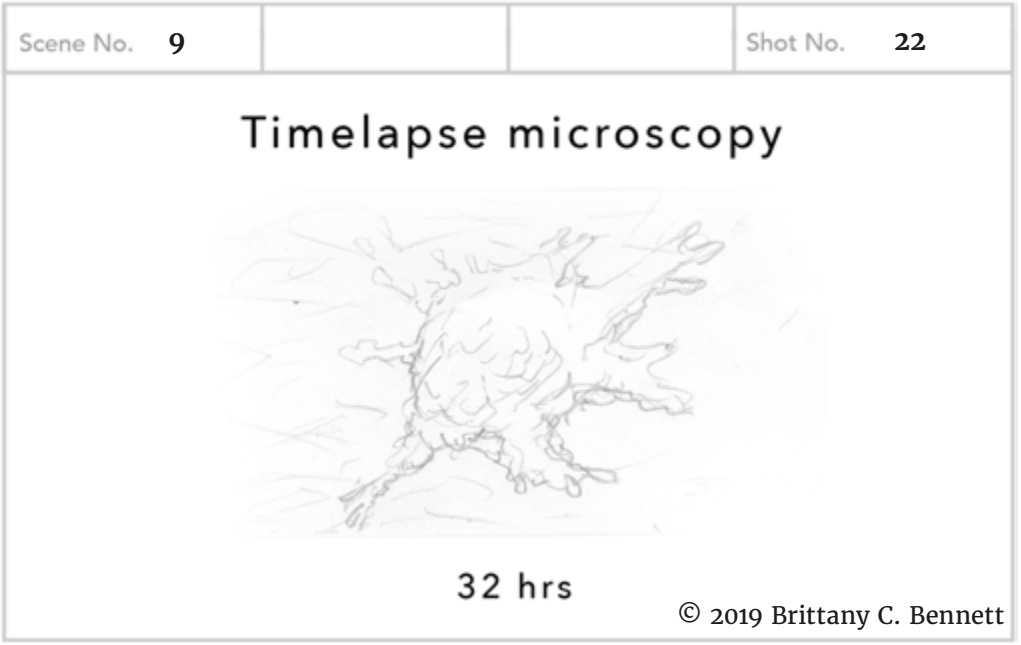

Video: Previous scene cross fades to footage of t

mor organoid proliferating.

Audio: "...and timelapse microscopy to identify molecular strategies that limit the growth and spread of epithelial tumors."

Figure 27.10. Animation storyboards 21–22.

Video: Time-lapse pauses and blurs. Text fades in on screen.

Audio: "This research supports a new model called Collective Epithelial Metastasis..."

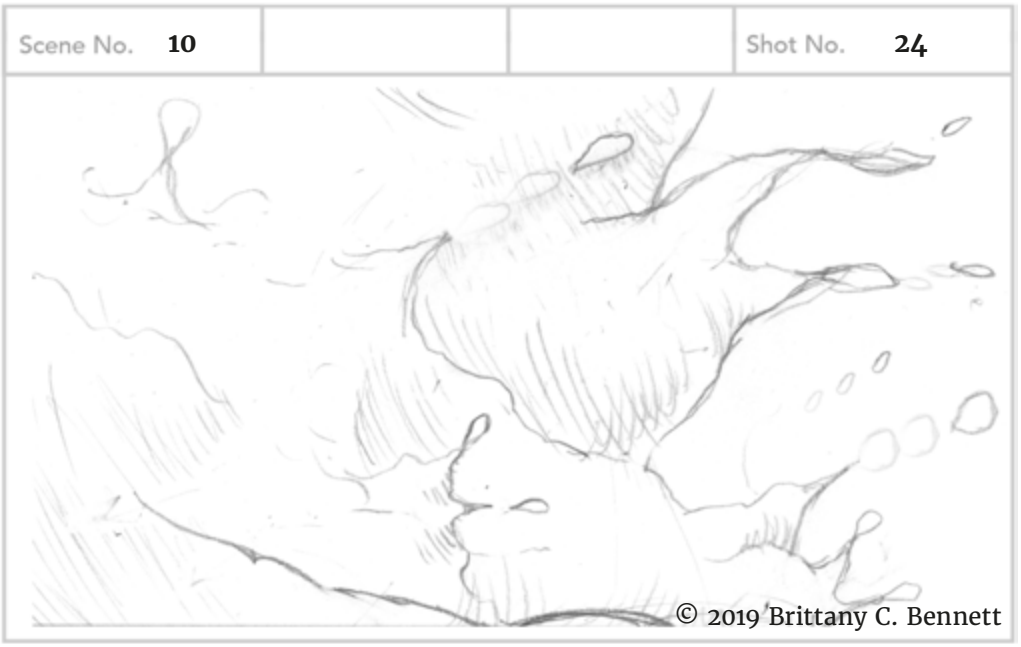

Video: Scene fades in and camera backs out accross surface of tumor. Cells are actively disseminating.

Audio: "...a model in which the danger is not just the escape of one rogue cancer cell,..."

Figure 27.11. Animation storyboards 23-24.

Video: Invasive strand comes into forground. Cell cluster detaches. Camera follows cluster for a moment then scene fades.

Audio: "...but also the cancer cells' ability to stick together and metastasize **pop sound effect**..."

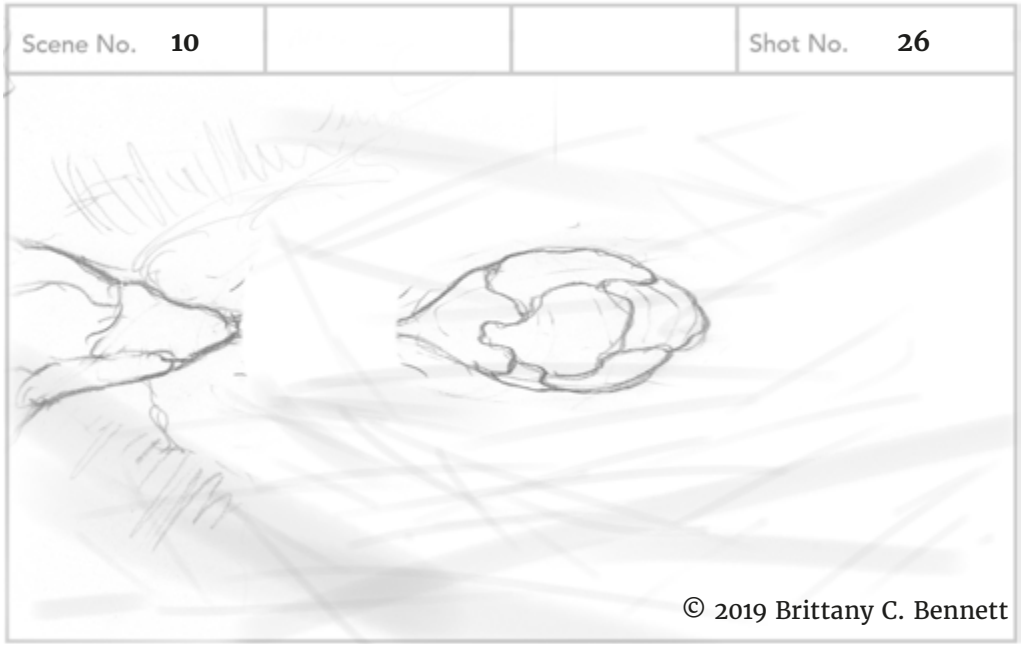

Video: Camera follows cell cluster as it disseminates through the matrix. Scene fades.

Audio: "...collectively."

Figure 27.12. Animation storyboards 25-26.

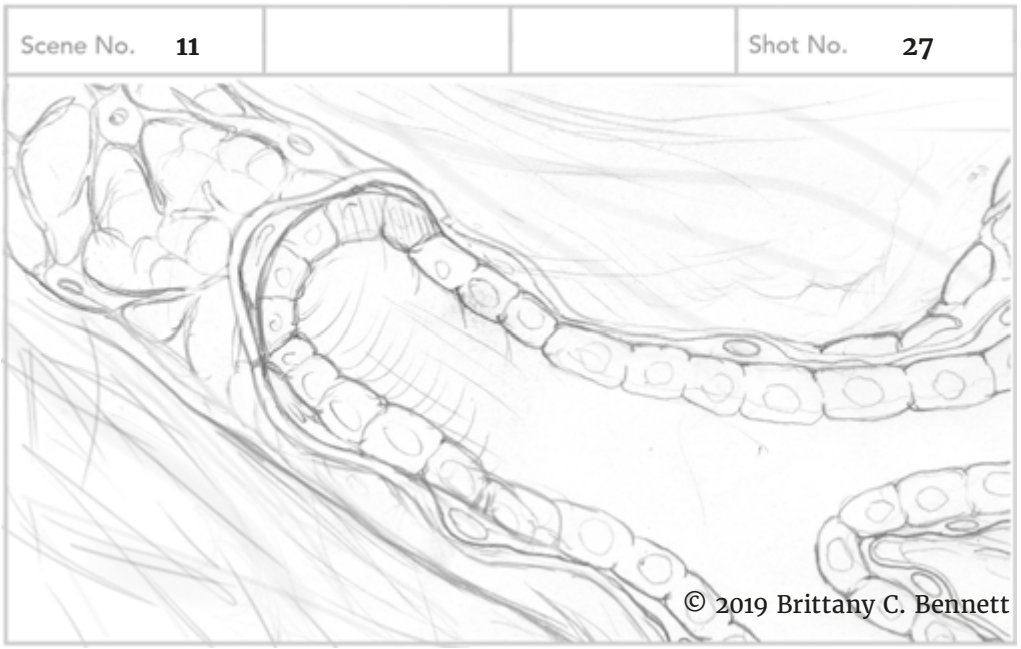

Video: Previous view of duct cross section fades in. Camera zooms in towards duct wall.
Audio: "Normal epithelial cells are tightly bound together…"

Video: Camera focuses on cells making up the duct wall. Adhesive junctions glow orange.
Audio: "…by a cell adhesion molecule…"

Figure 27.13. Animation storyboards 27–28.

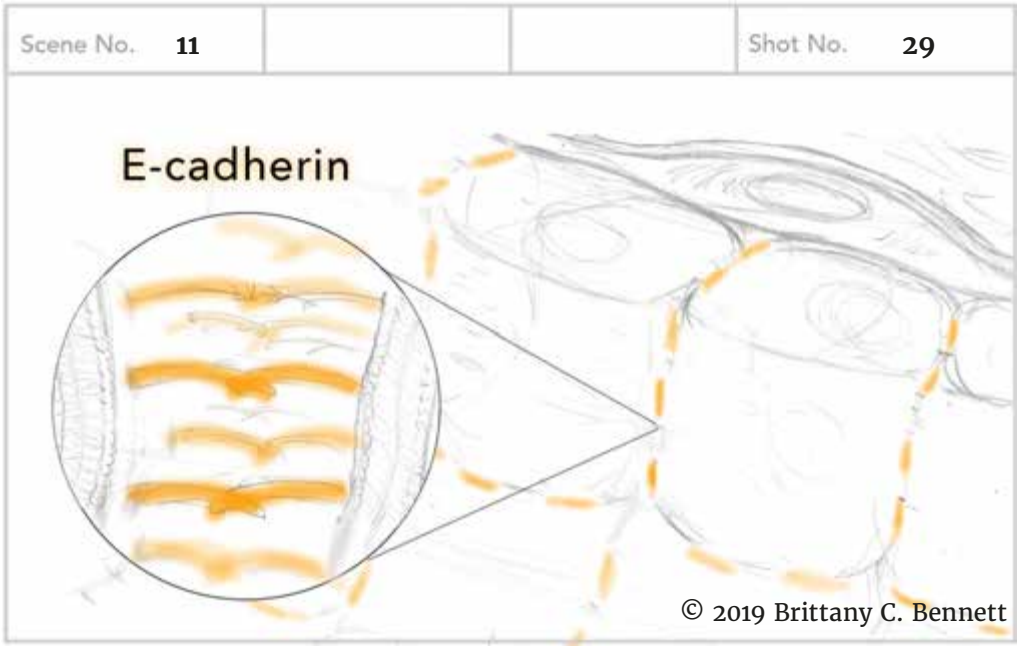

Video: Inset appears and magnifies view of cell junction with E-cad dimers holding cells together. On-screen text: "E-cadherin."

Audio: "...called E-cadherin, which holds epithelial cells in place and restricts the migration of cancer cells into surrounding tissue."

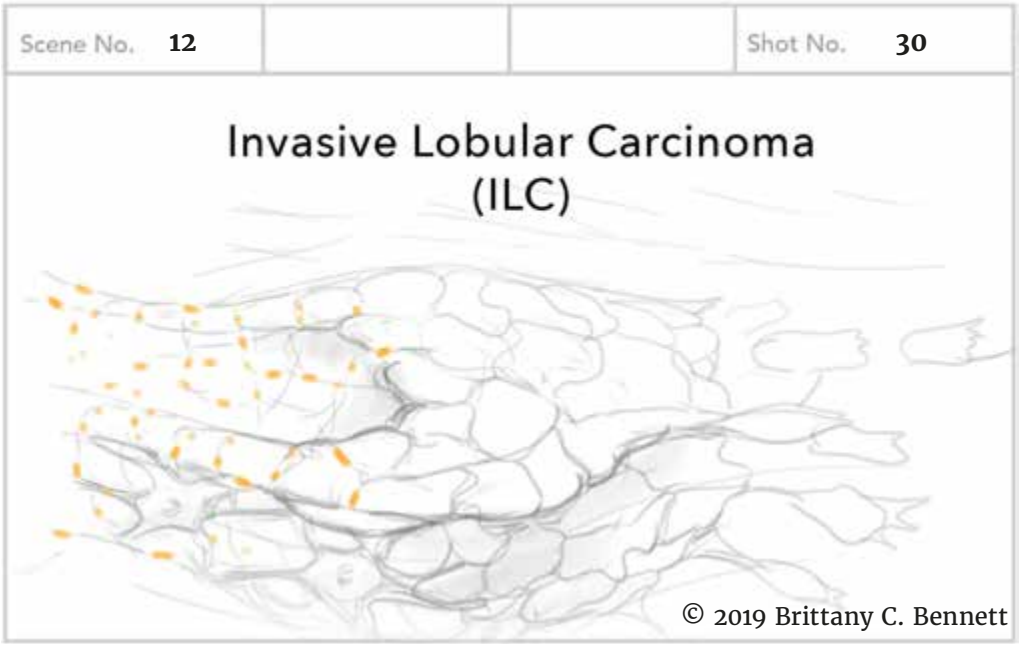

Video: Lobular scene. On-screen text: "Lobular Carcinoma In Situ." Epithelial cells in the lobule are lit up orange.

Audio: "To overcome this, some epithelial cancers lose E-cad to accelerate invasion..."

Figure 27.14. Animation storyboards 29-30.

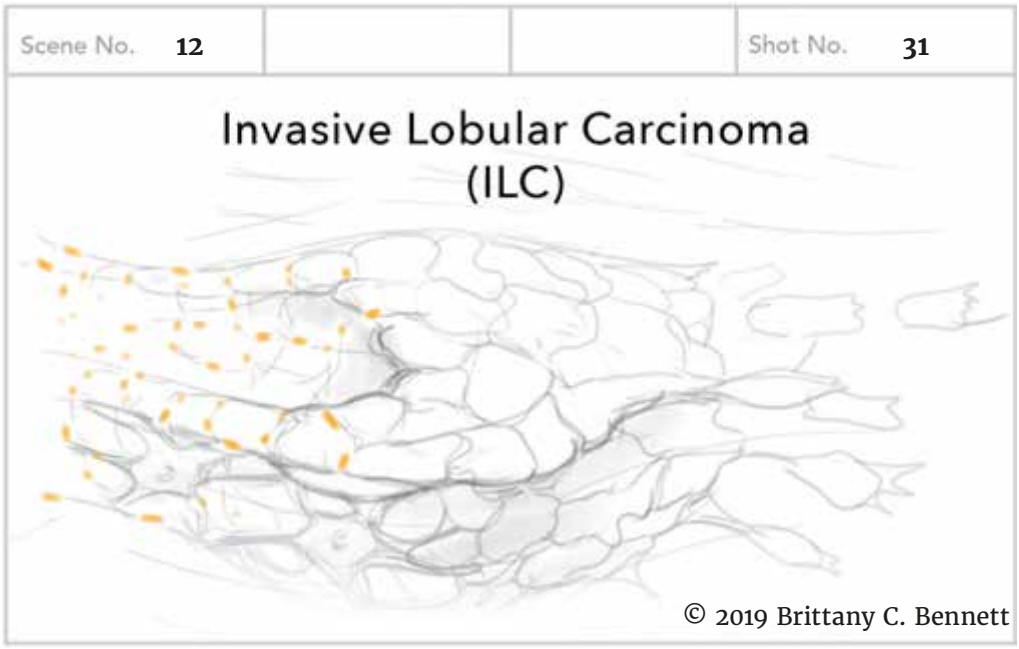

Video: E-cad flickers away until its gone, causing cells to disseminate.
Audio: "...to accelerate invasion... "

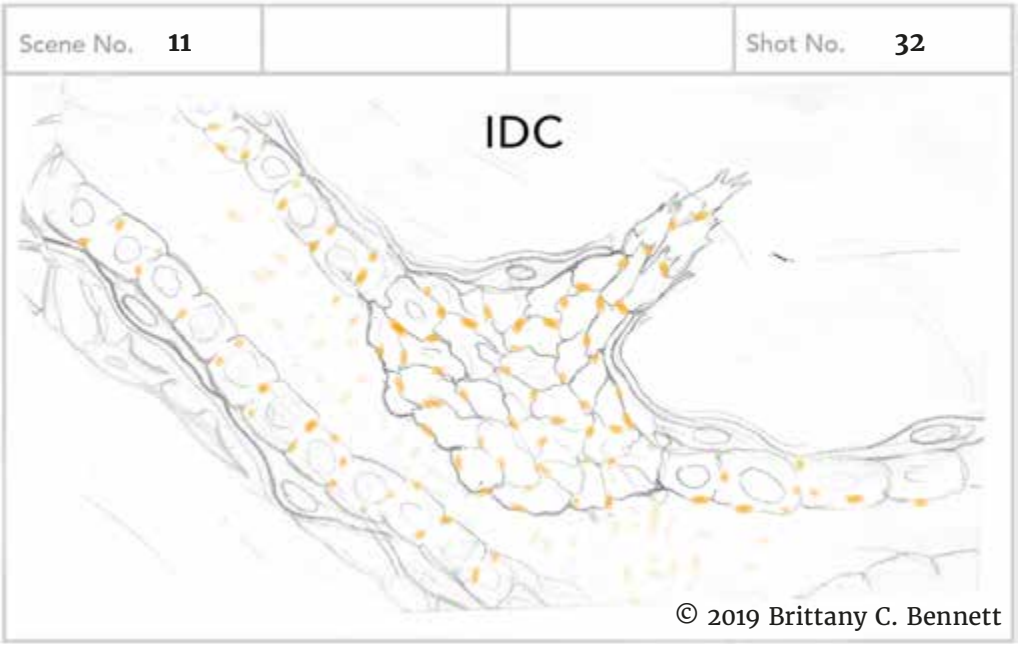

Video: Cells invade through basement membrane with E-cad lit up.
Audio: "...but Invasive Ductal Carcinoma not only retains cell adhesion with E-cad..."

Figure 27.15. Animation storyboards 31-32.

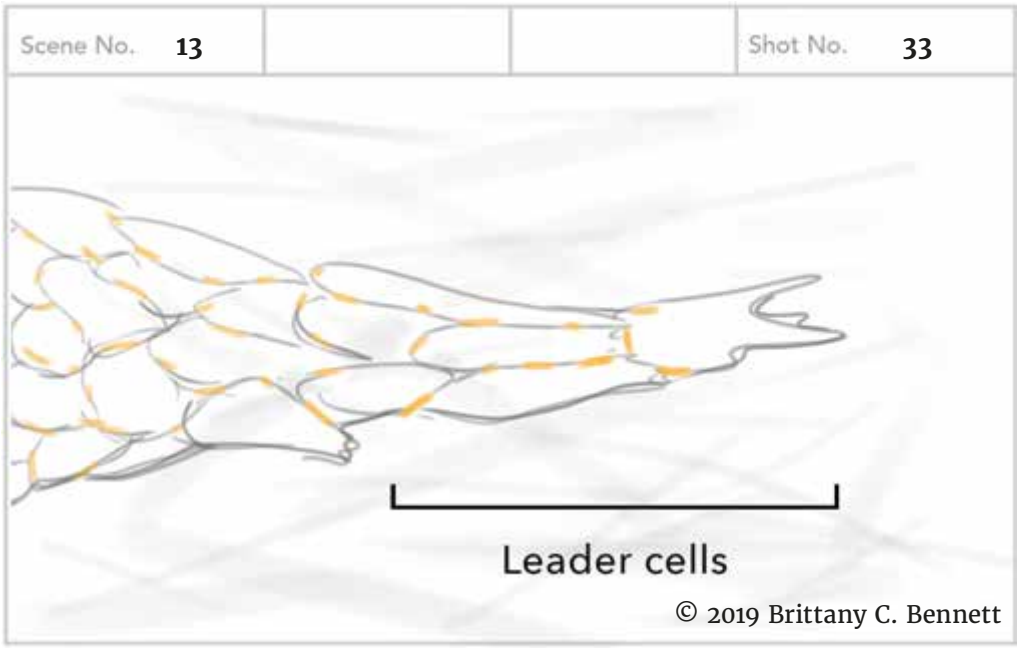

Video: Leading strand moves through matrix, E-cad lit up.

Audio: "...the cells leading the invasion require it."

Video: Zoom out to show that one tumor has multiple leader strands invading surrounding tissue. On-screen text appears after narration.

Audio: "Leader cells" are of interest to researchers because their molecular profile makes them the most invasive and the most dangerous."

Figure 27.16. Animation storyboards 33-34.

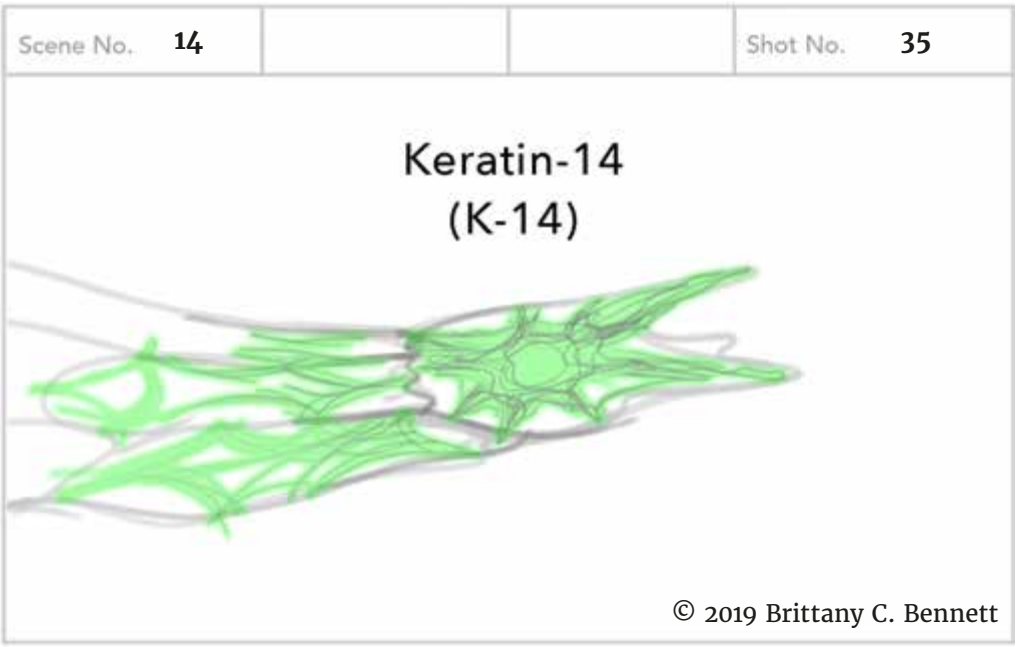

Video: Zoom in on leader cells, the filaments show through. On-screen text: Keratin-14 (K-14)

Audio: "In breast cancer, leader cells have one thing in common: an intermediate filament expressed in basal cells, called Keratin-14 (K-14)."

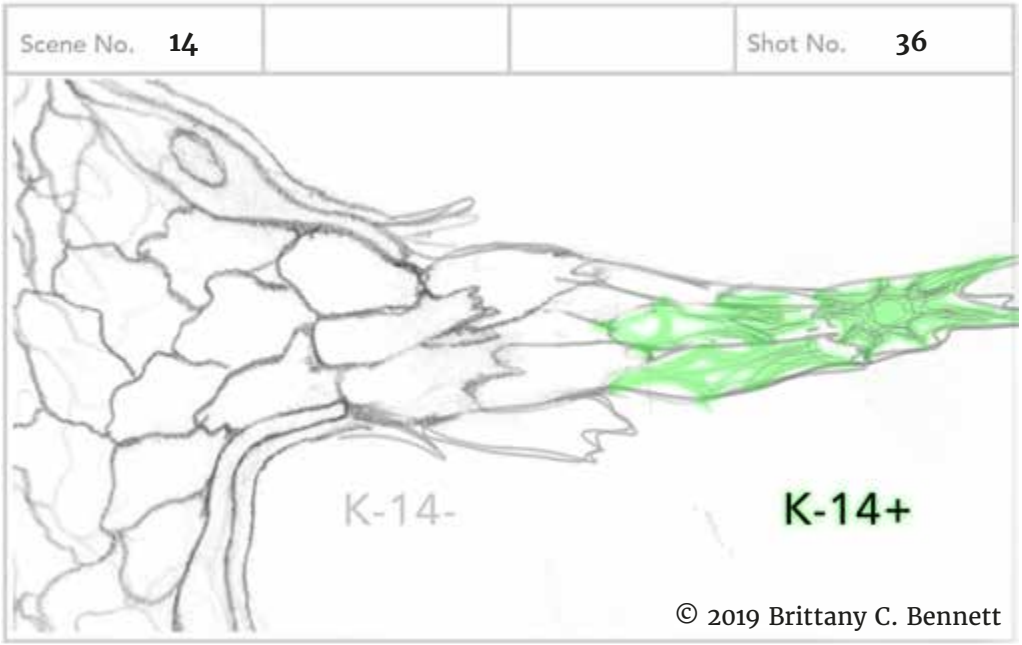

Video: Pan left to the margin of luminal cells with K-14 gradually fluorescing as they migrate forwards. On-screen text: K-14+

Audio: "Even luminal cells that don't normally have K-14, gradually induce K-14 expression, and become K-14+ before leading invasion."

Figure 27.17. Animation storyboards 35-36.

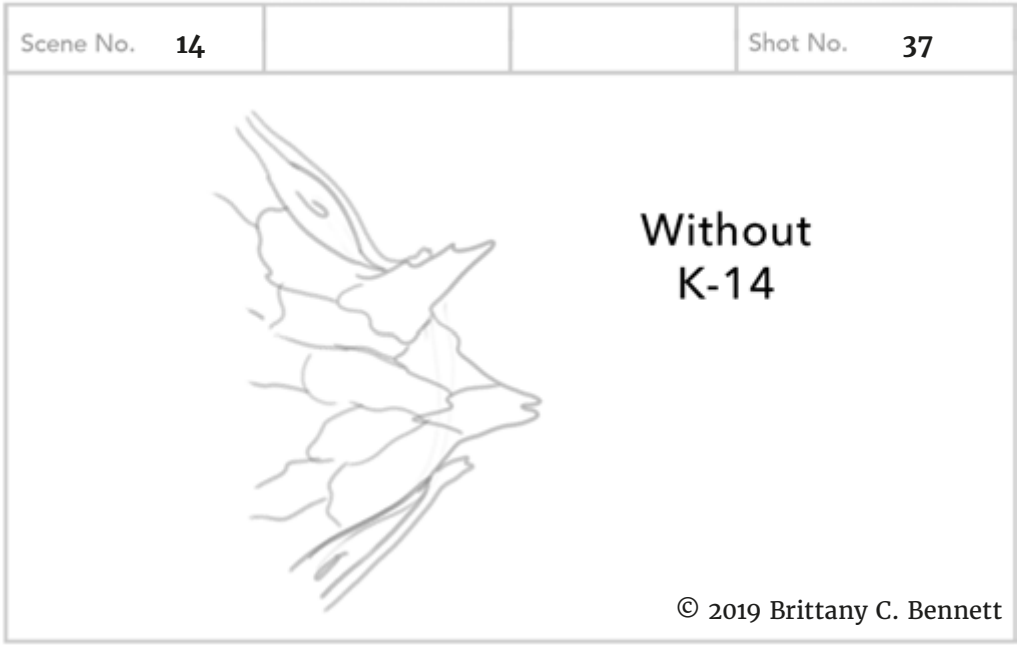

Video: A K-14-different tumor, same view cells making sub-cellular protrusions. On-screen text: K-14 –

Audio: "A tumor's failure to invade when K-14 is disrupted, shows that this protein is required for metastasis,..."

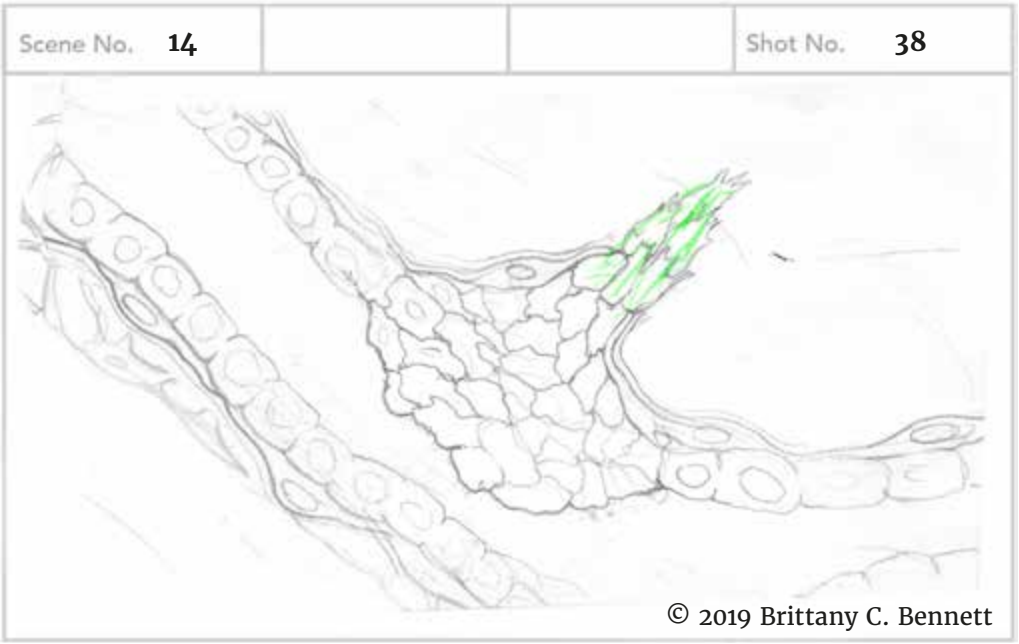

Video: K-14 lights up with"biomarker", KB zoom out.

Audio: "... and therefore, a useful biomarker to identify the metastatic potential of an individual patient's tumor."

Figure 27.18. Animation storyboards 37-38.

Video: Blur scene, On screen text: E-cad plays a versatile role throughout metastasis.

Audio: "E-cad plays a versatile role throughout metastasis."

Video: Dark scene, like underwater looking up, at silouette of duct and cell. An epithelial cell that hasn't disseminated very far looks like its struggling to get through the ECM, undergoes apoptosis.

Audio: "Single epithelial cells that have lost adhesion to their neighbors…"

Figure 27.19. Animation storyboards 39-40.

Video: Cell explodes (apoptosis).
Audio: "...are programed to self-destruct. "

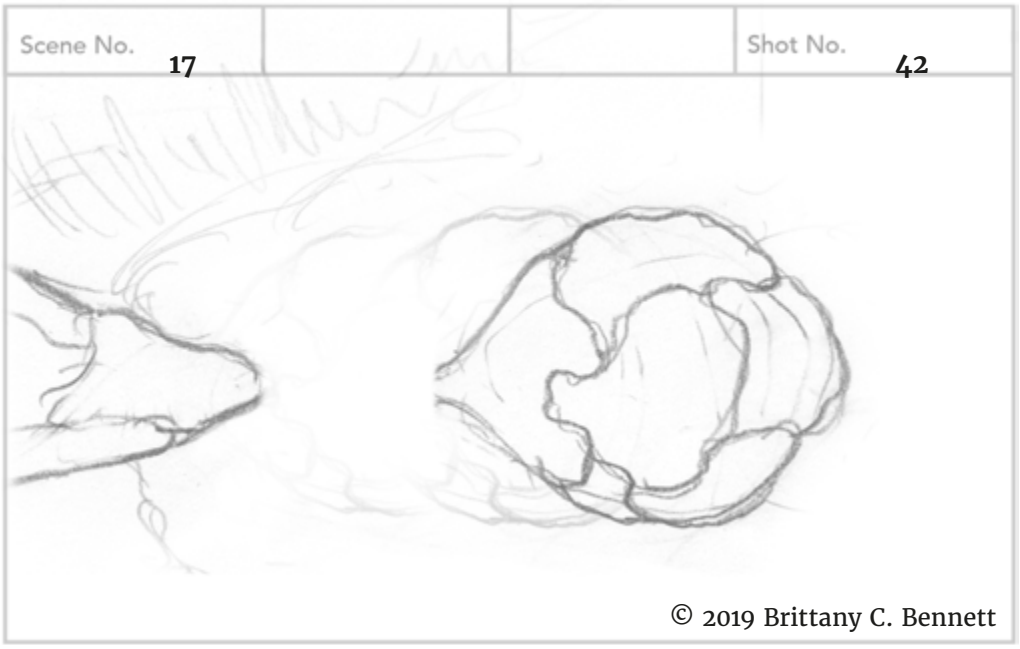

Video: Close up of disseminating cluster with E-cad labeled.
Audio: "Even though E-cad-mediated cell adhesion makes invasion difficult..."

Figure 27.20. Animation storyboards 41-42.

Video: Close up of disseminating cluster with E-cad labeled.
Audio: "...it enables cells to disseminate as clusters and evade self-destruction."

Video: Zoom out, where multiple clusters are seen disseminating through tissue.
Audio: "Epithelial cancers rely on their adhesive connections for survival,..."

Figure 27.21. Animation storyboards 43-44.

Video: Zoom out to tumor from the beginning.

Audio: "...making these adhesion-based survival pathways good targets for future research ..."

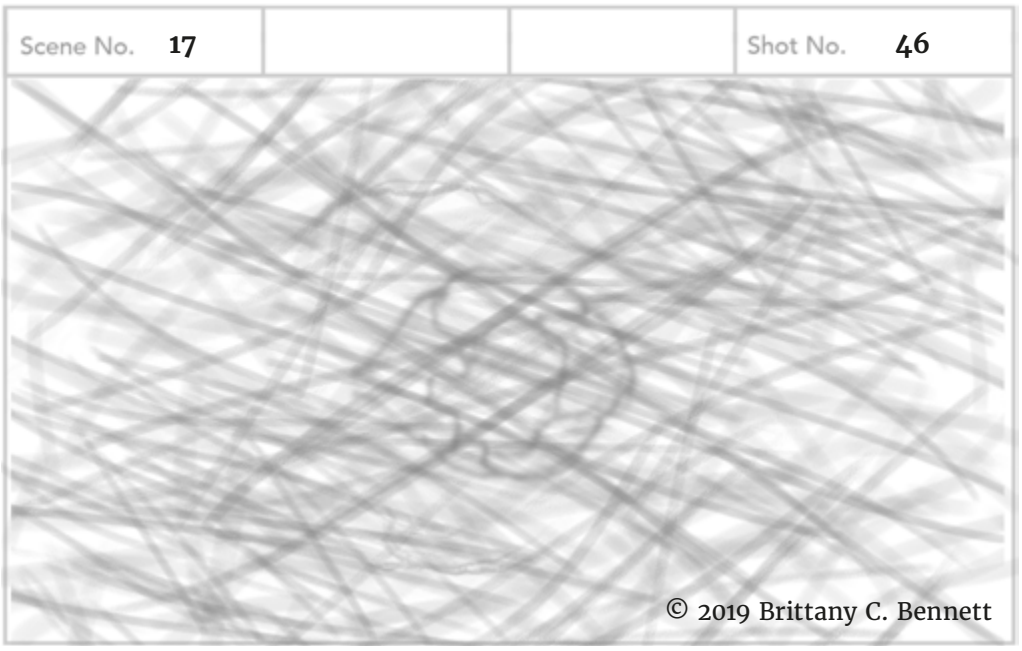

Video: Slow zoom out.

Audio: "...and new therapies." **Credit roll music**

Figure 27.22 Animation storyboards 45-46.

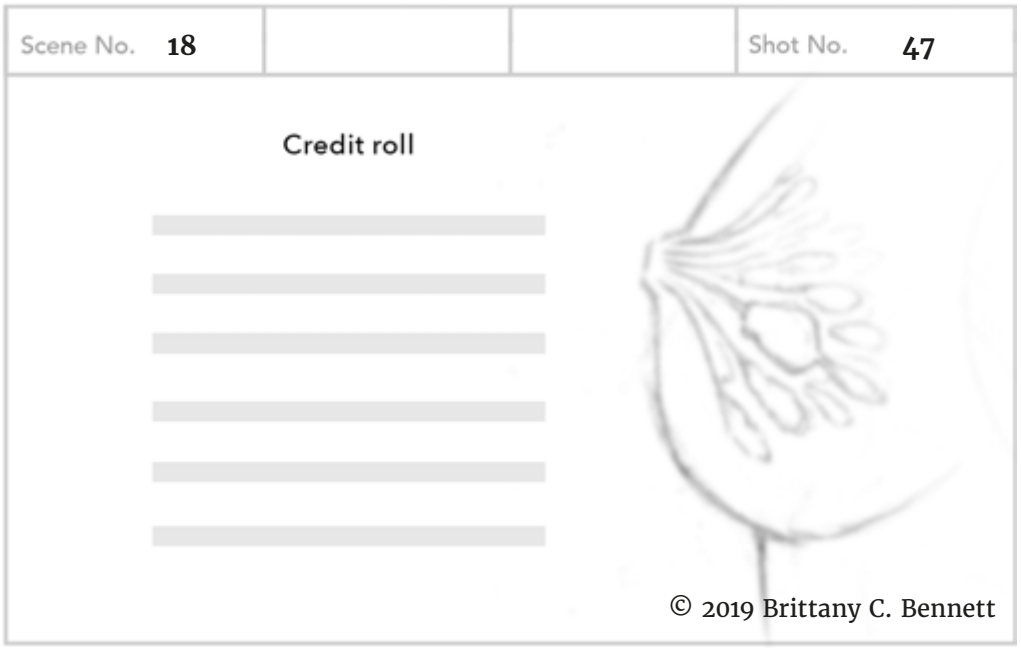

Video: Breast and tumor asset from begining appears, then blurs as credit roll plays.
Audio: *Credit roll music*

Figure 27.23. Animation storyboard 47.

Access to Assets Resulting from this Thesis

Access to the animation resulting from this thesis can be viewed at the web address, www.collectivemetastasis.com and www.bennettbiovisuals.com/collectivemetastasis, or by contacting the author at brittany@bennettbiovisuals.com. The author may also be reached through the Department of Art as Applied to Medicine via the website www.hopkinsmedicine.org/medical-art

DISCUSSION

Incorportation of Time-Lapse Microscopy Data into an Educational Animation

Technical Aspects

An OBJ Sequence Importer Plugin can be used to import a sequence of OBJ files into Cinema 4D as 3D models that correspond to 3D cell surface meshes created from a time-lapse microscopy data set. The result is contained in a null called "Sequence Controller," that animates the sequence of 3D models beginning on a specified frame in the timeline. The 3D models can be further modified by the application of deformers, generators, and materials. This is a novel method for visualizing time-lapse cellular events in Cinema 4D based on data. However, modifications like these can pose technical problems. Attention must be paid to whether the modification, such as rotating the model, is applied to the entire animated sequence or only one 3D model within the Sequence Controller. If the modification is applied to only one frame, the sequence may appear discontinuous when played.

Current State of Related Methods for Visualizing Time-Lapse Microscopy Datasets

Importing data-derived 3D cell surface meshes in animation programs, such as Cinema 4D, is a newly emerging method of biovisualization with opportunities to improve scientific communication. *Non-animated* cell surface meshes have been used to create manuscript figures (Fritz-Laylin 2017), for public outreach in educational web modules (Visual Guide to Human Cells 2019), and for viewing in virtual reality (University of Glasgow 2016). *Animated* 3D models of cell surface meshes have been used as figures in data for scientific communication to a specialized audience of cell biology researchers (Fritz-Laylin 2017). To the author's knowledge, *animated* 3D models of 3D cell surface meshes have not been incorporated into educational 3D

animations to communicate cellular events to a non-specialist audience.

Purpose of Incorporating Time-Lapse Microscopy Datasets into an Educational Animation

The time-lapse microscopy datasets from the Ewald Lab used in this project show cellular events that occur during breast cancer metastasis. The novel workflow to import and "reanimate" these cellular events in Cinema 4D made it possible to communicate the significance of these events in an educational 3D animation. This improves the accessibility of cell biology research by implementing collected data into a visual medium designed to communicate to audiences with minimal familiarity with the science.

A 3D rendering of a cell moving against a blank background with didactic color is powerful in its ability to communicate cellular topology, morphology, and spatiotemporal relationships to a specialist audience. However, this type of visual has no anatomical context and does not inherently include information about the process in which it takes place. The 3D animation produced in this project visualizes the cellular events within the context of a narrative. The narrative improves communication of the research represented by the dataset because it explains 1) the anatomical location of cellular events, 2) the scale at which the events take place, 3) the histological microenvironment which the event takes place in and interacts with, and 4) key definitions of pathological terminology relevent to the disease process in which the events take place.

Visualization Challenges Encountered during the Project

The goal of the animation was to communicate key conclusions from the Ewald Lab published from 2008-2018 to a non-specialist audience. The scale and

detail-level of the research conclusions made narrative design challenging. Briefly, the Ewald lab investigates how proteins play a role in causing cells to break away from a mammary duct tumor and survive as they disseminate and form distant metastasis. One challenge was to sift through an extensive amount of experimental results and microscopy images to condense the findings into a narrative that follows and communicates the logic of the primary research questions. This was addressed by creating an outline of the research questions and experimental conclusions of each primary study published by Ewald lab.

The defined audience has a vested interest in the current state of metastatic breast cancer research, such as patient advocates and benefactors. However, the audience is generally not expected to be able to independently interpret the significance of the research conclusions. The research conclusions tell a compelling story about how proteins, such as E-cadherin and Keratin-14, contribute to metastasis. In order to communicate the significance of these key conclusions, the audience must first be introduced to relevant anatomy, histological structures, and explanations of the pathology. For this reason, the research conclusions were conveyed within a narrative that teaches how a breast cancer tumor progresses from Ductal Carcinoma In-Situ to Invasive Ductal Carcinoma.

A scene of the histological mammary duct microenvironment was built in Cinema 4D using measurements of cell types and anatomical structures. The scene was created to balance histological accuracy with the filtering of extraneous levels of detail or unknown visual information in order to effectively teach specific cellular events that occur during collective epithelial metastasis. Two examples of this are the modeling of the extracellular matrix and the modeling of myoepithelial cells.

The extracellular matrix surrounding the mammary duct is a dense network of structural fibers and signaling molecules that cell clusters must traverse in order to collectively invade. This posed two challenges for the creation of the animation. First, an accurate depiction of the fibrous network surrounding the mammary duct would be visually distracting from the key events being taught. Second, the exact way in which cell clusters move through this fibrous network is currently disputed amongst experts. For these reasons, the extracellular matrix was depicted in a significantly reduced level of complexity by receding the fibers into the background and fading them out with atmospheric perspective.

Myoepithelial cells were observed to restrain and recapture luminal epithelial cells. However, the precise morphology of human myoepithelial cells was not determinately known during the creation of the animation. The 3D surfaces generated by Imaris were not precise due to poor thresholding of low-florescent intensity areas in the data set. To overcome this challenge, the decision was made to visually obstruct the myoepithelial cell layer with the basement membrane so the exact morphology of the cells was not readily apparent.

Summary

This project demonstrates that 3D time-lapse microscopy datasets can be incorporated into Cinema 4D and blend within the built anatomical and histological scene. The merging of data-derived animation with artist-created animation can improve scientific communication to audiences outside of cell biology.

APPENDIX A

Animation Learning Objectives:

Global Objectives

After watching the animation, the audience will...

- **Understand** the meaning of Collective Epithelial Metastasis (CEM)
- **Gain an appreciation for** how cellular and molecular research contributes to understanding the bigger picture of metastatic breast cancer and clinical efforts to develop new treatments.

Specific Learning Outcomes

After watching the animation, the audience will be able to...

- **Understand** the meaning of metastasis
- **Identify** the anatomical structures that are relevant to breast carcinoma (mammary gland, ducts, and lobules.)
- **Identify** the histological structures that are relevant to breast carcinoma (epithelium, epithelial cells, myoepithelial cells, basement membrane)
- **Visualize** some components of the stroma surrounding the relevant histological structures (Collagen I, elastin, and fibroblasts)
- **Distinguish** that epithelial cells are luminal and myoepithelial cells are basal
- **Contrast** normal epithelium, Ductal Carcinoma In Situ, and Invasive Ductal Carcinoma
- **Recognize** that myoepithelial cells can restrain luminal invasion
- **Recognize** how a tumor organoid grown in 3D culture mimics the anatomical and histological characteristics of ductal carcinoma in vivo.
- **Understand:**
    - ◊ That genetics, 3D cell culture, and time-lapse microscopy is used to study cell behavior during tumor growth

- ◊ The results of these studies supports CEM.
- ◊ The meaning of CEM as mode of cell migration.
- ◊ Identify a disseminated “cluster” of tumor cells
- ◊ Tumors disseminate collectively, rather than as a single cell
- ◊ The function of cell adhesion in normal mammary epithelium and in carcinomas
- ◊ Some carcinomas lose E-cadherin to facilitate invasion
- ◊ Invasive Ductal Carcinoma retains cell adhesion with E-cadherin
- ◊ E-cad suppresses invasion
- ◊ Leader cells require E-cadherin

- **Identify** an invasive “strand” and “leader cells”
- **Define** Keratin-14, a type of intermediate filament expressed in basal cells
- **Visualize:**
  - ◊ The motion of cells within a leading strand as it navigates through the stroma
  - ◊ How the invasive strand interacts with the collagen fibers as it moves
  - ◊ The effect of K14 inhibition on invasion

- **Understand (**about K-14):
  - ◊ Luminal cells do not express K-14, but gradually become K-14+ before leading invasion
  - ◊ K-14 could be a useful biomarker for metastatic potential of an individual patient’s tumor.

- **Understand** (about E-cad):
  - ◊ E-cad plays versatile roles throughout the process of metastasis
  - ◊ Epithelial cells that have lost adhesion to their neighbors are

programed to self-destruct.

- ◊ E-cad promotes metastasis at this stage, by facilitating adhesion within disseminating clusters, which are more successful metastatic seeds
- ◊ Epithelial cancer cells rely upon their adhesive connections for survival.
- ◊ Adhesion-based survival pathways may be good targets for new therapies.

APPENDIX B

“Cells in Motion: Collective Epithelial Metastasis” Script

Which cells in a breast tumor are the most dangerous to the patient?

The most dangerous cells are those that enable metastasis, a process in which cancer cells invade into the surrounding tissue and survive as they travel through the blood or lymphatic system to seed a secondary tumor in a distant organ. A deeper understanding of the mechanisms that drive dangerous cell behaviors enables scientists to develop new therapies to prevent and treat metastasis.

--

Most breast cancers arise from cells that line the ducts and lobules of the mammary gland, called the Epithelium. Mammary duct epithelium is made of luminal epithelial cells and basal myoepithelial cells, surrounded by a basement membrane. When luminal cells proliferate into the duct, but do not penetrate the basement membrane, this is called Ductal Carcinoma In-Situ (D-C-I-S). During cancer progression, myoepithelial cells can contract to restrain and re-capture luminal cells. But if they penetrate the basement membrane, it becomes Invasive Ductal Carcinoma (I-D-C), a malignant tumor that can become metastatic.

--

How do scientists study cellular mechanisms that drive metastasis?

Scientists use a novel combination of genetics, 3D culture, and time-lapse microscopy to identify molecular strategies that limit the growth and spread of epithelial tumors. This research supports a new model called Collective Epithelial Metastasis-- a model in which the danger is not just the escape of one rouge cancer cell, but also the cancer cells’ ability to stick together and metastasize collectively.

--

Normal epithelial cells are tightly bound together by a cell adhesion molecule called E-cadherin, which holds them in place and restricts the migration of cancer cells into surrounding tissue. To overcome this, some epithelial cancers lose E-cad to accelerate invasion, but Invasive Ductal Carcinoma not only retains cell adhesion with E-cad, the cells leading invasion require it.

--

Leader cells are of interest to researchers because their molecular profile makes them the most invasive and the most dangerous. In breast cancer, leader cells have one thing in common: an intermediate filament expressed in basal cells, called Keratin-14 (K-14). Even luminal cells that don't normally have K-14, gradually induce K-14 expression, and become K-14+ before leading invasion. A tumor's failure to invade when K-14 is disrupted, shows that this protein is required for metastasis, and therefore, a useful biomarker to identify the metastatic potential of an individual patient's tumor.

--

E-cad plays versatile roles throughout metastasis

Single epithelial cells that have lost adhesion to their neighbors are programed to self-destruct. Even though E-cad-mediated cell adhesion makes invasion difficult, it enables cells to disseminate as clusters and evade self-destruction. Epithelial cancers rely on their adhesive connections for survival, making these adhesion-based survival pathways good targets for future research and new therapies.

Narration time: 04:00

REFERENCES

American Cancer Society. "What Is Cancer?" Cancer Basics. Accessed November 19, 2018. https://www.cancer.org/cancer/cancer-basics/what-is-cancer.html

American Cancer Society. Breast Cancer Facts & Figures 2017-2018. Atlanta: American Cancer Society, Inc. 2017.

Andrechek, E. R., S. Mori, R. E. Rempel, J. T. Chang, and J. R. Nevins. "Patterns of Cell Signaling Pathway Activation That Characterize Mammary Development." Development 135, no. 14 (2008): 2403-413. doi:10.1242/dev.019018.

Adriance, Melissa C., Jamie L. Inman, Ole W. Petersen, and Mina J. Bissell. "Myoepithelial Cells: Good Fences Make Good Neighbors." Breast Cancer Research 7, no. 5 (2005). doi:10.1186/bcr1286

"Cancer Terms: Cancer, Neoplasia, Tumor, Neoplasm." SEER Training Modules. Accessed November 13, 2019. https://training.seer.cancer.gov/disease/cancer/terms.html.

Chen, Bi-Chang, Wesley R. Legant, Kai Wang, Lin Shao, Daniel E. Milkie, Michael W. Davidson, Chris Janetopoulos, Xufeng S. Wu, John A. Hammer, Zhe Liu, Brian P. English, Yuko Mimori-Kiyosue, Daniel P. Romero, Alex T. Ritter, Jennifer Lippincott-Schwartz, Lillian Fritz-Laylin, R. Dyche Mullins, Diana M. Mitchell, Joshua N. Bembenek, Anne-Cecile Reymann, Ralph Böhme, Stephan W. Grill, Jennifer T. Wang, Geraldine Seydoux, U. Serdar Tulu, Daniel P. Kiehart, and Eric Betzig. "Lattice Light-sheet Microscopy: Imaging Molecules to Embryos at High Spatiotemporal Resolution." Science (New York, N.Y.). October 24, 2014. Accessed March 16, 2019. https://www.ncbi.nlm.nih.gov/pmc/articles/PMC4336192/.

Cheung, Kevin J., Ed Gabrielson, Z. Werb, and Ewald J. Andrew. "Collective Invasion in Breast Cancer Requires a Conserved Basal Epithelial Program." Cell 155, no. 7, (2013): 1639-651. doi:10.1016/j.cell.2013.11.029.

Cheung, Kevin J., Veena Padmanaban, Vanesa Silvestri, Koen Schipper, Joshua D. Cohen, Amanda N. Fairchild, Michael A. Gorin, James E. Verdone, Kenneth J. Pienta, Joel S. Bader, and Andrew J. Ewald. "Polyclonal Breast Cancer Metastases Arise from Collective Dissemination of Keratin 14-Expressing Tumor Cell Clusters." PNAS, National Academy of Sciences, (2016). doi:https://doi.org/10.1073/pnas.1508541113

Christensen, Kent, Matthew Velkey, Lloyd M. Stoolman, Laura Hessler, and Diedra Mosley-Brower. "259 Mammary Gland Inactive." Compiled by Michael Hortsch. Virtual Slide List. Accessed December 20, 2019. http://virtualslides.med.umich.edu/Histology/Female Reproductive System/259_HISTO_20X.svs.

Clark, Kenneth, Bruce Vendt, Kirk Smith, John Freymann, Justin Kirby, Paul Koppel, Stephen Moore, Stanley Phillips, David Maffitt, Michael Pringle, Lawrence Tarbox, and Fred Prior. "The Cancer Imaging Archive (TCIA): Maintaining and Operating a Public Information Repository." Journal of Digital Imaging 26, no. 6 (2013): 1045-057. doi:10.1007/s10278-013-9622-7.

Cleator, S., and A. Ashworth. "Molecular Profiling of Breast Cancer: Clinical Implications." British Journal of Cancer 90, no. 6 (2004): 1120-124. doi:10.1038/sj.bjc.6601667.

Clermont, Yves, Michael Lalli, and Zsuzsanna Bencsath-Makkai. "Epithelial Cell of a Lactating Mammary Gland." Light Microscopy Histology Atlas. Accessed March 19, 2019. http://audilab.bmed.mcgill.ca/HA/html/frs_47_E.html.

Cobb, Matthew. "60 Years Ago, Francis Crick Changed the Logic of Biology." PLOS Biology 15, no. 9 (2017). doi:10.1371/journal.pbio.2003243.

Coleman, William B. "Neoplasia." In Molecular Pathology: The Molecular Basis of Human Disease, by William B. Coleman and Gregory J. Tsongalis, 71-97. Academic Press, 2018.

Cooper, Geoffrey M. The Cell: A Molecular Approach. New York: Sinauer Associates,

2019.

Creative Commons Legal Code. Accessed March 21, 2019. https://creativecommons.org/licenses/by-nc-sa/3.0/legalcode.

“Data Usage Policies and Restrictions.” The Cancer Imaging Archive User Guide. Accessed March 11, 2019. https://wiki.cancerimagingarchive.net/display/Public/Data Usage Policies and Restrictions.

Divoli, Anna, Eneida A. Mendonça, James A. Evans, and Andrey Rzhetsky. “Conflicting Biomedical Assumptions for Mathematical Modeling: The Case of Cancer Metastasis.” PLoS Computational Biology 7, no. 10 (2011). doi:10.1371/journal.pcbi.1002132.

Daly, Craig, Lauren Clunie, and Minhua Ma. “From Microscope to Movies: 3D Animations for Teaching Physiology.” Microscopy and Analysis 28(6) 28, no. 6 (September 2014): 7-10.

Ewald, A. J., R. J. Huebner, H. Palsdottir, J. K. Lee, M. J. Perez, D. M. Jorgens, A. N. Tauscher, K. J. Cheung, Z. Werb, and M. Auer. “Mammary Collective Cell Migragration Involves Transient Loss of Epithelial Features and Individual Cell Migration within the Epithelium.” Journal of Cell Science 125, no. 11 (2012): 2638-654. doi:10.1242/jcs.096875.

“The Ewald Lab.” Andrew Ewald, Ph.D. Accessed March 15, 2019. https://cellbio.jhmi.edu/people/faculty/andrew-ewald-phd.

Gartner, Leslie P. Textbook of Histology. Philadelphia, PA: Elsevier, 2017.

Friedl, Peter, Joseph Locker, Erik Sahai, and Jeffrey E. Segall. “Classifying Collective Cancer Cell Invasion.” Nature Cell Biology 14, no. 8 (2012): 777-83. doi:10.1038/ncb2548.

Fritz-Laylin, Lillian K., Megan Riel-Mehan, Bi-Chang Chen, Samuel J. Lord, Thomas D. Goddard, Thomas E. Ferrin, Susan M. Nicholson-Dykstra, Henry

Higgs, Graham T. Johnson, Eric Betzig, and R. Dyche Mullins. “Actin-based Protrusions of Migrating Neutrophils Are Intrinsically Lamellar and Facilitate Direction Changes.” ELife 6 (2017). Accessed March 5, 2019. doi:10.7554/elife.26990.

Haaksma, Carol J., Robert J. Schwartz, and James J. Tomasek. “Myoepithelial Cell Contraction and Milk Ejection Are Impaired in Mammary Glands of Mice Lacking Smooth Muscle Alpha-Actin1.” Biology of Reproduction 85, no. 1 (2011): 13-21. doi:10.1095/biolreprod.110.090639.

Hanahan, Douglas, and Robert A. Weinberg. “Hallmarks of Cancer: The next Generation.” Cell. March 04, 2011. Accessed January 2, 2019. https://www.ncbi.nlm.nih.gov/pubmed/21376230/.

Hohenester, Erhard, and Peter D. Yurchenco. “Laminins in Basement Membrane Assembly.” Cell Adhesion & Migration 7, no. 1 (2013): 56-63. doi:10.4161/cam.21831.

Iwasa, Janet H. “Bringing Macromolecular Machinery to Life Using 3D Animation.” Current Opinion in Structural Biology 31 (2015): 84-88. doi:10.1016/j.sbi.2015.03.015.

Junqueira, Luis Carlos., José Carneiro, and Robert O. Kelley. Basic Histology. 7th ed. London: Prentice-Hall International, 1992. 67-68.

Johns Hopkins Medicine Pathology Department, “Types of Breast Cancer,” Breast Cancer & Breast Pathology. Accessed December 20, 2018. https://pathology.jhu.edu/breast/my-results/types-of-breast-cancer pathology.jhu.edu/breast/my-results/types-of-breast-cancer.

Kalluri, Raghu, and Robert A. Weinberg. “The Basics of Epithelial-mesenchymal Transition.” Journal of Clinical Investigation 120, no. 5 (2010): 1786. doi:10.1172/jci39104c1.

Kierszenbaum, Abraham L., and Laura L. Tres. Histology and Cell Biology: An

Introduction to Pathology. Philadelphia: Elsevier, 2016.

Krinsky, G., N. M. Rofsky, and J. C. Weinreb. "Nonspecificity of Short Inversion Time Inversion Recovery (STIR) as a Technique of Fat Suppression: Pitfalls in Image Interpretation." American Journal of Roentgenology 166, no. 3 (1996): 523-26. doi:10.2214/ajr.166.3.8623620.

Martinez-Hernandez, Antonio, David J. Francis, and Steven G. Silverberg. "Elastosis and Other Stromal Reactions in Benign and Malignant Breast Tissue.An Ultrastructural Study." Cancer 40, no. 2 (1977): 700-06. doi:10.1002/1097-0142(197708)40:23.0.co;2-w.

Mayer, Richard E., and Roxana Moreno. "Aids to Computer-based Multimedia Learning." Learning and Instruction 12, no. 1 (2002): 107-19. doi:10.1016/s0959-4752(01)00018-4.

Merrienboer, Jeroen J. G. Van, Paul A. Kirschner, and Liesbeth Kester. "Taking the Load Off a Learners Mind: Instructional Design for Complex Learning." Educational Psychologist 38, no. 1 (2003): 5-13. doi:10.1207/s15326985ep3801_2.

Mindek, Peter, David Kouril, Johannes Sorger, Daniel Toloudis, Blair Lyons, Graham Johnson, M. Eduard Groller, and Ivan Viola. "Visualization Multi-Pipeline for Communicating Biology." IEEE Transactions on Visualization and Computer Graphics 24, no. 1 (2018): 883-92. doi:10.1109/tvcg.2017.2744518.

Nandakumar, Vivek, Laimonas Kelbauskas, Roger Johnson, and Deirdre Meldrum. "Quantitative Characterization of Preneoplastic Progression Using Single-cell Computed Tomography and Three-dimensional Karyometry." Cytometry Part A 79A, no. 1 (2010): 25-34. doi:10.1002/cyto.a.20997.

Neumann, Neil M., Matthew C. Perrone, Jim H. Veldhuis, Robert J. Huebner, Huiwang Zhan, Peter N. Devreotes, G. Wayne Brodland, and Andrew J. Ewald. "Coordination of Receptor Tyrosine Kinase Signaling and Interfacial Tension Dynamics Drives Radial Intercalation and Tube Elongation." Developmental

Cell 45, no. 1 (2018). doi:10.1016/j.devcel.2018.03.011.

Nguyen-Ngoc, K.V., and A.J. Ewald. "Mammary Ductal Elongation and Myoepithelial Migration Are Regulated by the Composition of the Extracellular Matrix." Journal of Microscopy 251, no. 3 (2013): 212-23. doi:10.1111/jmi.12017.

Noble, Denis. "General Discussion II." In Complexity in Biological Information Processing Novartis Foundation Symposia, by Gregory R. Bock and Jamie A. Goode. John Wiley & Sons, 2011. Accessed January 19, 2018. Google Books.

Ozzello, L., and P. Sanpitak. "Epithelial-stromal Junction of Intraductal Carcinoma of the Breast." Cancer 26, no. 6 (1970): 1186-198. doi:10.1002/1097-0142(197012)26:63.0.co;2-c.

Pollock, E., P. Chandler, and J. Sweller. "Assimilating Complex Information." Learning and Instruction 12, no. 1 (2002): 61-86. doi:10.1016/s0959-4752(01)00016-0.

Reil-Mehan, Megan. "Generating Obj Meshes and Ambient Occlusion Texture Maps for Use in THREE.js." Riel-Mehan Media. Accessed March 1, 2019. http://www.meganrielmehan.com/methods-and-notes/creating-obj-meshes-and-ambient-occlusion-texture-maps-for-use-in-threejs.

Rowley-Jolivet, Elizabeth. "Image as Text. Aspects of the Shared Visual Language of Scientific Conference Participants." ASp, no. 27-30 (2000): 133-54. doi:10.4000/asp.2093.

Sakorafas, G.h., and Michael Safioleas. "Breast Cancer Surgery: An Historical Narrative. Part III. From the Sunset of the 19th to the Dawn of the 21st Century." European Journal of Cancer Care 19, no. 2 (2010): 145-66. doi:10.1111/j.1365-2354.2008.01061.x.

Shamir, Eliah R., and Andrew J. Ewald. "Three-dimensional Organotypic Culture: Experimental Models of Mammalian Biology and Disease." Nature Reviews Molecular Cell Biology 15, no. 10 (2014): 647-64. doi:10.1038/nrm3873.

Shamir, Eliah R., Kester Coutinho, Dan Georgess, Manfred Auer, and Andrew J. Ewald. "Twist1-positive Epithelial Cells Retain Adhesive and Proliferative Capacity throughout Dissemination." Biology Open 5, no. 9 (2016): 1216-228. doi:10.1242/bio.019703.

Shamir, Eliah R., Elisa Pappalardo, Danielle M. Jorgens, Kester Coutinho, Wen-Ting Tsai, Khaled Aziz, Manfred Auer, Phuoc T. Tran, Joel S. Bader, and Andrew J. Ewald. "Twist1-induced Dissemination Preserves Epithelial Identity and Requires E-cadherin." The Journal of Cell Biology 204, no. 5 (2014): 839-56. doi:10.1083/jcb.201306088.

Sirka, Orit Katarina, Elijah R. Shamir, and Andrew J. Ewald. "Myoepithelial cells are a dynamic barrier to epithelial dissemination." J Cell Biology, 217, 10. (2018): 3368-3381, doi: 10.1083/jcb.201802144

Snyder, Shauna R. Stem Cell Orchestra: Interactive Didactic Animation for Cardiac Tissue Engineering. Master's thesis, Johns Hopkins School of Medicine, 2018.

Sparano, Joseph A. "Breast Cancer Treatment Protocols." Edited by John V. Kiluk. Medscape. Accessed January 17, 2019. https://emedicine.medscape.com/article/2006464-overview.

Turashvili, Gulisa, and Edi Brogi. "Tumor Heterogeneity in Breast Cancer." Frontiers in Medicine 4 (2017). doi:10.3389/fmed.2017.00227.

"Volume Modeling." MAXON. Accessed December 6, 2018. http://www.maxon.net/en/products/new-in-release-20/volume-modeling/.

University of Glasgow. "Virtual Reality with Dr Craig Daly." Youtube video, 3:48. March 26, 2016. https://www.youtube.com/watch?v=gSrjhaCU9Vo

Wang, James H.C., and Bhavani P. Thampatty. "Advances in Tendon Mechanobiology." Mechanobiology in Health and Disease, 2018, 127-55. doi:10.1016/b978-0-12-812952-4.00005-2.

Watanabe, Satoru. "The Metastasizability of Tumor Cells." Cancer 7, no. 2 (1954): 215-

23. doi:10.1002/1097-0142(195403)7:23.0.co;2-6.

Weigelt, Britta, Johannes L. Peterse, and Laura J. Vant Veer. “Breast Cancer Metastasis: Markers and Models.” Nature Reviews Cancer 5, no. 8 (2005): 591-602. doi:10.1038/nrc1670eer. “Breast Cancer Metastasis: Markers and Models.” Nature Reviews Cancer 5, no. 8 (2005): 591-602. doi:10.1038/nrc1670

“What Are Cell-cell Adhesions?” MBInfo. Accessed January 05, 2018. https://www.mechanobio.info/what-is-mechanosignaling/what-are-cell-cell-adhesions/#e-cadherin-mediated-cell-cell-adhesions.

VITA

Brittany Bennett was born in West Palm Beach, FL. She first explored her love of illustration while drawing pages of monsters with “pipes” (digestive tracts) from her imagination on scrap printer paper in her father’s office.

In 2011, she happily traded palm trees for the woodier fauna of the Northeast. She earned her BFA through a coordinated degree program at the University of Pennsylvania (UPenn) and the Pennsylvania Academy of the Fine Arts (Pafa) where she studied biology and fine art.

In August 2018, she began her education in the Medical and Biological Illustration program in the Department of Art as Applied to Medicine at Johns Hopkins University School of Medicine. She anticipates graduating in May of 2019 with a Master of Arts degree.

After graduation, Brittany will be pursuing a career in biomedical visualization. She strives to continue using art and visual storytelling to increase public understanding of science and accessibility to research.